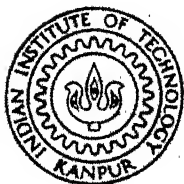


THERMOSYPHON ANALYSIS OF A CANDU REACTOR CORE IN THE EVENT OF LOSS-OF-FLOW ACCIDENTS

By

SUCHANDAN KUMAR DAS



NETP
31 TH
NETP/1981/14
D 264
S
E
NUCLEAR ENGINEERING AND TECHNOLOGY PROGRAMME

INDIAN INSTITUTE OF TECHNOLOGY KANPUR

JUNE, 1981

THERMOSYPHON ANALYSIS OF A CANDU REACTOR CORE IN THE EVENT OF LOSS-OF-FLOW ACCIDENTS

A Thesis Submitted
in Partial Fulfilment of the Requirements
for the Degree of
MASTER OF TECHNOLOGY

By
SUCHANDAN KUMAR DAS

to the

NUCLEAR ENGINEERING AND TECHNOLOGY PROGRAMME
INDIAN INSTITUTE OF TECHNOLOGY KANPUR
JUNE, 1981

TO

MY

BELOVED

PARENTS

WILLIAM
H. HARRISON
JANUARY 1891
NEW YORK

I. I. I. KANPUR
CENTRAL LIBRARY

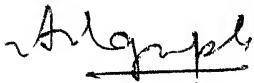
Acc. No. **A 66872**

3 SEP 1981

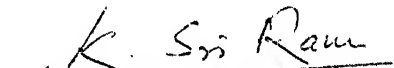
NETP - 1981 - M - DAS - THE

CERTIFICATE

This is to certify that this work entitled,
" THERMOSYPHON ANALYSIS OF A CANDU REACTOR CORE IN THE
EVENT OF LOSS-OF-FLOW ACCIDENTS " by Shri Suchandan Kumar
Das has been carried out under our supervision and has not
been submitted elsewhere for a degree.



(Dr. A. Sengupta)
Asst. Professor
Mechanical and Nuclear Engg.
Indian Institute of Technology
Kanpur.


(Dr. K. Sri Ram)
Professor and Head
Nuclear Engineering
Indian Institute of
Technology, Kanpur.

POST GRADUATE OFFICE

This thesis has been approved
for the award of the degree of
Master of Technology (M.Tech.)
in accordance with the
regulations of the Indian
Institute of Technology Kanpur
Dated.

ACKNOWLEDGEMENT

I have great pleasure in expressing my deep sense of gratitude to Professor K. Sri Ram and A. Sengupta for their constant encouragement, enlighting guidance and inexhaustible patience observed by them throughout the course of my thesis work.

I am extremely grateful to Prof. K. Sri Ram for suggesting the problem to me.

My sincere thanks are due to many people at IIT, Kanpur in particular to Messers M.S. Panesar, S.S. Pathak, V.S. Tomar, Gopal Tiwari and Manohar.

I owe my thanks to all my friends who helped me in more than one way throughout my stay at IIT, Kanpur.

Finally, I wish to acknowledge J.P. Gupta's excellent typing skill, R.S. Tripathi's (Panditjee) cyclostyling and D.K. Mishra's tracing work.

May 28, 1981

(SUCHANDAN KUMAR DAS)

IIT, KANPUR.

CONTENTS

	<u>Page</u>
LIST OF TABLES	i
LIST OF FIGURES	ii
SYNOPSIS	iv
CHAPTER I : INTRODUCTION	1
1.1 Safety of power reactors	1
1.2 Thermosyphon system	3
1.3 Review of literature	8
1.4 Description of CANDU reactor system	14
1.5 Scope of the thesis	17
CHAPTER II : FLOW MODELLING	20
2.1 Hydraulic transient analysis	20
2.2 Treatment of the primary flow circuit	23
2.3 Driving pressure in natural circulation	28
CHAPTER III : THERMAL MODELLING	31
3.1 Transient temperature distribution	31
3.2 Steady state natural convection (Thermosyphon) cooling	44
CHAPTER IV : NUMERICAL ANALYSIS OF THE SYSTEMS OF BOUNDARY LAYER DIFFERENTIAL EQUATIONS	59

LIST OF TABLES

	<u>Page</u>
TABLE I : Flow coastdown results	
TABLE II : Numerical results of the solution of system of equation (4.2.1)	78
TABLE III : Nusselt Number for isothermal and non-isothermal surface conditions on the fuel rod ($a=0.0$, $a=0.1$)	81
TABLE IV : Nusselt number for non-isothermal surface conditions on the fuel rod ($a=0.5$, $a=2.5$)	82

LIST OF FIGURES

	<u>Page</u>
Fig. 1.1 Vertical open thermosyphon	6
Fig. 1.2 Vertical closed thermosyphon	6
Fig. 1.3 Closed loop thermosyphon	6
Fig. 1.4 Schematic diagram for primary coolant circuit	15
Fig. 2.1 Flow channel	21
Fig. 2.2 Flow coastdown curve	27
Fig. 3.1 Sinusoidal heat flux distribution in the core	34
Fig. 3.5 A typical triangular lattice	45(s)
Fig. 3.6 Co-ordinate system	45(s)
Fig. 3.7 Buoyant force along the curved surface	45(s)
Fig. 4.1 Velocity distribution in the boundary layer	83
Fig. 4.2 Distribution of shear in the boundary layer	84
Fig. 4.3 Temperature distribution in the boundary layer	85
Fig. 4.4 Variation of temperature gradient	86
Fig. 4.5 Perturbations to the velocity ($X_2' \sim \eta$) curve	87

	<u>Page</u>
Fig. 4.6 Perturbations to the temperature ($Y_2 \sim \eta$) curve	88
Fig. 4.7 Perturbations to the velocity ($X'_3 \sim \eta$) curve	89
Fig. 4.8 Perturbations to the temperature ($Y_3 \sim \eta$) curve	90
Fig. 4.9 Isothermal surface condition on the fuel rod ($a = 0.0$)	91
Fig. 4.10 Non-isothermal surface conditions on the fuel rod (for $a = 0.1$)	92
Fig. 4.11 Non-isothermal surface condition on the fuel rod (for $a = 0.5$)	93
Fig. 4.12 Non-isothermal surface condition on the fuel rod (for $a = 2.5$)	94
Fig. 5.1 Flow chart of the main program	108
Fig. 5.2 Flow chart of the integration subroutine.	109

SYNOPSIS

In this study, hydraulic and thermosyphon models are formulated to investigate the transient and steady state flow and, thermal behaviour of a CANDU Reactor core in the event of loss-of-flow accidents, resulting from pumping failures. The hydraulic analysis leads to a flow coastdown, which determines mass flow rate versus time. The transient temperature behaviour is evaluated next. In view of safety assessment following the transients, major attention is directed towards the performance of thermosyphoning (Natural convection) effects in the vicinity of a horizontal cylindrical fuel rod to extract the after heat due to the decay of fission products, under both isothermal and non-isothermal surface conditions on the fuel rod. It is found that natural convection Nusselt number is approximately one-fifteenth of the forced convection (for coolant velocity 27.2 ft/sec) value. Furthermore, the surface temperature variation has a significant effect on the heat transfer from the fuel rod.

CHAPTER I

INTRODUCTION

1.1 SAFETY OF POWER REACTORS

The thorough safety assessment of a nuclear power plant necessarily involves consideration of the potentiality and consequences of a large number of reactor accidents, ranging from minor mishaps to truly catastrophic events. In recent years the efforts associated with assuring the safety of large nuclear power reactors has accelerated rapidly. The specifics of the accidents sequences that must receive attention depend strongly on reactors concept and on the details of design and operation of heat transport system, fission product barriers and safety systems. Among broad categories of reactor accidents, loss-of-flow accidents (LOFA) encompass one of the most conceivable nuclear power plant accidents.

Loss-of-flow accidents can result either from pumping failures or from obstruction in coolant loops. Flow obstructions are most likely to lead to local flow starvation in the core, whereas pumping failures are most likely to affect a major part or all of the core. Pumps, however, are normally in active state of operation and they are subject to rapid failure either from mechanical seizure or from power failure. A catastrophic mechanical seizure of pumps may occur nearly

instantaneously, causing a precipitous drop of the pump head to zero. But, pump failure due to loss of power does not result in an instantaneous loss of head, since even if pump motor suddenly fails, the rotational inertia of the pump impeller and flywheel cause the pump to coastdown gradually over a period of time that is often of the order of several seconds.

In loss-of-flow accidents, caused by a power failure to the all coolant pumps, the pressure drop across the core decreases, causing decreased mass flow rates and increased core temperature. Flow starvation may also take place, if there is an increase in the core hydraulic loss coefficient. Flow decrease results in deterioration of the heat transfer coefficient and coolant flow rate. As a result, the elevation of the coolant temperature may lead to a boiling crisis and subsequent insulation of the fuel element from the coolant. The equilibrium flow following the transient is quite small, since it is driven only by natural circulation. Thus, the most important action to be taken in the majority accident situations is the prompt shutdown of the nuclear chain reaction. This action rapidly reduces the power to the level of decay heat and therefore greatly alleviates the energy dissipation problem under adverse condition. .

Once reactor shutdown is achieved immediately, the primary problem is to assure an orderly path of removal of

decay heat. Otherwise, the energy imbalance would eventually lend to the meltdown of core and cause penetration of the primary system. Thus, a major engineered safety feature of any nuclear power plant is the emergency core cooling system. Equally important, in the event of a loss-of-flow accident is that, continuous core cooling must also be provided over a period of time required to actuate emergency core cooling system or in situations when emergency core cooling is not immediately available. The rate of decay heat production during this period after shutdown may still be capable of melting fuel elements.

Under such circumstances, thermosyphon system is extremely important and capable of transmitting fairly large rates of heat transfer in the earth's gravitational field. It determines amount of core cooling immediately available, even if the driving pressure following the transient fails to sustain natural circulation of coolant in the primary flow circuit. The reactor core consists of a number of flow channels, acts as a system of thermosyphons and provides essential cooling required during such emergent situations. A study of the thermosyphon systems reveals the nature of physical phenomena associated with the process of heat transfer.

1.2 THERMOSYPHON SYSTEM

The heat transfer system which has become known as the thermosyphon has many applications in engineering, ranging

from its' use in Bakers' oven to the cooling of turbine rotor blades, internal combustion engines and nuclear reactors. A thermosyphon is a circulating fluid system, whose motions are caused by density differences in a body force field. Davis and Morris [1] have suggested that thermosyphon can be categorized according to (i) nature of boundaries (whether the system is open or closed to mass flow), (ii) the regime of heat transfer (whether the process is purely natural convection or mixed natural and forced convection) and (iii) the nature of the body force (gravitational or rotational). The thermosyphon system has an intrinsic function of removing heat from a prescribed source and transferring heat and mass over a specific path (frequently a recirculation flow) and rejecting heat and mass to a prescribed sink. These flows are intrinsically driven by thermal buoyancy forces either locally or in overall sense. A simple loop flow may be the result of local buoyancy forces, but a multibranched flow circuit may easily incorporate sections in which the flow direction is contrary to the local buoyancy forces resulting from the pressure created by the overall system buoyancy forces.

The classification of thermosyphon systems mainly includes:

- (1) A common single phase, natural convection open system in the form of a vertical tube open at the top and closed at the bottom.

- (2) A simple single phase natural convection closed system in the form of a vertical tube closed at both ends.
- (3) The single phase closed loop thermosyphon.

Vertical Open Thermosyphon :

The vertical open thermosyphon as shown in Fig. 1.1 provides the starting point for considering thermosyphon systems. As can be noted that, the primary effect of heating the wall of an open thermosyphon should be to cause some type of flow upward along the wall due to the buoyancy effects and an associated return flow downward in the core via the law of continuity. It has been found that for large heat fluxes on the wall (as may be the case of nuclear reactors), the buoyancy forces are sufficiently intense near the wall so that a boundary layer regime is obtained. On the other hand for weaker heat fluxes, the buoyancy forces are less and the effect of shear is relatively enhanced owing to small inertial effects, causing the boundary layer to try to fill the entire tube. Hence, compared to the ordinary boundary layer flow, the flow is impended. For sufficiently weak fluxes this effect is found to be rather uniform and a similarity flow is observed. The first experiments on an open vertical thermosyphon were reported by Foyle [2], but those were of limited extent. His observations show that the heat transfer was independent of tube length beyond a certain critical value although, it increases quickly with increasing diameter of the tube. He also pointed out that, for increasing values of length to diameter ratio (L/a), larger values of Rayleigh number

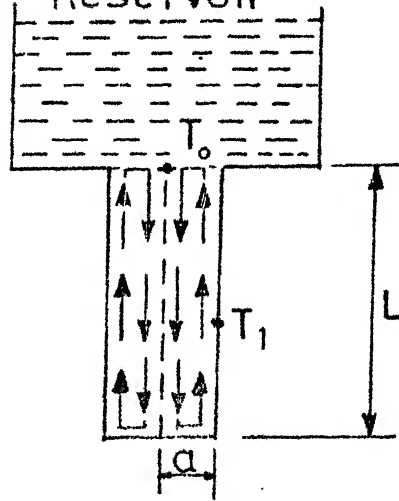


Fig.1.1 Vertical open thermosyphon

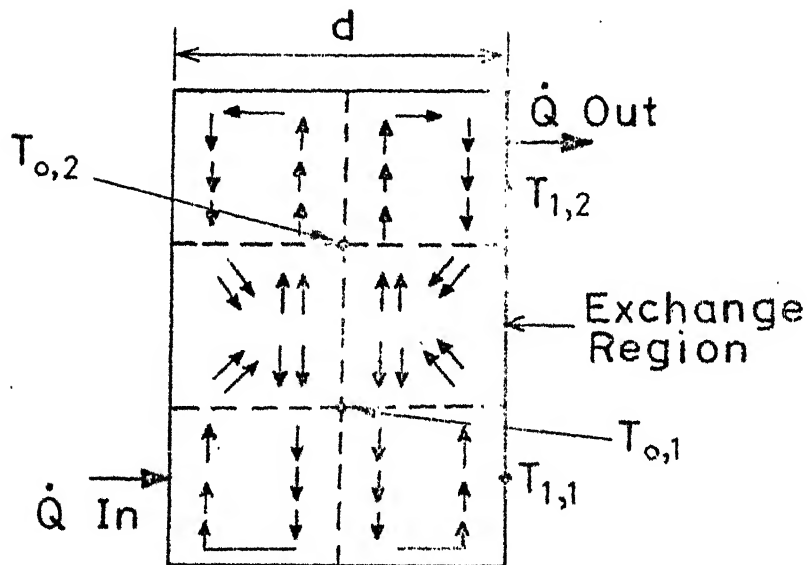
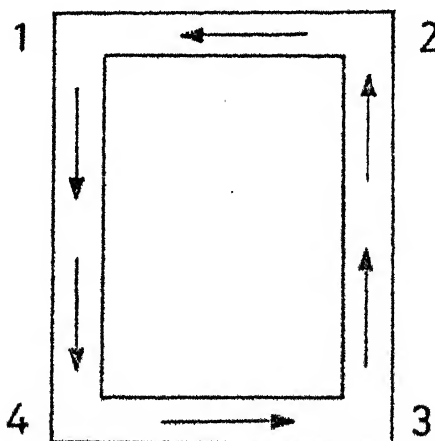


Fig.1.2 Vertical closed thermosyphon



are required to attain any given heat flux level.

Vertical Closed Thermosyphon :

The simple closed vertical thermosyphon as shown in Fig. 1.2 gained popularity as the problem of containment and pressurization became apparent in various application of open thermosyphon. It consists of a fluid completely enclosed in a tube situated in a body force field and lying parallel to the direction of the body force. Heat is applied to the 'lower' part of its length and cooled over the upper part, thus producing flow patterns as shown in Fig. 1.2. Referring to the figure, the first subscripts 0 and 1 associated with the temperature indicate core region and wall respectively. The second subscripts 1 and 2 refer to the top and bottom region of the thermosyphon. \dot{Q} gives the heatflow. It has been found that, when closed thermosyphon modelled carefully, it can be treated as a synthesis of two simple open thermosyphons approximately, joined at the mid tube exchange (coupling) region. Most of the modes of flow found for the open thermosyphon have been found for the closed thermosyphons. Primary problem concerned with the closed thermosyphon is that of modelling the exchange region i.e. to find temperatures T_{01} and T_{02} , to apply open thermosyphon results. For lower values of temperature difference between the bottom and upper wall, the exchange mechanism was found to be basically convective and for higher values, the convective process is less stable and degenerates to a mixing exchange process.

Closed Loop Thermosyphon :

A simple closed loop thermosyphon shown in Fig. 1.3 is a similar geometric configuration, which can be found in many industrial situations. The virtue which made closed loop thermosyphon interesting is that, it avoids chocking that occurs in open thermosyphon and diminishes exchange process as occurs in open and closed thermosyphons. The core boundary layer interaction is also minimized. In principle, there is no limit to the types of flow that could be obtained in a closed loop thermosyphon, subject to various thermal, geometric and body force conditions. Under the condition of rotation of this configuration, for a given temperature difference between the wall and the coolant, gives a strong increase to the heat transfer coefficient. The better known application of closed loop thermosyphon, is cooling of internal combustion engines and nuclear reactors, when driving pressure establishes a natural circulation.

1.3 REVIEW OF LITERATURE

The vertical thermosyphon systems and its various applications in engineering has been the subject of a good deal of research in recent years, although, probably because of the complexities of thermal buoyancy forces and their dependence on geometrical configurations and flow regimes, little attention has been given to it in its horizontal form. More attention has been directed towards the open thermosyphon in which the heated lower region opens at the top into a large reservoir of fluid

from which heat is removed by allowing evaporation to occur. Cohen and Baley [3], reported a number of such experiments using both static and rotating apparatus, concentrating mainly upon the evaporative system. The original application of this system to turbine cooling was given by Schmidt [4]. Experimental investigation to remove heat from the reservoir by means of an immersed cooling coil was carried out by Cohen and Hartnett et al. [5,6]. Under these conditions, it was found that, the fluid returning from the reservoir has free access to the "core" of the thermosyphon.

The analytical study presented by Lighthill [7] has served as the foundation for most vertical thermosyphon analyses (laminar) upto the present time. His treatment of flow in the open thermosyphon yielded three laminar flow regimes, depending upon wall heat fluxes. He considered basic laminar boundary layer flow equations for an open circular thermosyphon with variable fluid properties as follows :

$$\frac{\partial(\rho u R)}{\partial x} + \frac{\partial(\rho v R)}{\partial R} = 0 \quad (1.3.1)$$

$$u \frac{\partial u}{\partial x} + v \frac{\partial u}{\partial R} = -g - \frac{1}{\rho} \frac{\partial p}{\partial x} + \frac{1}{r R} \frac{\partial}{\partial R} (R \mu \frac{\partial u}{\partial R}) \quad (1.3.2)$$

$$\frac{\partial p}{\partial R} = 0 \quad (1.3.3)$$

$$u \frac{\partial(C_p T)}{\partial x} + v \frac{\partial(C_p T)}{\partial R} = \frac{1}{r R} \frac{\partial}{\partial R} (R K \frac{\partial T}{\partial R}) \quad (1.3.4)$$

$$\rho_1 = \rho [1 + \beta (T - T_1)] \quad (1.3.5)$$

where, u , v are velocities in x and R directions respectively, g is gravitational acceleration. K , P , β , ρ , C_p and μ are thermal conductivity, pressure, coefficient of thermal expansion, density, specific heat and dynamic viscosity respectively. Subscript 1 refers to the bottom of the thermosyphon.

With these equations, he treated the case of $Pr = \infty$, and thus neglecting the inertial terms after non-dimensionalizing the equations and estimated that, the analyses would give only 10 % error for $Pr = 2$. For different values of wall heat fluxes at the bottom of the thermosyphon, he used Blasius-Howarth Series solution to solve the problem. He finally established theoretically the existence of boundary layer flow regimes for large heat fluxes, impeded flow regimes for weaker heat fluxes and similarity flow regimes for sufficiently weak fluxes. Martins' [8] experimental results provided an excellent verification of Lighthills' flow models. His local heat transfer results for lower values of wall heat flux also verified the existence of laminar impeded regimes and similarity regimes.

Lighthill [7] again considered that the closed vertical thermosyphon system could be treated as a synthesis of open systems coupled together hydrodynamically in some manner by a region of limited extent. He suggested that complete mixing of the opposite streams in the coupling region would probably be a reasonable approximation. But it was left to Bayley and Lock [9], who made the first comprehensive experimental and analytical study of the closed thermosyphon. Their attempt was to analyse

the system for the laminar boundary layer regime. They found that, in each section of the tube a thin laminar boundary layer was formed adjacent to the tube wall, thus producing a central core of fluid which moves slowly in the opposite direction. Three limiting possibilities were suggested for the manner in which the open systems were coupled together depending upon the fluid properties. Those were :

- (1) The violent collision of the axially converging boundary layers giving rise to vigorous mixing.
- (2) The non-interactive crossing over of the boundary layers, each becoming the core of the opposite section.
- (3) The return of each boundary layer to its own section; thermal energy is thus transferred across the coupling region by axial conduction only.

They theoretically treated the above mentioned hydrodynamic couplings of the mid tube exchange mechanism and determined the effect of Prandtl number on heat transfer rates. Considering the integral form of the energy and momentum equation as cited below,

$$\nu \left(\frac{\partial u}{\partial y} \right)_o = \beta g \delta \int_0^1 (T - T_1) d(y/\delta) - \frac{d}{dx} \delta \int_0^1 u^2 d(y/\delta) \quad (1.3.6)$$

$$K \left(\frac{\partial T}{\partial y} \right)_o = - \frac{d}{dx} \delta \int_0^1 u (T - T_1) d(y/\delta) \quad (1.3.7)$$

where, δ is the boundary layer thickness. Other notations have their usual meaning and subscripts 'o' and '1' refer to wall and core respectively.

The approach developed by them permitted solutions to be obtained for vertical tubes of almost any cross section and including all fluid for which $1 < Pr < \infty$. The method is based on the assumptions that, the two dimensional form of the boundary layer equations are approximately valid near the tube wall and using VonKarman - Pohlhausen technique, they obtained the following expressions.

$$(\bar{Nu}_d)_H = 0.677 \left(\frac{Pr(t_d)_H}{Pr + 20/21} \right)^{1/4} \times \left\{ 1 - \frac{1}{0.382 \left(\frac{Pr(t_d)_H}{Pr + 20/21} \right)^{1/4} - 2} \right\} \quad (1.3.8)$$

for an isothermal wall and,

$$(\bar{Nu}_d)_H = 0.862 \left(\frac{Pr(t_d)_H}{Pr + 4/5} \right)^{1/4} \times \left\{ 1 - \frac{1}{0.410 \left(\frac{Pr(t_d)_H}{Pr + 4/5} \right) - 2} \right\}^{1/4} \quad (1.3.9)$$

for a uniformay heated wall. Subscripts 'd' and 'H' refer to the diameter and heated section respectively and t_d is the modified Rayleigh number.

Japikse and Winter [10] pointed out that, the wall temperature on each tube half should be used to model the flow processes in that tube half. This is of considerable importance to avoid error in heat transfer rates, in situations where non-isothermal wall condition exists.

However, the application of the above studies, mostly dealing with "vertical" thermosyphons are basically confined only to Light Water Reactors (LWR). Boiling Water Reactors (BWR) a

specific case of LWRs, have a vertical core configuration and easily actuate vertical thermosyphon cooling processes in the event of flow failure accidents. On the other hand, thermosyphoning for fluid enclosed in a horizontal tube or channels situated in a body force field and lying perpendicular to the direction of the body force on a horizontal plane, is known very little. Thus, for "horizontal" reactor core configuration e.g. CANDU Reactor (RAPP), this aspect is of considerable importance to assess the safety features involved in thermosyphon cooling in flow failure accidents.

No literature, however, found available, explicitly treating horizontal thermosyphon systems in the gravitational force field. Since, thermosyphoning is closely associated with natural convective heat transfer processes, some insight can be gained by reviewing natural convection processes around the horizontal objects.

For laminar flow around horizontal cylinders, Hyman et al. [11] found that the following equation for the average Nusselt number correlated data well for water, toluene, silicon, mercury etc.

$$\bar{Nu}_D = 0.53 \left[\left(\frac{Pr}{Pr + 0.952} \right) (Gr_D \cdot Pr) \right]^{1/4} \quad (1.3.10)$$

In some cases of horizontal cylinder, the entire surface may not be parallel to the body force caused by gravity. The variations of the angle between the surface and gravity vector was considered by Herman [12], who derived an equation for the local Nusselt number at various positions around a horizontal cylinder for air

(Pr = 0.74). The equation is

$$Nu_D = 0.604 Gr_D^{1/4} \phi(\theta) \quad (1.3.11)$$

The function $\phi(\theta)$ depends upon the value of θ , measured from the bottom of the cylinder. An integral approach to this problem by Levy [13] and a similarity solution approach by Eckert and Soehngen [14], also agree well with the calculated values by Herman.

On the basis of the foregoing reviews, the prime objective in the present investigation is to determine, thermosyphoning effects, to provide immediate core cooling in Reactors of horizontal core systems in the event of loss-of-flow accidents. A typical example is the CANDU (RAPP) type Reactor.

1.4 DESCRIPTION OF CANDU REACTOR SYSTEM

CANDU is a heavy water moderated pressurized heavy water cooled, UO_2 fuelled pressure tube reactor. The reactor has a horizontal cylindrical tank and tube assembly. This assembly is known as calandria. Natural Uranium in the form of pressed pellets is sheathed in Zircaloy tubes to form cylindrical fuel elements. Nineteen such elements are assembled to form a fuel bundle. Calandria tube contains thick walled coolant tube having a fuel bundle and primary coolant i.e., heavy water at high pressure. The calandria shell contains heavy water at high pressure and it is used as a moderator.

Heavy water essentially serves two purposes, namely as a moderator and as a coolant, each having its own closed

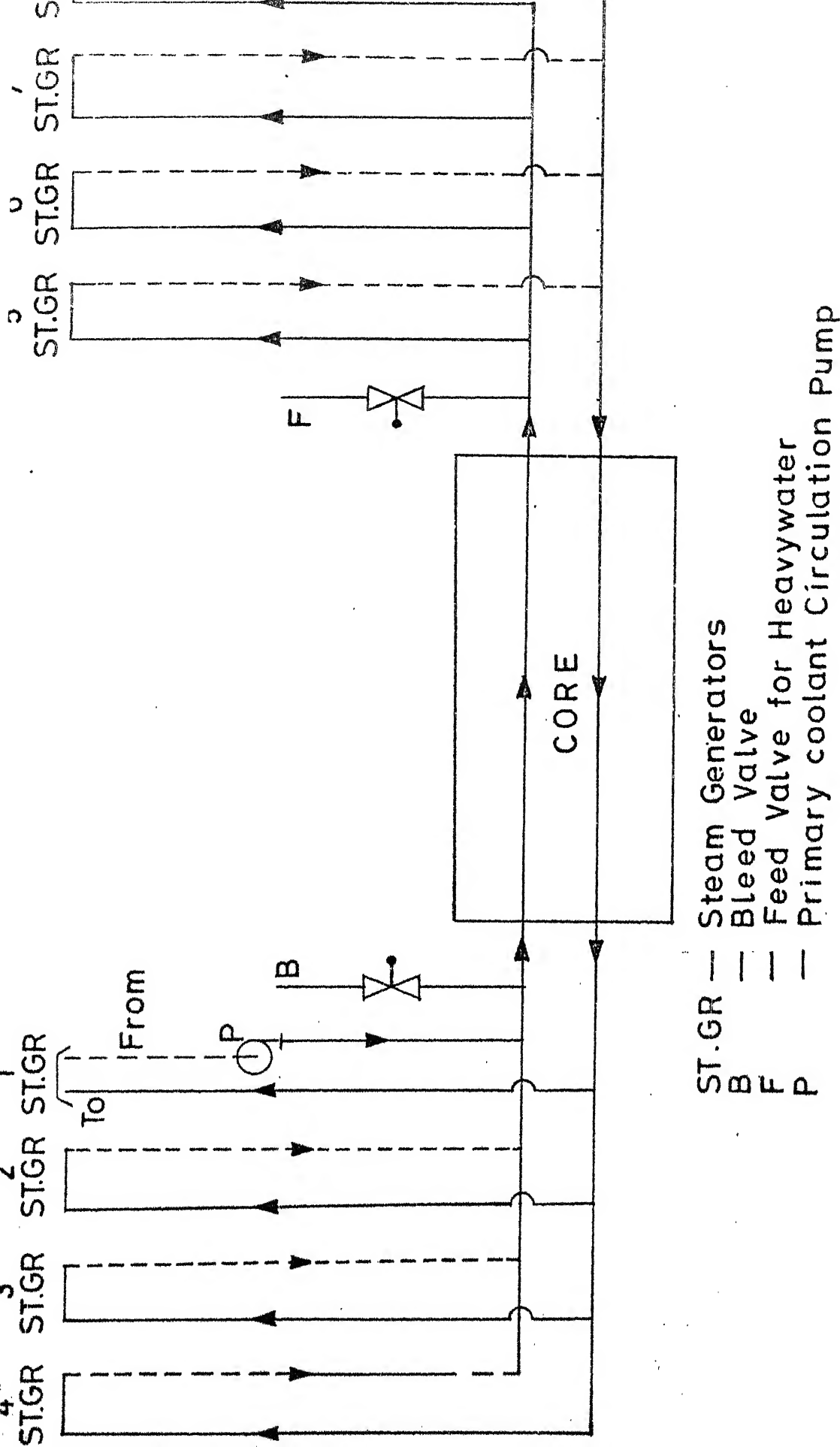


Fig.1-4 Schematic Diagram for Primary Coolant Circuit

circulating system. The fuel coolant system is called primary heat transport system is a high pressure and high temperature circuit with no bulk boiling. But, the moderator circuit is a low temperature low pressure circuit. Both circuits are insulated from each other in the reactor core by a gas annulus between the calandria tube and coolant tube.

Heat generated in the fuel elements is transferred to heat exchangers in the primary heat transport system, where the heat is utilized to generate steam in a secondary coolant system, consists essentially of two identical loops in series, one at each end of the reactor. Four boiler assemblies and four pumps in parallel are included in each loop. The primary coolant is circulated through alternate coolant tube assemblies in opposite directions. Each boiler assembly consists of ten vertical U type tubes and shell heat exchangers in parallel and a steam drum. The hot heavy water from the reactor enters the tube sides of the heat exchangers at the bottom of their recirculating sections. Then it returns from the bottom of the preheater legs of the heat exchangers to the reactor. Schematic diagram of the primary flow circuit is shown in Fig. 1.4.

The secondary coolant system consists of boiler feed-water entering the shell side of each heat exchanger at the bottom of the preheat leg. The feedwater is heated near to the saturation temperature. As a result, it boils in the upper portion of the leg and enters the steam drum above it. Water and steam are separated here. The water at saturation temperature flows through

downcomers to the bottom of heat exchanger recirculating leg, where it boils and returns to the steam drum. Saturated steam is supplied to the turbine unit. Discharge valves are provided in the steam mains to release steam to dump condenser in the case of pressure rise in steam drum. Such a facility is provided, in the case turbine is unable to accept enough steam. The turbine and reactor have adequate controls for safety and smooth operation of the power plant.

1.5 SCOPE OF THE THESIS

Scope of the present work is mainly centered on the investigation of thermosyphoning effects in CANDU Reactor System. It determines amount of core cooling immediately available as an essential safety requirement in loss-of-flow accidents particularly, in situations, when emergency core cooling is not immediately available and equilibrium driving pressure ceases to establish a natural circulation in the primary circuit. However, transient flow and temperature behaviours are also essential features of a loss-of-flow accident and must be evaluated prior to steady state analysis.

Under operating conditions the bulk of the fission product inventory remains trapped in the fuel. The fission products that escape from the fuel consists primarily of fraction of noble gases and other species of more volatile fission product. These collect in the fuel-cladding gap and in other void regions on the cladding envelope. Their existence may affect the gap

conductance and give rise to non-isothermal cladding surface conditions, resulting in a variation of steady state heat transfer across the surface.

In the investigation proposed here, the objectives will thus be to :

- (a) Study the flow coastdown during the transient, which determines decrease in mass flow rate with time.
- (b) Find out whether the driving pressure, following the total loss of pumping power can establish a natural circulation equilibrium flow in the primary circuit.
- (c) Determine the temperature distribution of the core during the transient and approximate evaluation of the time required to attain steady state.
- (d) Evaluate the important thermosyphoning (steady state natural convection) effect on the flow and heat transfer in terms of the distributions of velocity and temperature in the adjacent boundary layer regime of fuel elements, considering both isothermal and non-isothermal cladding surface conditions. Cases of linear and non-linear variations of surface temperatures are treated in non-isothermal conditions.

Obviously, detailed analysis of a project of this magnitude would be a lengthy one and requiring much time and effort. The analysis will thus be carried out only as far as is required to arrive at a qualitative conclusion for the objectives listed in items from (a) to (c). In the perspective of

thermosyphoning, listed in item (d), an asymptotic similarity solution of the equations of continuity, conservation of momentum and energy in the boundary layer regime will be sought by numerical methods for an axisymmetric, constant property, laminar boundary layer flow of a viscous, incompressible and newtonian fluid around a horizontal cylindrical fuel element. There is an arbitrary distribution of temperature on the surface of the fuel rod. Gravitational force field generates buoyancy forces responsible for thermosyphoning in the adjacent boundary layer.

For ease in formulation and analysis of the present problem as envisaged in the preceeding objectives, those may be mainly divided into two parts. The first part named as "Flow modelling", comprises first two objectives (a) and (b), which deals with transient and steady state flow behaviours in the primary system and the second part namely, "Thermal modelling" comprises rest two objectives (c) and (d), deals with transient temperature distribution in the core followed by thermosyphon cooling.

CHAPTER II

FLOW MODELLING

The determination of both transient and steady state flow behaviour following the transient, associated with reactor accidents, due to common mode power failure to pumps requires formulation of a hydraulic model for the reactor core and primary circuit. The mass flow rate versus time must be determined to gain an insight into the flow coastdown phenomena. Following the transient, equilibrium flow is quite small and driven only by natural circulation. It is required to verify that whether natural circulation can be sustained in the primary circuit.

2.1 HYDRAULIC TRANSIENT ANALYSIS

To accomplish objective (a) of Sec. 1.5, transient hydraulic analysis is formulated. Referring to Bird et al. [15] and Lewis [16]; control volume form of the continuity and mechanical energy balance equations in Eulerian frame are utilized to arrive at a relationship between mass flow rate and pressure drop for a flow channel.

Mass and mechanical energy balance equations are written as follows:

$$\frac{\partial}{\partial t} \iiint_{c.v.} \rho \, dV + \iint_{c.s.} \rho \hat{n} \cdot \vec{v} \, ds = 0 \quad (2.1.1)$$

$$\begin{aligned}
& \frac{\partial}{\partial t} \iiint_{c.v.} \left(\frac{1}{2} \rho v^2 \right) dV + \iint_{c.s.} \left(\frac{1}{2} \rho v^2 \right) \hat{n} \cdot \vec{v} ds \\
& = - \iiint_{c.v.} \vec{v} \cdot \nabla P dV + \iiint_{c.v.} \vec{v} \cdot \vec{g} dV - E_v + E_p \quad (2.1.2.)
\end{aligned}$$

where, ρ = fluid density, V = fluid volume, s = surface of the volume V , \hat{n} = outward normal to s , v = fluid speed, \vec{v} = fluid velocity, P = pressure, \vec{g} = gravitational force vector, E_v = Rate of mechanical energy dissipation due to viscous force and E_p = Rate of mechanical energy generation due to pump.

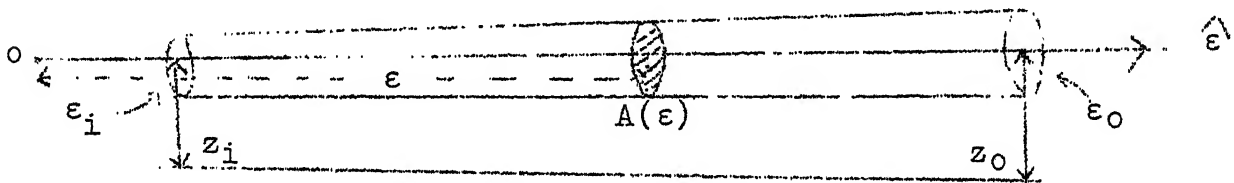


Fig. 2.1 : Flow channel.

Let us consider a specific flow channel as shown in Fig.(2.1). ϵ is the distance along the centreline and $dV = A(\epsilon)d\epsilon$, where $A(\epsilon)$ is channel area at ϵ . Fluid velocity, speed, density and pressure are considered function of ϵ and time.

$$v = v(\epsilon, t), \quad \vec{v} = \vec{v}(\epsilon, t) \hat{\epsilon}$$

$$\rho = \rho(\epsilon, t), \quad P = P(\epsilon, t)$$

Considering the volume V between an inlet ϵ_i and outlet ϵ_o , equations (2.1.1) and (2.1.2) may be written as

$$\frac{\partial}{\partial t} \int_{\epsilon_i}^{\epsilon_o} \rho(\epsilon, t) A(\epsilon) d\epsilon + \rho(\epsilon_o, t) v(\epsilon_o, t) A(\epsilon_o) - \rho(\epsilon_i, t) v(\epsilon_i, t) A(\epsilon_i) = - \int_{\epsilon_i}^{\epsilon_o} \vec{v} \cdot \nabla P dV + \int_{\epsilon_i}^{\epsilon_o} \vec{v} \cdot \vec{g} dV - E_v + E_p$$

$$\begin{aligned}
& \frac{\partial}{\partial t} \int_{\varepsilon_i}^{\varepsilon_0} \frac{1}{2} \rho(\varepsilon, t) v^2(\varepsilon, t) A(\varepsilon) d\varepsilon + \frac{1}{2} \rho(\varepsilon_0, t) v(\varepsilon_0, t)^3 A(\varepsilon) \\
& \quad - \frac{1}{2} \rho(\varepsilon_i, t) v(\varepsilon_i, t)^3 A(\varepsilon_i) \\
& = - \int_{\varepsilon_i}^{\varepsilon_0} v(\varepsilon, t) A(\varepsilon) \frac{\partial P(\varepsilon, t)}{\partial \varepsilon} d\varepsilon - g \int_{\varepsilon_i}^{\varepsilon_0} \rho(\varepsilon, t) v_z(\varepsilon, t) A(\varepsilon) d\varepsilon - E_v + E_p
\end{aligned}
\tag{2.1.4}$$

where, g is the magnitude of gravity vector and v_z vertical component of v .

In the absence of boiling, we can treat primary system flow transients by assuming incompressible flow, i.e. $\frac{\partial \rho}{\partial t} = 0$, which means that $\rho = \rho(\varepsilon)$. Time independence of ρ causes the first term of equation (2.1.3) to vanish, and we have

$$\rho(\varepsilon_0) v(\varepsilon_0, t) A(\varepsilon_0) = \rho(\varepsilon_i) v(\varepsilon_i, t) A(\varepsilon_i) \tag{2.1.5}$$

Since, ε_0 is arbitrary, it gives mass flow rate $\rho(\varepsilon) v(\varepsilon, t) A(\varepsilon) t$ to be independent of ε . Thus, mass flow rate at any point along the channel is given as

$$W(t) = \rho(\varepsilon) v(\varepsilon, t) A(\varepsilon) \tag{2.1.6}$$

Using these incompressible flow approximations and carrying out the mathematics involved, the expression for pressure drop follows from equation (2.1.4)

$$\Delta P = \frac{L}{A} \frac{dW}{dt} + \left[\left(\frac{\bar{\rho} \bar{A}}{\rho_0 A_0} \right)^2 - \left(\frac{\bar{\rho} \bar{A}}{\rho_i A_i} \right)^2 \right] \frac{W^2}{2 \bar{\rho} \bar{A}^2} + \bar{\varepsilon}_1 \frac{W^2}{2 \bar{\rho} \bar{A}^2} + \bar{\rho} g (z_0 - z_i) - \bar{\rho} g H_p
\tag{2.1.7}$$

where, $P = P_i - P_0$, $L = \varepsilon_i - \varepsilon_0$, $\bar{\rho} = \frac{1}{V} \int_{\varepsilon_i}^{\varepsilon_0} \rho(\varepsilon) A(\varepsilon) d\varepsilon$,

$$\frac{1}{\bar{A}} = \frac{\bar{\rho}}{L} \int_{\epsilon_i}^{\epsilon_o} \frac{d\epsilon}{\rho(\epsilon)A(\epsilon)}, \quad \bar{E}_v = \frac{E_v}{W(t)}, \quad H_p = \frac{E_p}{gW(t)},$$

ϵ_1 , is an empirical loss coefficient and subscripts 'o' and 'i' refer to outlet and inlet respectively.

The sum of contributions to the pressure drop come from inertial, viscous, hydrostatic and pump energy term respectively. Combining, viscous and acceleration pressure drop expressions, eqn. (2.1.7) can be written in a contracted form.

$$\Delta P = \frac{L}{\bar{A}} \frac{dW}{dt} + K \frac{W^2}{2\bar{\rho}\bar{A}^2} + \bar{\rho}g\Delta z - \bar{\rho}gH_p \quad (2.1.8)$$

where, $K = \bar{\epsilon}_1 + \left(\frac{\bar{\rho}\bar{A}}{\rho_o A_o}\right)^2 - \left(\frac{\bar{\rho}\bar{A}}{\rho_i A_i}\right)^2$, known as hydraulic resistance of the channel, and $\Delta z = z_o - z_i$.

2.2 TREATMENT OF THE PRIMARY FLOW CIRCUIT

The standard pressure drop and flow relationship given in equation (2.1.8) can be applied to CANDU system. Considering a simplified assumption that all pumps behave identically following a power failure and pump inertia following the loss of power is taken into account in the expression for pressure drop.

With the above assumption, the accident can be treated in terms of the reactor core and N identical coolant loops (The loop consists of series of paths through the hot and cold legs and the heat exchangers). Core is characterized by a loss coefficient K_c and flow area A_T . Each of the coolant loops has a loss coefficient K_1 and flow area A_1 . Normalized flow resistance i.e., $\bar{K}_c = K_c/A_T^2$ and $\bar{K}_1 = K_1/A_1^2$ are defined to eliminate flow area

from the pressure drop equation.

Excluding hydrostatic term for a horizontal core ($\because \Delta z = z_o - z_i = 0$) in the pressure drop relationship, we write core pressure drop as

$$\Delta P_c = \left(\frac{L}{A}\right)_c \frac{dW}{dt} + \bar{K}_c \frac{W^2}{2\bar{P}} \quad (2.2.1)$$

and for coolant loops

$$\Delta P_l = \left(\frac{L}{A}\right)_l \frac{dW_l}{dt} + \bar{K}_l \frac{W_l^2}{2\bar{P}} + g(\bar{P}\Delta z)_l + \bar{P}g \left(\frac{\omega}{\omega_o}\right)^2 H_p \quad (2.2.2)$$

Where, W_o and W_l are flow rates in the core and in each flow loop respectively. The term $\left(\frac{\omega}{\omega_o}\right)^2$ multiplies the initial pump head in order to approximate the decreasing speed of the pump during the transient. ω_o is the initial pump speed and ω is the decreasing speed during the transient.

Applying, Kirchoffs laws for pressure drop around any loop of the channel and hydraulic junction law for flows in a hydraulic circuit, we have :

$$\Delta P_c + \Delta P_l = 0 \quad (2.2.3)$$

$$W = NW_l \quad (2.2.4)$$

Now, combining expressions (2.2.1) and (2.2.2), we find that the core flow is determined from

$$\left(\frac{L}{A}\right)_p \frac{dW}{dt} + \bar{K}_p \frac{W^2}{2\bar{P}} + g(\bar{P}\Delta z)_p - \bar{P}g \left(\frac{\omega}{\omega_o}\right)^2 H_p = 0 \quad (2.2.5)$$

where for the primary system,

$$\left(\frac{L}{A}\right)_p = \left(\frac{L}{A}\right)_c + \frac{1}{N} \left(\frac{L}{A}\right)_1$$

$$\bar{K}_p = \bar{K}_c + \frac{1}{N^2} K_1 \quad \text{and} \quad (\bar{P} \Delta z)_p = (\bar{P} \Delta z)_1$$

Subscript p refers to primary circuit.

Hydrostatic head is small compared to pump head during the first stage of the transient and can be neglected from equation (2.2.5). It is only predominant after pump head vanishes at a later stage.

Referring to Burgreen [17] to model the pump speed, we write the equation of motion :

$$I \frac{d\omega(t)}{dt} = -c\omega^2(t) \quad (2.2.6)$$

subject to initial condition $\omega(t)|_{t=0} = \omega_0$ where, I is the moment of inertia of the pump, c is a loss coefficient relating to windage torque. Solution of (2.2.6) gives

$$\omega = \frac{\omega_0}{1 + t/t_p} \quad (2.2.7)$$

Where, $t_p = I/c\omega_0$ is the pump halftime. Substituting equation (2.2.7) in (2.2.5) and neglecting hydrostatic term in accordance with previous argument, we obtain

$$\left(\frac{L}{A}\right)_p \frac{dW}{dt} + \bar{K}_p \frac{W^2}{2\bar{P}} = \frac{\bar{P} g H_p}{(1 + t/t_p)^2} \quad (2.2.8)$$

subject to initial condition

$$K_p \frac{W_0^2}{2\bar{P}} - \bar{P} g H_p = 0 \quad (2.2.9)$$

The nonlinear differential equation can be written in terms of the normalized core flow utilizing the initial condition, as

$$t_1 \cdot \frac{d}{dt} \left(\frac{W}{W_0} \right) + \left(\frac{W}{W_0} \right)^2 = \frac{1}{(1 + t/t_p)^2} \quad (2.2.10)$$

where, $t_1 = \frac{2 \bar{P}}{W_0 \bar{K}_p (\frac{A}{L})_p}$ designated as loop halftime.

A solution of equation (2.2.10) gives the flow coast-down relation in terms of the normalized flow as a function of time. For CANDU reactors designed with sufficiently large flywheels, the pump inertia may be made much larger than that of the fluid, and hence $t_p \gg t_1$. If this is the case, the normalized flow rate varies much slowly with time and it is reasonable to neglect the time derivative in equation (2.2.10). This approximately gives flow coastdown by

$$\frac{W}{W_0} = \frac{1}{1 + t/t_p} \quad (2.2.11)$$

For a typical recirculation pump, the pump halftime, t_p is calculated to be 5 seconds. Table I gives numerical results of variation of normalized flow with respect to time, normalized with pump halftime, using relation (2.2.11). A flow coastdown plot of these results is given in Figure (2.2).

When t_1 and t_p are of the same order of magnitude, a solution of nonlinear equation (2.2.10) must be sought. As such, no standard method in terms of elementary functions found applicable to it. Some aspects of the solution is given in Appendix A.

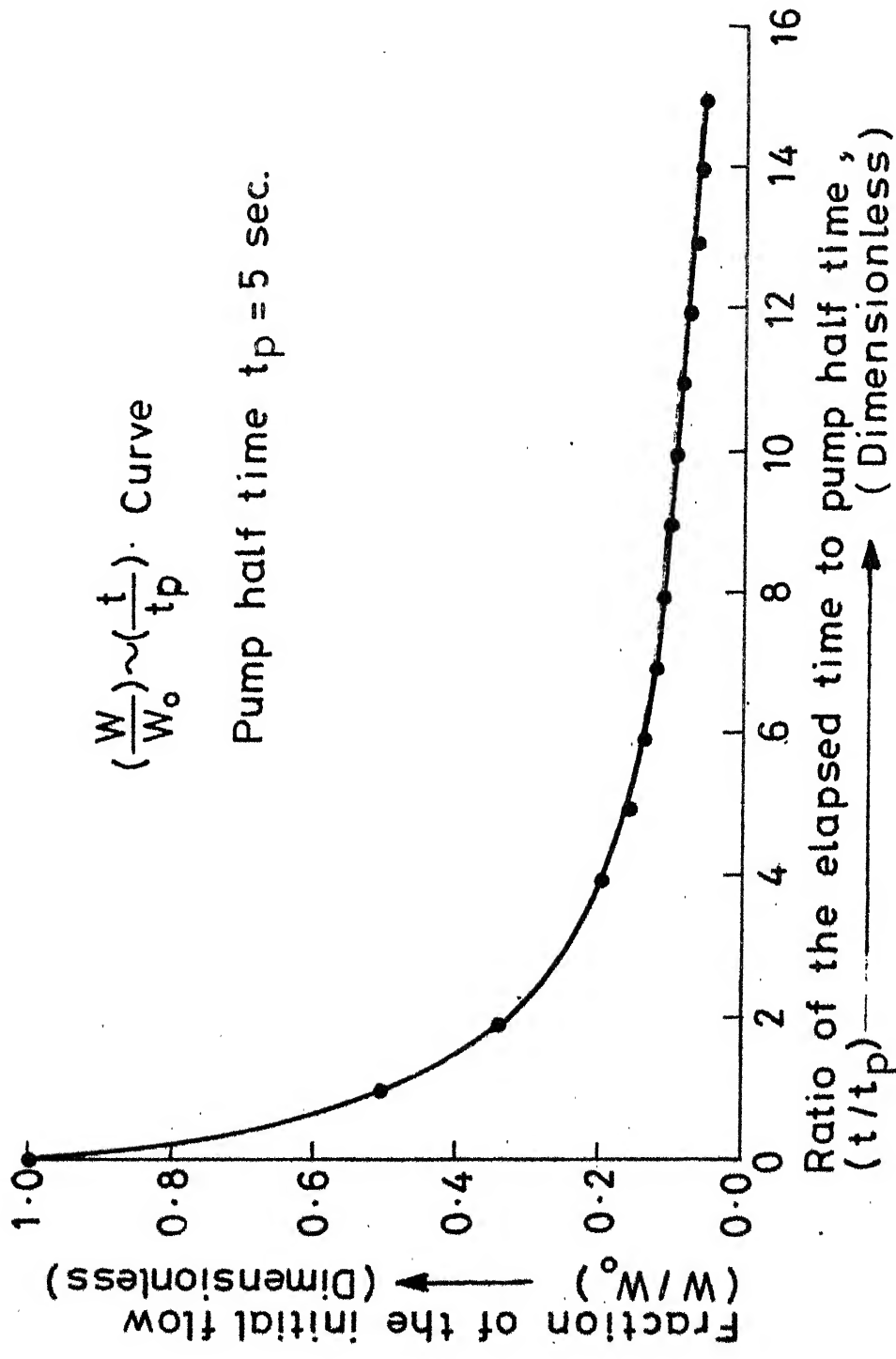


Fig. 2.2 Flow coast-down curve

Table I

(Flow Coastdown Results)

Pump Halftime = t_p = 5 sec.

Ratio of the elapsed time to the pump halftime, (t/t_p)	Fraction of initial flow, W/W_0 (Normalized flow)
0	1.0
1	0.5
2	0.33
3.	0.25
4	0.20
5	0.16
6	0.14
7	0.12
8	0.11
9	0.10
10	0.09
11	0.08
12	0.076
13	0.071
14	0.066
15	0.062

2.3 DRIVING PRESSURE IN NATURAL CIRCULATION

The second important aspect in flow modelling i.e., objective (b) Sec. 1.5, is to verify whether natural circulation can be sustained in the primary circuit following the total loss of pumping power. Because of the density differential between the coolant in the downcomer and that in the riser, a driving pressure is established. Provided the reactor is shutdown fast enough to prevent any damage, a central question then becomes whether an equilibrium state can be established for natural circulation to remove decay heat.

To establish such an equilibrium state the driving pressure must equal to the total system losses at the desired rate of flow of coolant in the channel. This must be verified. Following El-Wakil [18], the system losses are given by

$$\sum \Delta P = \sum \Delta P_f + \sum \Delta P_a + \sum \Delta P_r \quad (2.3.1)$$

Where, $\sum \Delta P$ = Total pressure losses in lbf/ft²,

$\sum \Delta P_f$ = Sum of frictional pressure losses, in core riser and downcomer,

$\sum \Delta P_a$ = Sum of the acceleration pressure losses,

$\sum \Delta P_r$ = Sum of the pressure losses due to resistance to flow such as, due to drag of submerged bodies like spacers, fuel element handle etc.

The total system losses found out from RAPP data is 1.413 lbf/in². The driving pressure may be evaluated as follows:

$$\begin{aligned} \Delta P_d &= (\text{hydrostatic pressure in downcomer}) \\ &\quad - (\text{hydrostatic pressure in riser}) \\ &= \bar{\rho}_d H \frac{g}{g_c} - \bar{\rho}_r H \frac{g}{g_c} = (\bar{\rho}_d - \bar{\rho}_r) H \frac{g}{g_c} \end{aligned} \quad (2.3.2)$$

where, H is the height of the downcomer as well as the riser and $\bar{\rho}_d$, $\bar{\rho}_r$ are mean densities in the downcomer and riser respectively. g is the gravitational acceleration and g_c is the conversion constant.

In standard gravity $g/g_c = 1.0$. Substituting corresponding values in equation (2.3.2), ΔP_d is found out to be 26.31 lbf/ft^2 i.e., 0.182 lbf/in^2 .

Now, in the case the computed driving pressure being less than the total system losses, the coolant rate of flow decreases and natural circulation cannot be sustained. The flow **ultimately** comes to a stagnation as the steady state is attained.

CHAPTER III

THERMAL MODELLING

A comprehensive analysis of the problem of thermal modelling for a reactor core under accident conditions and steady state immediately following the transient, frequently requires the numerical solution of large systems of partial differential equations for transient heat conduction, fluid flow, transient and steady state convection and a host of other phenomena likely to occur during and after the course of a transient. Simple lumped parameter models basing on energy balances, however, often provides sufficient accuracy when the primary objectives are to gain an understanding of the interaction of various phenomena involved and to make rough estimates of the consequences of the accident. But, the present formulation of the problem largely revolves around two important aspects, namely, the transient temperature distributions in the core and steady state thermosyphoning cooling effects following the transient, which is of paramount importance in view of safety assessment.

3.1 TRANSIENT TEMPERATURE DISTRIBUTION

Accurate description of the temperature distribution that appear in the reactor core under accident conditions requires that the time dependent mass, momentum and energy balance conservation equations to such situations, Mayer [20], must be solved successively by numerical methods. The complexity in the process of solution is due to the time involvement and

severe nonlinearity for the presence of convective terms in the inertial force expression. This can be further aggravated owing to the reactivity effects through temperature feedback.

For the present investigation as proposed in the objective (c) sec. 1.5, we try to formulate a simple transient conduction analysis to arrive at an expression for the solution of this equation subject to given boundary conditions. In the process, we shall deal with the analytical method to derive a solution, in order to gain an insight into the procedure of solution for non-homogeneous boundary conditions. Limited resources of data and inadequate informations regarding the boundary conditions of the reactor core during the process of transient, puts a constraint for arriving at a complete solution of the problem. The analytical treatment will be general, and a solution can be immediately sought, once the required boundary conditions are known.

In the case of very severe transients, the analytical technique may not provide the desired accuracy due to large changes in fuel temperature and coolant conditions. This fact coupled with obvious complexities of analytical technique and availability of digital computers has led to an increased use of numerical techniques. The mathematical apparatus required for the finite difference

solution of parabolic equation of heat conduction type and required convergence criteria for explicit finite difference solution was comprehensively treated by Crank and Nicholson [21].

In treating the problem of transient temperature distribution in the reactor core by a conduction analysis, some simplifying assumptions are made.

These are :

1. The radial dimension of the fuel bundle placed in the core is small compared to the axial i.e. horizontal dimension.
2. While the axial heat flux distribution (i.e. volumetric thermal energy) in the core varies sinusoidally, the radial distribution shows relatively small changes. Thus, the neutron flux and consequently the volumetric thermal source strength q''' , are considered as functions of only the axial coordinate.
3. It will be also assumed that the physical properties of the coolant and the fuel (e.g. density, specific heat, thermal conductivity) remain constant and independent of temperature.
4. Core is considered to be of constant cross-sectional dimension.

The sinusoidal core heat flux distribution can be utilized to find out the initial temperature distribution in the core with the help of the boundary conditions at the inlet and outlet prior to the transient. The volumetric thermal energy distribution is shown in Fig. 3.1. The distribution is of sine form with respect to the origin situated at the inlet and positive axial co-ordinate is taken towards the outlet. T_1 and T_2 are the inlet and outlet temperatures respectively, prior to the transient. Their numerical values are quoted in Appendix III. These values refer to the reactor conditions during steady state operation i.e. prior to the initiation of transients.

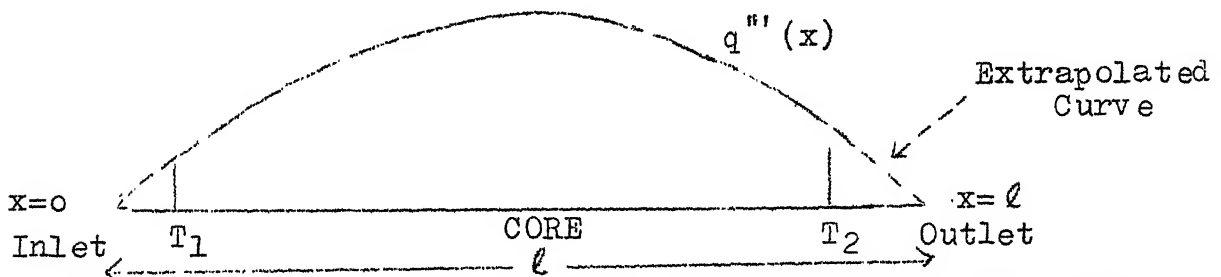


Fig.3.1: Sinusoidal Heat flux distribution in the core.

The total length of the core is considered to be $l = 16.404$ ft. (This includes extrapolation distance.) Under transient conditions with an initial sinusoidal volumetric thermal energy distribution in the axial direction, the general conduction equation for heat flow considered only in one dimension (i.e. one space variable) assumes the well known form.

$$C_p \rho \frac{\partial T(x,t)}{\partial t} = K \frac{\partial^2 T(x,t)}{\partial x^2} \quad (3.1.1)$$

where, t represents time, x axial coordinate, C_p specific heat, ρ density and K thermal conductivity and $T(x,t)$ is the temperature distribution. The initial volumetric thermal energy distribution assumes the following form

$$q'''(x) = q_0''' \sin\left(\frac{\pi x}{\ell}\right) \quad (3.1.2)$$

where, q_0''' is the peak value of the thermal energy inside the core.

The initial and boundary conditions to this boundary value problem is stated as follows:

$$T(0, 0) = T_1 \quad \text{at } t = 0 \quad (3.1.3)$$

$$T(\ell, 0) = T_2$$

$$T(0, t) = \alpha_1(t) \quad \text{for } t > 0 \quad (3.1.4)$$

$$T(\ell, t) = \alpha_2(t)$$

A complete solution of the present formulation to evaluate the transient temperature distribution i.e. seeking a particular solution to the conduction equation demands that the functions $\alpha_1(t)$ and $\alpha_2(t)$ should be explicitly

defined as a function of time. No experimental data or theoretical estimates of the nature of functions $\alpha_1(t)$ and $\alpha_2(t)$ during the process of transient is available. However, a general solution to the problem can be sought by analytical method such that the transient temperature behaviour during the course of flow transient can be known, if the functions $\alpha_1(t)$ and $\alpha_2(t)$ are specified.

Initial temperature distribution in the core :

The initial temperature distribution can be evaluated from the steady state conduction equation and thermal energy distribution, which represents a source factor.

Thus, from equation (3.1.1) and (3.1.2) for $t = 0$, we have

$$\frac{d^2 T(x,0)}{dx^2} + \frac{q_0'''}{K} \sin\left(\frac{\pi x}{\ell}\right) = 0 \quad (3.1.5)$$

Above equation integrates twice to give

$$T(x,0) = C_1 + C_2 x + \left(\frac{\pi}{\ell}\right)^2 \sin\left(\frac{\pi x}{\ell}\right) \quad (3.1.6)$$

where, C_1 and C_2 are constants of integration.

Initial temperature distribution at any position can be determined by evaluating these integration constants with the help of the conditions enumerated in eqn.(3.1.3).

This gives two simultaneous equations in two unknowns C_1 and C_2 .

$$\begin{pmatrix} 1 & 0 \\ 1 & \ell \end{pmatrix} \begin{pmatrix} C_1 \\ C_2 \end{pmatrix} = \begin{pmatrix} T_1 \\ T_2 \end{pmatrix}$$

which is solved to give,

$$C_1 = T_1 \quad \text{and} \quad C_2 = \frac{T_2 - T_1}{\ell}$$

Hence, from equation (3.1.6), the core initial temperature distribution follows as,

$$T(x, 0) = T_1 + \left(\frac{T_2 - T_1}{\ell}\right)x + \left(\frac{\pi}{\ell}\right)^2 \sin\left(\frac{\pi x}{\ell}\right) \quad (3.1.7)$$

Analytical method :

The complete boundary value problem will be:

$$\frac{\partial T(x, t)}{\partial t} = \frac{K}{\rho C_p} \frac{\partial^2 T(x, t)}{\partial x^2}$$

With boundary conditions; and initial conditions :

$$T(x, 0) = T_1 + \left(\frac{T_2 - T_1}{\ell}\right)x + \left(\frac{\pi}{\ell}\right)^2 \sin\left(\frac{\pi x}{\ell}\right) = T(x)$$

$$T(0, t) = \alpha_1(t), \quad T(\ell, t) = \alpha_2(t)$$

For non-homogeneous boundary conditions prescribed in the given problem, it becomes necessary to split up the boundary conditions into groups of partial conditions, and solutions of the differential equations satisfying each group separately.

must be sought. Then, their sum automatically satisfies the heat conduction equation, on accounts of it's linearity. The original division into partial conditions should be carried out in a correct manner such that, the boundary conditions will also be satisfied.

The scheme for the decomposition of the boundary conditions and of the complete solution $T(x,t)$ in partial solutions $v(x,t)$ and $w(x,t)$ is carried out as follows.

$$T(x,t) = v(x,t) + w(x,t) \quad (3.1.8)$$

Then equation (3.1.1) becomes

$$\frac{\partial v(x,t)}{\partial t} + \frac{\partial w(x,t)}{\partial t} = \frac{K}{\rho C_p} \left[\frac{\partial^2 v(x,t)}{\partial x^2} + \frac{\partial^2 w(x,t)}{\partial x^2} \right] \quad (3.1.9)$$

The transformed boundary conditions will be :

$$\begin{aligned} v(0,t) + w(0,t) &= \alpha_1(t) \\ v(\ell,t) + w(\ell,t) &= \alpha_2(t) \end{aligned} \quad (3.1.10)$$

and the initial condition becomes,

$$v(x,0) + w(x,0) = T(x) \quad (3.1.11)$$

Now, $w(x,t)$ can be chosen such that,

$$\begin{aligned} \frac{\partial^2 w}{\partial x^2} &= 0 \\ w(0,t) &= \alpha_1(t) \\ w(\ell,t) &= \alpha_2(t) \end{aligned} \quad (3.1.12)$$

Hence, we obtain, $w(x,t) = a(t)x + b(t)$ (3.1.13)

Applying the boundary conditions (3.1.12) we have,

$$b(t) = \alpha_1(t)$$

and

$$a(t) = [\alpha_2(t) - \alpha_1(t)]/\ell$$

Now, $v(x,t)$ satisfies the partial differential equation,

$$\frac{\partial v(x,t)}{\partial t} - \frac{K}{\rho C_p} \frac{\partial^2 v(x,t)}{\partial x^2} = - \frac{\partial w(x,t)}{\partial t} \quad (3.1.14)$$

where $w(x,t)$ is a known function of x and t .

The initial and boundary conditions becomes

$$\text{I.C.} \quad v(x,0) = T(x) - w(x,0) = g(x)$$

$$\text{B.C.} \quad v(0,t) = 0; \quad v(\ell, t) = 0 \quad (3.1.15)$$

where, $w(x,t)$ is given by,

$$w(x,t) = \frac{1}{\ell} [\alpha_2(t) - \alpha_1(t)]x + \alpha_1(t) \quad (3.1.16)$$

Therefore,

$$- \frac{\partial w}{\partial t} = - \frac{x}{\ell} \left(\frac{d\alpha_2(t)}{dt} - \frac{d\alpha_1(t)}{dt} \right) + \frac{d\alpha_1(t)}{dt}$$

Let us use the notation,

$$f(x,t) = - \frac{x}{\ell} \left(\frac{d\alpha_2(t)}{dt} - \frac{d\alpha_1(t)}{dt} \right) + \frac{d\alpha_1(t)}{dt}$$

Thus, our equation for $v(x,t)$ becomes

$$\frac{\partial v(x,t)}{\partial t} = \alpha^2 \frac{\partial^2 v(x,t)}{\partial x^2} + f(x,t) \quad (3.1.17)$$

where, $\alpha^2 = K/\rho C_p$, with boundary conditions

$$v(0,t) = 0, \quad v(\ell, t) = 0 \quad (3.1.18)$$

and initial condition

$$v(x,0) = T(x) - w(x,0) \quad (3.1.19)$$

This is an inhomogeneous equation with homogeneous boundary conditions.

Let us seek a solution to this boundary value problem in the form

$$v(x,t) = \sum_{n=1}^{\infty} T_n(t) \sin \frac{n\pi x}{\ell} \quad (3.1.20)$$

So that the boundary conditions (3.1.18) should be satisfied.

Let us suppose that the function $f(x,t)$, regarded as a function of x , can be expanded in Fourier series.

$$f(x,t) = \sum_{n=1}^{\infty} f_n(t) \sin \frac{n\pi x}{\ell} \quad (3.1.21)$$

$$\text{where, } f_n(t) = \frac{2}{\ell} \int_0^{\ell} f(x,t) \sin \frac{n\pi x}{\ell} dx$$

Substituting the series (3.1.20) and (3.1.21) into equation (3.1.17), we obtain,

$$\left[\frac{dT_n(t)}{dt} - \left(\frac{n\pi\alpha}{\ell} \right)^2 T_n(t) - f_n(t) \right] \sin \frac{n\pi x}{\ell} = 0$$

Let us put $\frac{n\pi\alpha}{\ell} = \beta_n$, we obtain

$$\frac{dT_n(t)}{dt} - \beta_n^2 T_n(t) = f_n(t) \quad (3.1.22)$$

By using the initial condition for $v(x,t)$

$$v(x,0) = \sum_{n=1}^{\infty} T_n(0) \sin \frac{n\pi x}{\ell} = g(x)$$

We obtain initial condition for $T_n(t)$:

$$T_n(0) = \frac{2}{\ell} \int_0^{\ell} g(x) \sin \frac{n\pi x}{\ell} dx$$

The solution of eq. (3.1.22) becomes

$$T_n(t) = e^{\beta_n^2 t} \left[T_n(0) + \int_0^t e^{-\beta_n^2(t-\tau)} f_n(\tau) d\tau \right] \quad (3.1.23)$$

Substituting (3.1.23) in (3.1.20) we have, the complete expression for, $v(x,t)$ follows as,

$$v(x,t) = \sum_{n=1}^{\infty} \left\{ e^{\beta_n^2 t} \left[T_n(0) + \int_0^t e^{-\beta_n^2(t-\tau)} f_n(\tau) d\tau \right] \right\} \sin\left(\frac{n\pi x}{\ell}\right) \quad (3.1.24)$$

$$\text{where, } T_n(0) = \frac{2}{\ell} \int_0^{\ell} g(x) \sin\left(\frac{n\pi x}{\ell}\right) dx$$

Thus, the complete solution to the problem is the combination of both the partial solutions $v(x,t)$ and $w(x,t)$, i.e.

$$\begin{aligned} T(x,t) = & \sum_{n=1}^{\infty} \left\{ e^{\beta_n^2 t} \left[T_n(0) + \int_0^t e^{-\beta_n^2(t-\tau)} f_n(\tau) d\tau \right] \right\} \sin\left(\frac{n\pi x}{\ell}\right) \\ & + \frac{1}{\ell} [\alpha_2(t) - \alpha_1(t)]x + \alpha_1(t) \end{aligned} \quad (3.1.25)$$

Transient Numerical Technique :

When the transients are severe and the transient boundary conditions are of such form that a mathematical solution to the problem is not possible. In these cases, the problems are best handled by a numerical technique with hand calculator or computers depending upon the accuracy desired.

In the setup for the problem the second derivatives in equation (3.1.1) is approximated by

$$\frac{\partial^2 T(x,t)}{\partial x^2} = \frac{1}{(\Delta x)^2} (T_{m+1}^n - 2 T_m^n + T_{m-1}^n)$$

and

$$\frac{\partial T(x,t)}{\partial t} = \frac{T_m^{n+1} - T_m^n}{\Delta t}$$

In this relation, the superscript designates the time increment and subscript corresponds to space increment. Combining the relations above, the difference equation equivalent to Eq.(3.1.1) is

$$\frac{T_{m+1}^n - 2 T_m^n + T_{m-1}^n}{\Delta x^2} = \frac{1}{\alpha^2} \frac{T_m^{n+1} - T_m^n}{\Delta t} \quad (3.1.24)$$

Thus, if the temperature of the various nodes are known at any particular time, the temperature after an increment of time Δt may be calculated by writing an equation like eqn.(3.1.24) for each node and obtaining values of T_m^{n+1} . The procedure may be repeated to obtain the distribution after any desired number of time increments. Equation (3.1.24) can be conveniently written as,

$$T_m^{n+1} = \frac{\alpha^2 \Delta t}{\Delta x^2} (T_m^n + T_{m-1}^n) + [1 - \frac{2\alpha^2 \Delta t}{\Delta x^2}] T_m^n \quad (3.1.25)$$

In this explicit finite difference method an approximation associated with difference equation (3.1.25) is that, while the temperatures at T_m^n changes during a small interval

to a value T_m^{n+1} , the values of T_{m+1}^n and T_{m-1}^n are assumed to remain constant.

If the time and distance increments are chosen such that $M = \frac{(\Delta x)^2}{\alpha^2 \Delta t} = 2$, the temperature of node m after the time increment is given as the arithmetic average of the two adjacent nodal temperatures at the beginning of the time increment. The solution of the value of the parameter $M = \frac{(\Delta x)^2}{\alpha^2 \Delta t}$ is important, as it governs the case with which we may proceed to effect the numerical solution.

Once the distance increment and the value of M are established, the time increment is fixed. The smaller values of Δx and Δt in the iteration process gives better accuracy. One important thing to note is that, if $M < 2$ the coefficients of equation (3.1.25) becomes negative and a condition is generated that the 2nd law of thermodynamics is violated.

The difference equation given above is useful for determining the internal temperature in the core as a function of space and time. Once the boundary conditions are specified, their finite difference approximations can be made and used to start the iteration process.

3.2 STEADY STATE NATURAL CONVECTION (THERMOSYPHON) COOLING

The most important aspect of the present work is concerned with the natural convection cooling (thermosyphoning) in the horizontal CANDU reactor core in the vicinity of each fuel rod following the transient, specifically in situations, when equilibrium natural circulation in the primary system cannot be established and auxiliary recirculation pumps become inoperative. A central question then becomes, whether thermosyphoning in the horizontal core plays dominant role in determining availability of adequate cooling following the accident, by directly extracting heat from the surface of the each fuel rod.

Problem Formulation :

A fuel bundle in a CANDU reactor core is a circular array of circular cylindrical fuel elements placed according to a specified array geometry. The array is generally divided into triangular lattice cells as shown in Fig. 3.5, and coolant channel is characterized by its' hydraulic diameter, $D_e = \frac{4A_c}{P}$, where, A_c is the cross sectional area of the lattice cell and P is the wetted perimeter. To formulate the problem, we consider individual fuel rods in the lattice cells, which are isolated from each other and try to develop an analysis for a single fuel rod. Without any ambiguity, the treatment can be extended for all the fuel rods assuming that these are all in the same thermal state. This seems reasonable because, the steady state heat flux distribution in the core has been considerably flattened compared to the initial sinusoidal distribution. As a result, this gives

approximately a constant uniform heat flux throughout the core.

With the aid of the argument given by Lighthill [7], it is recalled that a boundary layer regime will be developed in the vicinity of each fuel rod because of the existence of considerably high heat flux inside the core. Calculation of steady state Grashoff number indicates that the boundary layer regime is laminar in nature. Since, the thickness of the thermal and hydrodynamic boundary layers are approximately equal in the fluids with Prandtl number close to unity, therefore, no separate boundary layers will be considered in the present treatment. The region near the fuel rod surface in the boundary layer regime, where velocity is found to be significant. The fluid beyond the boundary layer regime is assumed to be stationary, since the buoyant force due to gravity, causes the lighter fluid near the fluid to move and it becomes insignificant at a larger distance from the surface. The fluid velocity, therefore, be zero at the fuel rod surface, increase to a maximum value in the immediate neighbourhood, and then decreases asymptotically to zero at the outer edge of the boundary layer. The motion of the flow is restricted to a region close to the fuel rod surface. For the present treatment the following assumptions are made :

- (1) Mutual influences of the fuel rods on their individual flow in the boundary layer regime is disregarded.
- (2) The interaction of the boundary layer of a fuel rod with its' neighbouring one is also disregarded.
- (3) The results derived for a single fuel rod is equally

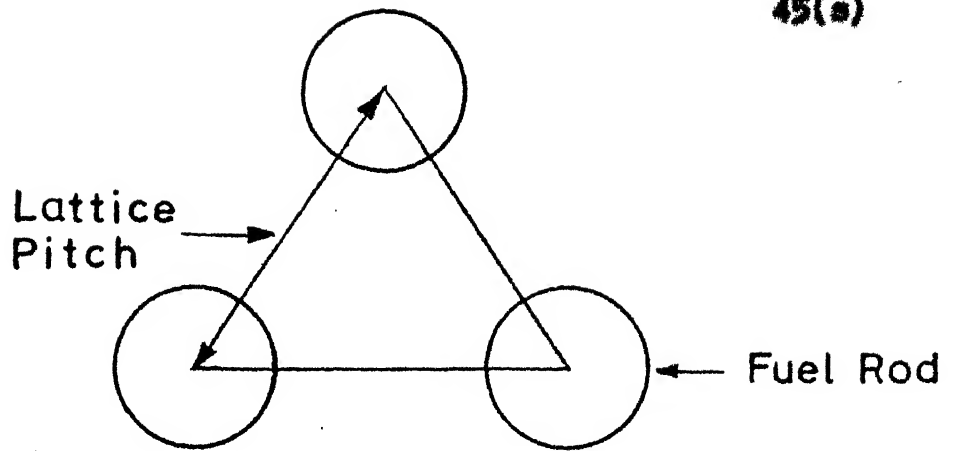


Fig.3.5 A Typical Triangular Lattice Cell

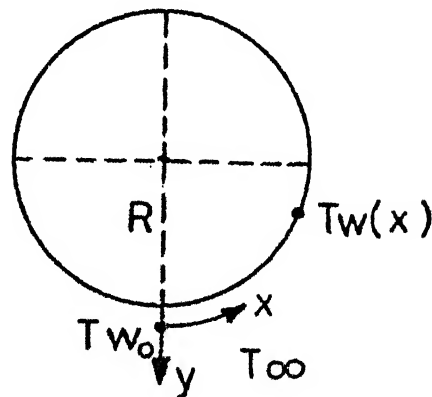


Fig. 3.6 Co-ordinate System

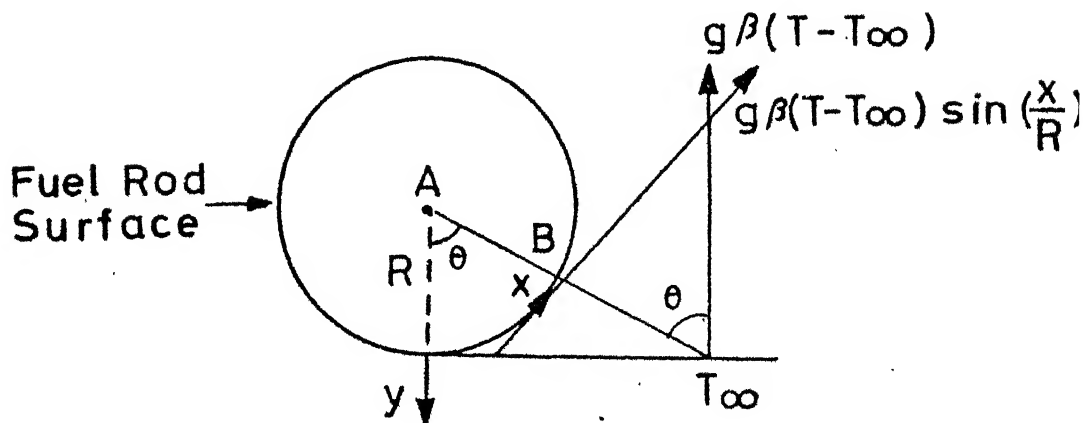


Fig. 3.7 Buoyant Force along the curved surface

applicable to all the rods inside a fuel bundle according to foregoing arguments.

Usually, Nusselt number and Grashoff number are based on the diameter of the cylinder, the significant length in all free convection problems with horizontal cylinders. A coordinate system suggested by Koh and Price [22] to treat axially symmetric horizontal objects in free convection is well suited for the present problem. This helps immensely to construct the buoyant force term. The coordinate system is shown in Fig. 3.4. It is located with the origin at the lower end of the cylinder. x coordinate varies across the fuel rod surface as shown in the figure and y axis is normal to the surface. Here T_{w_0} , $T_w(x)$ and T_∞ are temperatures at origin, at a point with coordinate x on the fuel rod surface and, ambient fluid (coolant) temperature respectively.

Isothermal and Non-isothermal surface conditions on the fuel rod :

As previously pointed out that, accumulation of volatile fission products in the fuel cladding gap and in other void regions in the cladding envelope is likely to affect the gap conductance and give rise to non-isothermal surface conditions on the fuel rod. In such situations, the temperature varies in an arbitrary manner with the coordinate x across the fuel rod surface. At $x = 0$, a stagnation point is formed. For the present situation, the surface temperature is assumed to vary in both linear and nonlinear manner as two separate cases. The surface

temperature is assumed to take the following forms:

For linear variation ;

$$(T_w - T_\infty) = (T_{w_0} - T_\infty) \left[1 + a \left(\frac{x}{R} \right) \right] \quad (3.2.1)$$

For nonlinear variation ;

$$(T_w - T_\infty) = (T_{w_0} - T_\infty) \left[1 + a \left(\frac{x}{R} \right)^2 \right] \quad (3.2.2)$$

Where, a is an arbitrary constant and the surface temperature is always higher than the free stream (ambient) temperature T_∞ .

In isothermal surface condition, there is no variation of temperature occurs across the surface of the fuel rod, which implies that $a = 0$. Hence, it is reasonable to suppose that the free convection heat transfer from a non-isothermal surface would be significantly different from that of an isothermal one.

Construction of the buoyant force term :

The density has been considered as only variable in forming the buoyancy force term. Variation of all other properties are neglected. The body force is assumed to be significant only in the vertically upward direction, then body force per unit volume in the vertical direction is $g\beta(T-T_\infty)$, where, g is the gravitational force vector and β is the thermal expansion coefficient. In order to construct the body force expression for a curved surface, a tangent is drawn at any point B on the fuel rod surface as shown in the Fig. 3.7. If R is the radius of the fuel rod and x is the coordinate of the point B, then the angle θ subtended at the centre of the circle

is equal to x/R . The direction of the buoyant force at the point B is along the direction of the tangent drawn at that point and its magnitude is $g\beta(T - T_{\infty})\sin(x/R)$. Thus, generalizing the buoyancy force at any point on the curved surface of the fuel rod has a direction along the tangent drawn at that point and magnitude equal to $=g\beta(T - T_{\infty})\sin(x/R)$, which is a function of the coordinate x .

Governing Differential Equations :

The two dimensional equations expressing conservation of mass, momentum, and energy for steady, laminar flow in a boundary layer on a horizontal cylindrical fuel element can be expressed, without any loss of generality in Cartesian coordinates as follows :

$$\frac{\partial u}{\partial x} + \frac{\partial v}{\partial y} = 0 \quad (3.2.3)$$

$$u \frac{\partial u}{\partial x} + v \frac{\partial u}{\partial y} = \nu \frac{\partial^2 u}{\partial y^2} + g\beta(T - T_{\infty})\sin\left(\frac{x}{R}\right) \quad (3.2.4)$$

$$u \frac{\partial T}{\partial x} + v \frac{\partial T}{\partial y} = \frac{\nu}{Pr} \frac{\partial^2 T}{\partial y^2} \quad (3.2.5)$$

where, u and v are velocity components along x and y directions, respectively. ν is the kinematic viscosity and Pr is the Prandtl number.

Viscous dissipation and work against the gravity field have been omitted from the energy equation since they are negligibly small. The appropriate boundary conditions are :

$$\begin{array}{lll} y = 0 & u = v = 0 & T = T_w(x) \\ y \rightarrow \infty & u \rightarrow 0 & T \rightarrow T_{\infty} \end{array}$$

First boundary conditions is the no slip condition on the surface and second one is the asymptotic boundary condition at the edge of the free convection boundary layer. Equation (3.2.3) can be automatically satisfied if a stream function is introduced such that

$$u = \frac{\partial \psi}{\partial y} \quad v = - \frac{\partial \psi}{\partial x} \quad (3.2.6)$$

The momentum and energy equations may be converted into dimensionless forms by introducing suitable similarity parameters as shown by Schmidt [23] and Valentine [24] for laminar free convection problems. The similarity parameters are given as:

$$\begin{aligned} \bar{x} &= \frac{x}{R} \\ \eta &= \left[\frac{g\beta(T_{w_0} - T_{\infty}) R^3}{\nu^2} \right]^{1/4} \frac{y}{R} = (Gr)^{1/4} \frac{y}{R} \\ M(\bar{x}, \eta) &= \left[\frac{\nu^2}{g\beta(T_{w_0} - T_{\infty}) R^3} \right]^{1/4} \frac{\psi}{\nu} = \frac{1}{(Gr)^{1/4}} \frac{\psi}{\nu} \\ \theta(\bar{x}, \eta) &= \frac{T - T_{\infty}}{T_{w_0} - T_{\infty}} \end{aligned} \quad (3.2.7)$$

In the above transformations, the first two quantities, i.e. \bar{x} and η represent dimensionless coordinates. $M(\bar{x}, \eta)$ and $\theta(\bar{x}, \eta)$ are dimensionless stream function and temperature respectively. The reasoning behind the selection of this form for the similarity parameters is rather involved and specific for particular type of problem. Using these transformation we deduce the following

$$u = \frac{\partial \psi}{\partial y} = \frac{\nu}{R} (Gr)^{1/2} \frac{\partial M}{\partial \eta}$$

$$v = - \frac{\partial \psi}{\partial x} = - \frac{(Gr)^{1/4} \nu}{R} \frac{\partial M}{\partial \bar{x}}$$

$$\frac{\partial u}{\partial y} = \frac{\nu}{R^2} Gr^{3/4} \frac{\partial^2 M}{\partial \eta^2}$$

$$\frac{\partial u}{\partial x} = \frac{\nu}{R^2} Gr^{1/2} \frac{\partial^2 M}{\partial \bar{x} \partial \eta}$$

$$\frac{\partial^2 u}{\partial y^2} = \frac{\nu}{R^3} Gr \frac{\partial^3 M}{\partial \eta^3}$$

$$\frac{\partial T}{\partial x} = \frac{1}{R} (T_{w_0} - T_{\infty}) \frac{\partial \theta}{\partial \bar{x}}$$

$$\frac{\partial T}{\partial y} = (T_{w_0} - T_{\infty}) \frac{Gr^{1/4}}{R} \frac{\partial \theta}{\partial \eta}$$

$$\frac{\partial^2 T}{\partial y^2} = (T_{w_0} - T_{\infty}) \frac{Gr^{1/4}}{R^2} \frac{\partial^2 \theta}{\partial \eta^2}$$

Substituting the above results, the momentum and energy equations i.e. equation (3.2.4) and (3.2.5) may be rewritten in the following dimensionless form :

$$\frac{\partial M}{\partial \eta} \frac{\partial^2 M}{\partial \bar{x} \partial \eta} - \frac{\partial^2 M}{\partial \eta^2} \frac{\partial M}{\partial \bar{x}} = \frac{\partial^3 M}{\partial \eta^3} + \theta \sin \bar{x} \quad (3.2.8)$$

$$\frac{\partial M}{\partial \eta} \frac{\partial \theta}{\partial \bar{x}} - \frac{\partial M}{\partial \bar{x}} \frac{\partial \theta}{\partial \eta} = \frac{1}{Pr} \frac{\partial^2 \theta}{\partial \eta^2} \quad (3.2.9)$$

In terms of the new variables, the boundary conditions are

$$\eta = 0 \quad M = \frac{\partial M}{\partial \bar{x}} = \frac{\partial M}{\partial \eta} = 0 \quad (3.2.10)$$

and, $\phi = 1$ (Isothermal case)

$$\phi = (1 + a\bar{x}) \quad (\text{Linear variation of temperature})$$

$$\phi = (1 + a\bar{x}^2) \quad (\text{Non-linear variation of temperature})$$

$$\eta \longrightarrow \infty \quad \frac{\partial M}{\partial \eta} \longrightarrow 0 \quad \phi \longrightarrow 0$$

Solution Procedure :

Equations (3.2.8) and (3.2.9) together with the boundary conditions can be solved by using Blasius-Howarth series approximation technique for the dimensionless stream function M and dimensionless temperature ϕ as discussed by Chiang and Kaye [25]. Thus, the series approximations for M and ϕ take the following forms for non-linear and linear variations of the fuel rod surface temperature. For non-linear case :

$$M(\bar{x}, \eta) = \bar{x} F_0(\eta) + \bar{x}^3 F_1(\eta) + \dots \quad (3.2.11)$$

$$\phi(\bar{x}, \eta) = G_0(\eta) + \bar{x}^2 G_1(\eta) + \dots$$

and For linear case :

$$M(\bar{x}, \eta) = \bar{x} F_0(\eta) + \bar{x}^2 F_1(\eta) + \dots \quad (3.2.12)$$

$$\phi(\bar{x}, \eta) = G_0(\eta) + \bar{x} G_1(\eta) + \dots$$

The first terms in each of these series expansion is the dominating one with respect to the other terms. Higher order terms are treated as perturbations to the first term. The great advantage lies with these series expansions, which convert the governing partial differential equation to a set of ordinary differential equations.

Dr. KIANPUR
CENTRAL LIBRARY

No. A 66872

Sin \bar{x} in equation (3.2.8) is approximated by the first two terms of its power series as follows :

$$\sin \bar{x} = \bar{x} - \frac{\bar{x}^3}{3!} + \dots \quad (3.2.13)$$

When equations (3.2.11) and sine series approximation (3.2.13) are substituted into equation (3.2.8) and (3.2.9) and terms arranged in ascending power of \bar{x} gives.

$$\begin{aligned} & \bar{x} \left[\frac{d^3 F_0}{d\eta^3} + G_0 - \left(\frac{dF_0}{d\eta} \right)^2 + F_0 \frac{d^2 F_0}{d\eta^2} \right] + \bar{x}^3 \left[\frac{d^3 F_1}{d\eta^3} + G_1 - \frac{G_0}{6} - \frac{dF_1}{d\eta} \frac{dF_0}{d\eta} \right] \\ & + \bar{x}^5 \left[3F_1 \frac{d^2 F_1}{d\eta^2} - 3 \left(\frac{dF_1}{d\eta} \right)^2 - \frac{G_1}{6} \right] + \left[3 \frac{dF_0}{d\eta} \frac{dF_1}{d\eta} + 3F_1 \frac{d^2 F_0}{d\eta^2} + F_0 \frac{d^2 F_1}{d\eta^2} \right] = 0 \end{aligned}$$

and, (3.2.14)

$$\begin{aligned} & \left(\frac{1}{Pr} \frac{d^2 G_0}{d\eta^2} + F_0 \frac{dG_0}{d\eta} \right) + \bar{x}^2 \left(\frac{1}{Pr} \frac{d^2 G_1}{d\eta^2} - 2G_1 \frac{dF_0}{d\eta} + F_0 \frac{dG_1}{d\eta} + 3F_1 \frac{dG_0}{d\eta} \right) \\ & + \bar{x}^4 \left(F_0 \frac{dG_1}{d\eta} - 2 \frac{dF_1}{d\eta} G_1 \right) = 0 \end{aligned} \quad (3.2.15)$$

Now, setting the coefficient of \bar{x}^α to zero for each non-negative integer $\alpha \leq 3$ and neglecting the coefficient of higher order terms in \bar{x} , yields the following sets of ordinary differential equation

$$\begin{aligned} & \frac{d^3 F_0}{d\eta^3} + F_0 \frac{d^2 F_0}{d\eta^2} - \left(\frac{dF_0}{d\eta} \right)^2 + G_0 = 0 \\ & \frac{1}{Pr} \frac{d^2 G_0}{d\eta^2} + F_0 \frac{dG_0}{d\eta} = 0 \end{aligned} \quad (3.2.16)$$

$$\begin{aligned} & \frac{d^3 F_1}{d\eta^3} + F_0 \frac{d^2 F_1}{d\eta^2} - 4 \frac{dF_0}{d\eta} \frac{dF_1}{d\eta} + 3 \frac{d^2 F_0}{d\eta^2} F_1 + G_1 - \frac{1}{6} G_0 = 0 \end{aligned} \quad (3.2.17)$$

$$\frac{1}{Pr} \frac{d^2 G_1}{d\eta^2} + F_0 \frac{dG_1}{d\eta} - 2 \frac{dF_0}{d\eta} G_1 + 3 \frac{dG_0}{d\eta} F_1 = 0$$

The boundary conditions are

$$\begin{aligned} \eta = 0 \quad F_0 = \frac{dF_0}{d\eta} = 0 \quad G_0 = 1 \\ F_1 = \frac{dF_1}{d\eta} = 0 \quad G_1 = a \quad (3.2.18) \\ \eta \rightarrow \infty \quad \frac{dF_0}{d\eta} \rightarrow 0 \quad G_0 \rightarrow 0 \\ \frac{dF_1}{d\eta} \rightarrow 0 \quad G_1 \rightarrow 0 \end{aligned}$$

Similarly, when equations (3.2.12) together with the sine series expansion (3.2.13) are substituted into equations (3.2.8) and (3.2.9) and terms arranged in ascending powers of \bar{x} , the setting to zero of the coefficients of \bar{x}^α for each non-negative integer $\alpha \leq 2$ yields the same sets of ordinary differential equations as given above.

An inspection of equations (3.2.16) to (3.2.18) reveals that the present problem involves two parameters, Pr and a . However, for isothermal surface condition 'a' becomes zero. For non-isothermal conditions, for each combination of Pr and a it would be necessary to solve two pairs of simultaneous equations. The Prandtl number is considered to be a constant. However, a can have different values as it is taken to be an arbitrary constant. Hence, it may be desired to solve equations (3.2.16) to (3.2.18) for different values of a . Consequently, referring to Struble [26], the following transformations are used to transform

the original equations and boundary conditions to new sets of differential equations and boundary conditions which are free of the parameter a .

$$\begin{aligned} F_0(\eta) &= X_1(\eta) & G_0(\eta) &= Y_1(\eta) \\ F_1(\eta) &= aX_2(\eta) + X_3(\eta) & G_1(\eta) &= aY_2(\eta) + Y_3(\eta) \end{aligned} \quad (3.2.19)$$

Substituting these transformations into equations (3.2.16) to (3.2.18), and with little algebra yields the new differential equations together with their boundary conditions.

$$\frac{d^3 X_1}{d\eta^3} + X_1 \frac{d^2 X_1}{d\eta^2} - \left(\frac{dX_1}{d\eta}\right)^2 + Y_1 = 0 \quad (3.2.20)$$

$$\frac{d^2 Y_1}{d\eta^2} + \text{Pr} X_1 \frac{dY_1}{d\eta} = 0$$

$$\eta = 0 \quad X_1 = 0 \quad \frac{dX_1}{d\eta} = 0 \quad Y_1 = 1$$

$$\eta \rightarrow \infty \quad \frac{dX_1}{d\eta} \rightarrow 0 \quad Y_1 \rightarrow 0$$

$$\frac{d^3 X_2}{d\eta^3} + X_1 \frac{d^2 X_2}{d\eta^2} - 4 \frac{dX_1}{d\eta} \frac{dX_2}{d\eta} + 3 \frac{d^2 X_1}{d\eta^2} X_2 - Y_2 = 0$$

$$\frac{d^2 Y_2}{d\eta^2} + \text{Pr} \left[X_1 \frac{dY_2}{d\eta} - 2 \frac{dX_1}{d\eta} Y_2 + 3X_2 \frac{dY_1}{d\eta} \right] = 0 \quad (3.2.21)$$

$$\eta = 0 \quad X_2 = 0 \quad \frac{dX_2}{d\eta} = 0 \quad Y_2 = 1$$

$$\eta \rightarrow \infty \quad \frac{dX_2}{d\eta} \rightarrow 0 \quad Y_2 \rightarrow 0$$

$$\frac{d^3 X_3}{d\eta^3} + X_1 \frac{d^2 X_3}{d\eta^2} - 4 \frac{dX_1}{d\eta} \frac{dX_3}{d\eta} + 3X_3 \frac{d^2 X_1}{d\eta^2} + Y_3 - \frac{1}{6} Y_1 = 0$$

$$\frac{d^2 Y_3}{d\eta^2} + \text{Pr} \left[X_1 \frac{dY_3}{d\eta} - 2 \frac{dX_1}{d\eta} Y_3 + 3X_3 \frac{dY_1}{d\eta} \right] = 0 \quad (3.2.22)$$

$$\eta = 0 \quad X_3 = 0 \quad \frac{dX_3}{d\eta} = 0 \quad Y_3 = 0$$

$$\eta \rightarrow \infty \quad \frac{dX_3}{d\eta} \rightarrow 0 \quad Y_3 \rightarrow 0$$

The equations (3.2.20) to (3.2.22) are free of the parameter a and hence solutions of these equations are applicable for different values of a .

It is noted that equations (3.2.20) are non-linear, while remainder of the equations are linear (assuming that solutions of equations (3.2.20) are known). All of these three sets of equations are coupled third order ordinary differential equations with asymptotic boundary conditions. Inspection of equations (3.2.20) reveals that these are very much similar to the boundary value problem for the free convection flow about a vertical plate referring to Ostrach [27]. Equations (3.2.21) and (3.2.22) involve four dependent variables each, and X_1 and Y_1 are two of these four variables. These asymptotic boundary value problems are virtually impossible to solve by an analytical method. Extensive numerical analysis of these equations are required to solve them fairly accurately by a reasonably good numerical technique. The mathematical apparatus required for the numerical solution of these equations will be introduced in

succeeding chapter.

Velocity, Temperature and Heat transfer :

Substituting the transformations given by equations (3.2.19) into equations (3.2.11) and (3.2.12), the dimensionless stream functions and temperature assumes the following forms respectively for non-linear and linear variation of surface temperature.

$$M(\bar{x}, \eta) = \bar{x} X_1(\eta) + \bar{x}^3 (aX_2(\eta) + X_3(\eta)) \quad (3.2.23)$$

$$\vartheta(\bar{x}, \eta) = Y_1(\eta) + \bar{x}^2 (aY_2(\eta) + Y_3(\eta))$$

$$M(\bar{x}, \eta) = \bar{x} X_1(\eta) + \bar{x}^2 (aX_2(\eta) + X_3(\eta)) \quad (3.2.24)$$

$$\vartheta(\bar{x}, \eta) = Y_1(\eta) + \bar{x} (aY_2(\eta) + Y_3(\eta))$$

From the expression for similarity parameter related to dimensionless stream function M , given in equation (3.2.7), we have

$$\psi = M \frac{(Gr)^{1/4}}{y} \eta, \quad \text{which gives,}$$

$$u = \frac{\partial \psi}{\partial y} = \frac{(Gr)^{1/2}}{R} \eta \frac{\partial M(\bar{x}, \eta)}{\partial \eta}$$

Substituting for $\frac{\partial M}{\partial \eta}$ from the equations (3.2.23) and (3.2.24) into the above equation, the expression for velocity distribution in the boundary layer follows for both non-linear and linear cases of thermal condition on the surface :

$$u = \frac{(Gr)^{1/2}}{R} \eta \left[\bar{x} \frac{dX_1}{d\eta} + \bar{x}^3 \left(a \frac{dX_2}{d\eta} + \frac{dX_3}{d\eta} \right) \right]$$

$$u = \frac{(Gr)^{1/2}}{R} \eta \left[\bar{x} \frac{dX_1}{d\eta} + \bar{x}^2 \left(a \frac{dX_2}{d\eta} + \frac{dX_3}{d\eta} \right) \right] \quad (3.2.25)$$

Now, equating Fourier law of heat flow on the surface in terms of θ and heat flux, q/A given as,

$$q/A = -K(T_{w_o} - T_{\infty}) \frac{Gr^{1/4}}{R} \frac{\partial \theta}{\partial \eta} \Big|_{\eta=0}$$

and Newton's law of cooling for the heat converted away from the surface given as,

$$q/A = h (T_{w_o} - T_{\infty})$$

One finds the following equation,

$$h = -K \frac{Gr^{1/4}}{R} \frac{\partial \theta}{\partial \eta} \Big|_{\eta=0}$$

The dimensionless heat transfer i.e., Nusselt number may be given as,

$$Nu_D = \frac{hR}{K} = -(Gr)^{1/4} \frac{\partial \theta}{\partial \eta} \Big|_{\eta=0} \quad (3.2.26)$$

where, Nu_D based upon the radius (i.e. diameter) of the fuel rod. Substituting for $\frac{\partial \theta}{\partial \eta} \Big|_{\eta=0}$ from equations (3.2.23) and (3.2.24) into the above equation, the expression for Nusselt number follows for both non-linear and linear cases of thermal condition on the surface

$$Nu_D = -Gr^{1/4} \left[\frac{dY_1(0)}{d\eta} + \bar{x}^2 \left(a \frac{dY_2(0)}{d\eta} + \frac{dY_3(0)}{d\eta} \right) \right] \quad (3.2.27)$$

$$Nu_D = -Gr^{1/4} \left[\frac{dY_1(0)}{d\eta} + \bar{x} \left(a \frac{dY_2(0)}{d\eta} + \frac{dY_3(0)}{d\eta} \right) \right]$$

The equations representing, velocity and Nusselt number for non-linear and linear cases are similar except for the power of \bar{x} involved in those expressions. The velocity distribution in the

boundary layer accounts for the thermosyphoning effects, in the form of eddies in the vicinity of each fuel rod. In order to compute the velocity and Nusselt number, the derivatives in the corresponding expressions must be evaluated which are functions of η , the measure of the dimensionless distance from the surface of the fuel rod.

CHAPTER IV

NUMERICAL ANALYSIS OF THE SYSTEMS OF BOUNDARY LAYER DIFFERENTIAL EQUATIONS

4.1 INTRODUCTION

The numerical integration of the ordinary differential equations, obtained from Blasius-Hawarth series with appropriate transformations, involves the satisfaction of asymptotic boundary conditions. That is, some boundary conditions are specified at the initial point or wall and other are specified as limits that must be approached at relatively large values of the independent variable, corresponding to the edge of the boundary layer. In order to integrate the differential equations numerically from the wall to the edge of the boundary layer, it is necessary to specify as many additional conditions at the wall as there are conditions to be satisfied at the edge of the boundary layer. All methods that have been used to find the proper initial conditions rely on the fact that, for relatively large values of the independently variable, the integrals of the differential equations depend on the initial conditions. Among the broad categories of numerical methods, two widely applicable techniques are namely :

- (i) Initial value method, Fox [28].
- (ii) Quasilinearization method, Radbill [29].

Initial value method, that has been used to find proper initial conditions, is that of obtaining integrals of the differential equations with guessed initial conditions, that is an attempt is made to integrate the differential equations to the edge of the boundary layer. If this can be accomplished, corrections are made for the initial guesses by suitable iterative method and the process is repeated until desired accuracy is achieved. In order to carry out these iterations, additional differential equations have to be integrated. The additional differential equations are obtained by differentiating the terms of the original differential equations with respect to initial conditions. The integrals of these additional differential equations, referred to as perturbation equations, give the rate of change of the integrals of the original differential equations with respect to the initial conditions.

Quasilinearization is similar in principle to the initial value method, except that the original differential equations, if non-linear, are linearized. The resulting linear differential equations for the current approximation are inhomogeneous, since they also contain the previous approximation as members. In application, the two methods are different in that, in the quasilinearization method, the complementary solutions are used to obtain solutions to the inhomogeneous linear differential equations, whereas in initial value method, the integrals of the perturbation equations are used to adjust the starting values at the initial point.

A disadvantage associated with quasilinearization method is that, the solution of the inhomogeneous equations obtained by combining complementary solution and a particular integral is usually not well determined except near the origin or initial point as pointed out by Hartree [30]. Thus initial value method has an edge over the latter, as solutions of perturbation equations can be used to determine the proper initial conditions closely. Since, boundary conditions specified as a limit that must be approached at higher values of the independent variable, the integration should be stopped at a value of the independent variable, so that various functions are approaching their asymptotic and physically acceptable values. This value of the independent variable may be called approximately the edge of the boundary layer. This value of independent variable is obtained by suitable guess and trial effort.

In an effort to adapt the initial value method to the solution of differential equations with asymptotic boundary condition, an iterative method developed by Nachtsheim and Swigert [31] to correct the initial conditions, is applied. This method of solution is capable of satisfying boundary layer correctly. This is accomplished by choosing the additional initial conditions so that the mean square error between the computed variable and asymptotic variable is minimized. This method of solution is based on least square error criterion and the edge of the boundary layer is approached in steps.

4.2 DESCRIPTION OF THE METHOD

A description and application of the initial value method can best be given, referring to any one of the set of differential equations as an example. However, the general iterative formulas derived by using first set of non-linear equation (3.2.20) are equally applicable to all the sets of equations.

Using 'primes', to denote differentiation with respect to independent variable η , the measure of the dimensionless distance from the wall, we have:

$$\frac{dX_1}{d\eta} = X_1' , \quad \frac{d^2X_1}{d\eta^2} = X_1'' , \quad \frac{d^3X_1}{d\eta^3} = X_1''' .$$

Now, set of equations (3.2.20) can be rewritten as

$$\begin{aligned} X_1''' &= - (X_1 X_1'' - X_1'^2 + Y_1) \\ Y_1' &= - \text{Pr } X_1 Y_1' \end{aligned} \tag{4.2.1}$$

with boundary conditions:

$$\eta = 0, \quad X_1(\eta) = X_1'(\eta) = 0, \quad Y_1(\eta) = 1$$

$$\eta \rightarrow \infty, \quad Y_1(\eta) = X_1'(\eta) \rightarrow 0$$

The dependent variables, X_1 and Y_1 related to dimensionless stream function and temperature respectively.

In practice, the asymptotic boundary conditions is replaced by conditions that $X_1' = 0$ and $Y_1 = 0$, to a sufficient degree of accuracy at $\eta = \eta_{\text{edge}}$, where η_{edge} is the value of

the independent variable. The boundary value problem of this coupled differential equation is equivalent to the problem of finding values of $X_1''(0)$ and $Y_1'(0)$ for which the boundary conditions at the edge of the boundary layer is satisfied, i.e. it is desired to find solutions of equations

$$X_1' \text{ edge} [X_1''(0), Y_1'(0)] = 0 \quad (4.2.2)$$

$$Y_1 \text{ edge} [X_1''(0), Y_1'(0)] = 0 \quad (4.2.3)$$

where, $X_1' \text{ edge} \equiv X_1'(\eta_{\text{edge}})$ and $Y_1 \text{ edge} \equiv Y_1(\eta_{\text{edge}})$.

Since there are two asymptotic boundary conditions to satisfy, two additional initial conditions $X_1''(0)$ and $Y_1'(0)$ at the wall will have to be adjusted, that is, values of these are sought that will satisfy simultaneously the above equations. The functions $X_1' \text{ edge} [X_1''(0), Y_1'(0)]$ and $Y_1 \text{ edge} [X_1''(0), Y_1'(0)]$ in this problem are not, in general, explicit; those will be expressed as functions of $X_1''(0)$ and $Y_1'(0)$ through integration of equation (4.2.1).

Using notations^{*}, $x = X_1''(0)$ and $y = Y_1'(0)$, we observed that, small changes Δx and Δy in the initial conditions change X_1' and Y_1 by the amounts $\frac{\partial X_1'}{\partial x} \Delta x + \frac{\partial X_1'}{\partial y} \Delta y$ and $\frac{\partial Y_1}{\partial x} \Delta x + \frac{\partial Y_1}{\partial y} \Delta y$ respectively. The necessary correction to the first approximation comes from the solution of the linear equations

$$X_1' + \frac{\partial X_1'}{\partial x} \Delta x + \frac{\partial X_1'}{\partial y} \Delta y = 0 \quad (4.2.4)$$

$$Y_1 + \frac{\partial Y_1}{\partial x} \Delta x + \frac{\partial Y_1}{\partial y} \Delta y = 0 \quad (4.2.5)$$

at $\eta = \eta_{\text{edge}}$.

* The notations here should not be confused with the coordinates.

The initial value method again demands that all higher derivatives of the independent variables vanish at the outer boundary i.e. at $\eta = \eta_{\text{edge}}$. Hence, satisfaction of both pair of boundary conditions i.e. $X_1' = 0$, $X_1'' = 0$ and $Y_1 = 0$, $Y_1' = 0$ at $\eta = \eta_{\text{edge}}$ ensures that X_1' and Y_1 approach zero asymptotically as η approaches infinity. Thus, in order to satisfy asymptotic conditions at a finite value of η , both pair of above conditions must be imposed. Hence, in order to satisfy, asymptotic boundary conditions, the preceeding equations (4.2.2) and (4.2.3) must be supplemented by

$$X_1'' \text{ edge } [X_1''(0), Y_1'(0)] = 0 \quad (4.2.6)$$

$$Y_1'' \text{ edge } [X_1''(0), Y_1'(0)] = 0 \quad (4.2.7)$$

Again for small changes Δx and Δy in the initial conditions, the necessary correction to the first approximation, as previously given, comes from the solution of linear equations

$$X_1'' + \frac{\partial X_1''}{\partial x} \Delta x + \frac{\partial X_1''}{\partial y} \Delta y = 0 \quad (4.2.8)$$

$$Y_1' + \frac{\partial Y_1'}{\partial x} \Delta x + \frac{\partial Y_1'}{\partial y} \Delta y = 0 \quad (4.2.9)$$

at $\eta = \eta_{\text{edge}}$.

The solution of both pairs of equations i.e. (4.2.4), (4.2.5) and (4.2.8), (4.2.9) can be performed, provided that the partial derivatives involved in those equations with respect to x and y can be evaluated at $\eta = \eta_{\text{edge}}$. The partial derivatives can be evaluated by forming and integrating perturbation

equations for the functions X_1' , X_1'' and Y_1' , Y_1'' . These equations are obtained by differentiating the terms in the original equations (4.2.1) approximately with respect to x and y respectively.

The perturbation differential equation for x derivatives are :

$$\frac{\partial X_1'''}{\partial x} = - \left(\frac{\partial X_1}{\partial x} X_1'' + X_1 \frac{\partial X_1''}{\partial x} \right) + 2X_1' \frac{\partial X_1'}{\partial x} - \frac{\partial Y_1}{\partial x} \quad (4.2.10)$$

$$\frac{\partial Y_1''}{\partial x} = - \text{Pr} \left(\frac{\partial X_1}{\partial x} Y_1' + X_1 \frac{\partial Y_1'}{\partial x} \right)$$

with the initial conditions

$$\eta = 0: \quad \frac{\partial X_1}{\partial x} = \frac{\partial X_1'}{\partial x} = \frac{\partial Y_1}{\partial x} = \frac{\partial Y_1'}{\partial x} = 0, \quad \frac{\partial X_1''}{\partial x} = 1$$

The perturbation differential equations for the y derivatives are

$$\frac{\partial X_1'''}{\partial y} = - \left(\frac{\partial X_1}{\partial y} X_1'' + X_1 \frac{\partial X_1''}{\partial y} \right) + 2X_1' \frac{\partial X_1'}{\partial y} - \frac{\partial Y_1}{\partial y} \quad (4.2.11)$$

and

$$\frac{\partial Y_1''}{\partial y} = - \text{Pr} \left(\frac{\partial X_1}{\partial y} Y_1' + X_1 \frac{\partial Y_1'}{\partial y} \right)$$

with initial conditions

$$\eta = 0: \quad \frac{\partial X_1}{\partial y} = \frac{\partial X_1'}{\partial y} = \frac{\partial X_1''}{\partial y} = \frac{\partial Y_1}{\partial y} = 0, \quad \frac{\partial Y_1'}{\partial y} = 1.$$

Although, the equations for the y derivatives are the same as the equations for the x derivatives, but the integrals of these equations will differ since the initial conditions are different. It is also noted that there are as many system of

perturbation equations to integrate as there are asymptotic boundary conditions to meet.

Now, corrections to the initial conditions Δx and Δy so chosen that these four equations (4.2.2), (4.2.3), (4.2.8) and (4.2.9) are satisfied at $\eta = \eta_{\text{edge}}$. This is, in general, impossible since there are four equations and only two adjustable parameters. However, a satisfactory solution that is consistent with the idea that the boundary conditions can't be satisfied exactly at a finite value of η , is to seek least square solutions of those four equations.

4.3 NACHTSHEIM-SWIGERT ITERATION SCHEME

The method developed by Nachtsheim and Swigert [31] can be applied to these four equations to solve for Δx and Δy basing on least square error criteria. According to the method, Δx and Δy should be found such that, the sum of the squares of the error in these four equations must be minimum. Hence, considering discrepancies δ_1 , δ_2 , δ_3 and δ_4 in these equations respectively (deviations from their asymptotic values), where,

$$\begin{aligned}
 X_1' + \frac{\partial X_1'}{\partial x} \Delta x + \frac{\partial X_1'}{\partial y} \Delta y &= \delta_1 \\
 Y_1 + \frac{\partial Y_1}{\partial x} \Delta x + \frac{\partial Y_1}{\partial y} \Delta y &= \delta_2 \\
 X_1'' + \frac{\partial X_1''}{\partial x} \Delta x + \frac{\partial X_1''}{\partial y} \Delta y &= \delta_3 \\
 Y_1' + \frac{\partial Y_1'}{\partial x} \Delta x + \frac{\partial Y_1'}{\partial y} \Delta y &= \delta_4
 \end{aligned} \tag{4.3.1}$$

It is equivalent of saying that, the original equations (4.2.2)

and (4.2.3) along with the supplemented equations (4.2.6) and (4.2.7) are associated with these discrepancies δ_1 , δ_2 , δ_3 and δ_4 respectively. We have :

$$\begin{aligned}
 X_1' \text{ edge } [X_1''(0), Y_1'(0)] &= \delta_1 \\
 Y_1 \text{ edge } [X_1''(0), Y_1'(0)] &= \delta_2 \\
 X_1'' \text{ edge } [X_1''(0), Y_1'(0)] &= \delta_3 \\
 Y_1' \text{ edge } [X_1''(0), Y_1'(0)] &= \delta_4
 \end{aligned}
 \tag{4.3.2}$$

Solution of set of equations (4.3.1) in least square sense requires determination of minimum values of the error,

$$E = \delta_1^2 + \delta_2^2 + \delta_3^2 + \delta_4^2$$

So differentiating E with respect to x and y respectively and equating to zero i.e. we evaluate: For x derivatives,

$$\begin{aligned}
 \frac{\partial E}{\partial x} &= \frac{\partial}{\partial x} (\delta_1^2 + \delta_2^2 + \delta_3^2 + \delta_4^2) = 0. \text{ Substituting for } \delta_1^2, \delta_2^2, \\
 \delta_3^2 \text{ and } \delta_4^2 \text{ from the set of equations (4.3.1), we have after} \\
 \text{rearranging terms:} \\
 [(\frac{\partial X_1'}{\partial x})^2 + (\frac{\partial Y_1}{\partial x})^2 + (\frac{\partial X_1''}{\partial x})^2 + (\frac{\partial Y_1'}{\partial x})^2] \Delta x &+ [\frac{\partial X_1'}{\partial x} \frac{\partial X_1'}{\partial y} + \frac{\partial Y_1}{\partial x} \frac{\partial Y_1}{\partial y} \\
 + \frac{\partial X_1''}{\partial x} \frac{\partial X_1''}{\partial y} + \frac{\partial Y_1'}{\partial x} \frac{\partial Y_1'}{\partial y}] \Delta y &= - (X_1' \frac{\partial X_1'}{\partial x} + Y_1 \frac{\partial Y_1}{\partial y} + X_1'' \frac{\partial X_1''}{\partial x} + Y_1' \frac{\partial Y_1'}{\partial x})
 \end{aligned}
 \tag{4.3.3}$$

Similarly, for y derivative, equating $\frac{\partial E}{\partial y}$ to zero, and rearranging terms,

$$\begin{aligned}
& \left[\frac{\partial X_1'}{\partial x} \frac{\partial X_1'}{\partial y} + \frac{\partial Y_1}{\partial x} \frac{\partial Y_1}{\partial y} + \frac{\partial X_1''}{\partial x} \frac{\partial X_1''}{\partial y} + \frac{\partial Y_1''}{\partial x} \frac{\partial Y_1'}{\partial y} \right] \Delta x + \left[\left(\frac{\partial X_1'}{\partial y} \right)^2 + \left(\frac{\partial Y_1}{\partial y} \right)^2 \right. \\
& \left. + \left(\frac{\partial X_1''}{\partial y} \right)^2 + \left(\frac{\partial Y_1'}{\partial y} \right)^2 \right] \Delta y = - \left(X_1' \frac{\partial X_1'}{\partial y} + Y_1 \frac{\partial Y_1}{\partial y} + X_1'' \frac{\partial X_1''}{\partial y} + Y_1' \frac{\partial Y_1'}{\partial y} \right)
\end{aligned}
\tag{4.3.4}$$

Equations (4.3.3) and (4.3.4) can be written as a system of linear equations in two unknowns in a simplified form.

$$\begin{aligned}
A_{xx} \Delta x + A_{xy} \Delta y &= B_1 \\
A_{xy} \Delta x + A_{yy} \Delta y &= B_2
\end{aligned}
\tag{4.3.5}$$

and in matrix notation,

$$\begin{pmatrix} A_{xx} & A_{xy} \\ A_{xy} & A_{yy} \end{pmatrix} \begin{pmatrix} \Delta x \\ \Delta y \end{pmatrix} = \begin{pmatrix} B_1 \\ B_2 \end{pmatrix}$$

where,

$$\begin{aligned}
A_{xx} &= \left(\frac{\partial X_1'}{\partial x} \right)^2 + \left(\frac{\partial Y_1}{\partial x} \right)^2 + \left(\frac{\partial X_1''}{\partial x} \right)^2 + \left(\frac{\partial Y_1'}{\partial x} \right)^2 \\
A_{xy} &= \left(\frac{\partial X_1'}{\partial x} \frac{\partial X_1'}{\partial y} + \frac{\partial Y_1}{\partial x} \frac{\partial Y_1}{\partial y} + \frac{\partial X_1''}{\partial x} \frac{\partial X_1''}{\partial y} + \frac{\partial Y_1'}{\partial x} \frac{\partial Y_1'}{\partial y} \right) \\
A_{yy} &= \left(\frac{\partial X_1'}{\partial y} \right)^2 + \left(\frac{\partial Y_1}{\partial y} \right)^2 + \left(\frac{\partial X_1''}{\partial y} \right)^2 + \left(\frac{\partial Y_1'}{\partial y} \right)^2 \\
B_1 &= - \left(X_1' \frac{\partial X_1'}{\partial x} + Y_1 \frac{\partial Y_1}{\partial x} + X_1'' \frac{\partial X_1''}{\partial x} + Y_1' \frac{\partial Y_1'}{\partial x} \right) \\
B_2 &= - \left(X_1' \frac{\partial X_1'}{\partial y} + Y_1 \frac{\partial Y_1}{\partial y} + X_1'' \frac{\partial X_1''}{\partial y} + Y_1' \frac{\partial Y_1'}{\partial y} \right)
\end{aligned}$$

Solving equations (4.3.5) for the two unknowns Δx and Δy , we have,

$$\Delta x = \frac{B_1 A_{yy} - B_2 A_{xy}}{A_{xx} A_{yy} - A_{xy}^2} \quad (4.3.6)$$

and

$$\Delta y = \frac{A_{xx} B_2 - B_1 A_{xy}}{A_{xx} A_{yy} - A_{xy}^2} \quad (4.3.7)$$

This calculation yields values of Δx and Δy corresponding minimum of the sum $\delta_1^2 + \delta_2^2 + \delta_3^2 + \delta_4^2$. The magnitude of error E , evaluated for a given range of independent variable approached in steps, gives an indication how unsatisfactory the asymptotic boundary conditions are. The error term can also be written as

$$E = X_1'^2 + Y_1^2 + X_1''^2 + Y_1'^2 \quad (4.3.8)$$

The minimum of E with respect to x and y , say E_{\min} , corresponds to no deviations in the required initial conditions, that permits the asymptotic boundary conditions to be approximately satisfied at a finite value of the independent variable. The edge of the boundary layer, taken to be some guessed value of η consistent with our assumptions, for which E_{\min} is less than some preassigned small value for this range of integration, gives the desired solutions.

These modifications to the initial value method come from the corrections to the initial conditions given by equations (4.3.6) and (4.3.7) in a least square sense. These are generalized correction formulas and can be applied to any system of coupled third order differential equations, if the subscript '1' associated with X and Y is ignored. However, the main difference

lies with the evaluation of corresponding partial derivatives involved in correction equations, which would be different for different set of equations and also correspondingly their perturbation equations.

Application to systems of equations (3.2.21) and (3.2.22):

In primed notations as stated before, these equations can be rewritten as:

$$\begin{aligned} X_2''' &= - (X_1 X_2'' - 4X_1' X_2' + 3X_1'' X_2 - Y_2) \\ Y_2'' &= - \text{Pr} (X_1 Y_2' - 2X_1' Y_2 + 3Y_1' X_2) \end{aligned} \quad (4.3.9)$$

with boundary conditions:

$$\begin{aligned} \eta = 0, \quad X_2 = X_2' = 0, \quad Y_2 = 1 \\ \eta \rightarrow \infty, \quad X_2' \rightarrow 0 \quad Y_2 \rightarrow 0 \end{aligned}$$

and,

$$\begin{aligned} X_3''' &= - (X_1 X_3'' - 4X_1' X_3' + 3X_3 X_1'' + Y_3 - \frac{1}{6} Y_1) \\ Y_3'' &= - \text{Pr} (X_1 Y_3' - 2X_1' Y_3 + 3X_3 Y_1') \end{aligned} \quad (4.3.10)$$

with boundary conditions:

$$\begin{aligned} \eta = 0, \quad X_3 = X_3' = 0, \quad Y_3 = 0 \\ \eta \rightarrow \infty, \quad X_3' \rightarrow 0 \quad Y_3 \rightarrow 0 \end{aligned}$$

In the above equations, dependent variables each. These equations can only be solved by knowing the solution, namely, the values of corrected initial conditions $X_1''(0)$ and $Y_1(0)$ of

equation (2.4.1). Method of solution of these equations is exactly same as given in the foregoing analysis, once the values of the initial conditions are evaluated. The only difference lies with the evaluation of partial derivatives involved implicitly in the expressions (4.3.6) and (4.3.7), which would be different for different system of coupled equations depending upon the integrals of corresponding perturbation equations.

The perturbation differential equations for the coupled equations (4.3.9) are obtained by differentiating original equations with respect to the initial conditions x and y , respectively. For x derivative,

$$\begin{aligned} \frac{\partial X_2'''}{\partial x} = & - \left(\frac{\partial X_1}{\partial x} X_2'' + X_1 \frac{\partial X_2''}{\partial x} - 4X_1' \frac{\partial X_2'}{\partial x} - 4 \frac{\partial X_1'}{\partial x} X_2' \right. \\ & \left. + 3 \frac{\partial X_1''}{\partial x} X_2 + 3X_1'' \frac{\partial X_2}{\partial x} - \frac{\partial Y_2}{\partial x} \right) \end{aligned} \quad (4.3.11)$$

$$\begin{aligned} \frac{\partial Y_2''}{\partial x} = & - \text{Pr} \left(X_1 \frac{\partial Y_2'}{\partial x} + Y_2' \frac{\partial X_1}{\partial x} - 2X_1' \frac{\partial Y_2}{\partial x} \right. \\ & \left. - 2 \frac{\partial X_1'}{\partial x} Y_2 + 3X_2 \frac{\partial Y_1'}{\partial x} + 3 \frac{\partial X_2}{\partial x} Y_1' \right) \end{aligned}$$

With initial conditions:

$$\eta=0: \quad \frac{\partial X_2}{\partial x} = \frac{\partial X_2'}{\partial x} = \frac{\partial Y_2}{\partial x} = \frac{\partial Y_2'}{\partial x} = 0, \quad \frac{\partial X_2''}{\partial x} = 1$$

$$\eta=0: \quad \frac{\partial X_1}{\partial x} = \frac{\partial X_1'}{\partial x} = \frac{\partial Y_1}{\partial x} = \frac{\partial Y_1'}{\partial x} = 0, \quad \frac{\partial X_1''}{\partial x} = 1$$

For y derivatives,

$$\begin{aligned} \frac{\partial^3 X_2}{\partial y} = & - \left(\frac{\partial X_1}{\partial y} X_2'' + X_1 \frac{\partial^2 X_2}{\partial y} - 4X_1' \frac{\partial X_2'}{\partial y} - 4 \frac{\partial X_1'}{\partial x} X_2' \right. \\ & \left. + 3 \frac{\partial X_1''}{\partial y} X_2 + 3X_1'' \frac{\partial X_2}{\partial y} - \frac{\partial Y_2}{\partial x} \right) \end{aligned} \quad (4.3.12)$$

$$\frac{\partial^2 Y_2}{\partial y} = -Pr \left(X_1 \frac{\partial Y_2'}{\partial y} + Y_2' \frac{\partial X_1}{\partial y} + 3X_2 \frac{\partial Y_1'}{\partial x} + 3 \frac{\partial X_2}{\partial x} Y_1' \right)$$

With initial conditions:

$$\eta=0: \quad \frac{\partial X_2}{\partial y} = \frac{\partial X_2'}{\partial y} = \frac{\partial^2 X_2}{\partial y} = \frac{\partial Y_2}{\partial y} = 0, \quad \frac{\partial Y_2'}{\partial y} = 1$$

$$\eta=0: \quad \frac{\partial X_1}{\partial y} = \frac{\partial X_1'}{\partial y} = \frac{\partial^2 X_1}{\partial y} = \frac{\partial Y_1}{\partial y} = 0, \quad \frac{\partial Y_1'}{\partial y} = 1$$

Similarly, the perturbation differential equations for the system of coupled differential equations (4.3.10) are as follows:

For x derivative,

$$\begin{aligned} \frac{\partial^3 X_3}{\partial x} = & - \left(\frac{\partial X_1}{\partial x} X_3'' + X_1 \frac{\partial^2 X_3}{\partial x} - 4X_1' \frac{\partial X_3'}{\partial x} - 4 \frac{\partial X_1'}{\partial x} X_3' \right. \\ & \left. + 3 \frac{\partial X_1''}{\partial x} X_3 + 3X_1'' \frac{\partial X_3}{\partial x} + \frac{\partial X_3}{\partial x} - \frac{1}{6} \frac{\partial Y_1}{\partial x} \right) \end{aligned} \quad (4.3.13)$$

$$\begin{aligned} \frac{\partial^2 Y_3}{\partial x} = & -Pr \left(X_1 \frac{\partial Y_3'}{\partial x} + Y_3' \frac{\partial X_1}{\partial x} - 2 \frac{\partial X_1'}{\partial x} Y_3 - 2X_1' \frac{\partial Y_3}{\partial x} \right. \\ & \left. + 3X_3 \frac{\partial Y_1'}{\partial x} + 3 \frac{\partial X_3}{\partial x} Y_1' \right) \end{aligned}$$

With initial conditions:

$$\eta=0: \quad \frac{\partial X_3}{\partial x} = \frac{\partial X_3'}{\partial x} = \frac{\partial Y_3}{\partial x} = \frac{\partial Y_3'}{\partial x} = 0, \quad \frac{\partial X_3''}{\partial x} = 1$$

$$\eta=0: \quad \frac{\partial X_1}{\partial x} = \frac{\partial X_1'}{\partial x} = \frac{\partial Y_1}{\partial x} = \frac{\partial Y_1'}{\partial x} = 0, \quad \frac{\partial X_1''}{\partial x} = 1$$

For y derivatives:

$$\begin{aligned} \frac{\partial X_3'''}{\partial y} = & -\left(\frac{\partial X_1}{\partial y} X_3'' + X_1 \frac{\partial X_3''}{\partial y} - 4X_1' \frac{\partial X_3'}{\partial y} - 4 \frac{\partial X_1'}{\partial y} X_3' \right. \\ & \left. + 3 \frac{\partial X_1''}{\partial y} X_3 + 3X_1'' \frac{\partial X_3}{\partial y} + \frac{\partial Y_3}{\partial y} - \frac{1}{6} \frac{\partial Y_1}{\partial y}\right) \end{aligned} \quad (4.3.14)$$

$$\begin{aligned} \frac{\partial Y_3''}{\partial y} = & -Pr\left(X_1 \frac{\partial Y_3'}{\partial y} + Y_3' \frac{\partial X_1}{\partial y} - 2 \frac{\partial X_1'}{\partial y} Y_3 - 2X_1' \frac{\partial Y_3}{\partial y} \right. \\ & \left. + 3X_3 \frac{\partial Y_1'}{\partial y} + 3 \frac{\partial X_3}{\partial y} Y_1\right) \end{aligned}$$

with initial conditions:

$$\eta=C: \quad \frac{\partial X_3}{\partial y} = \frac{\partial X_3'}{\partial y} = \frac{\partial X_3''}{\partial y} = \frac{\partial Y_3}{\partial y} = 0, \quad \frac{\partial Y_3'}{\partial y} = 1,$$

$$\eta=0: \quad \frac{\partial X_1}{\partial y} = \frac{\partial X_1'}{\partial y} = \frac{\partial X_1''}{\partial y} = \frac{\partial Y_1}{\partial y} = 0, \quad \frac{\partial Y_1'}{\partial y} = 1.$$

As stated previously, the partial derivatives with respect to x and y, that appears in the generalized correction equations (4.3.6) and (4.3.7) can be evaluated for these system of equations by integrating corresponding perturbation equations for the functions X_2' , X_2'' , Y_2 , Y_2' and X_3' , X_3'' , Y_3 , Y_3' respectively.

4.4 COMPUTATIONAL PROCEDURE

Usually, a boundary value problem is recasted as an initial value problem by the application of initial value method. Hence, the boundary layer and corresponding perturbation differential equations were rewritten as equivalent systems of first order differential equations. With proper initial guesses these were integrated by fourth order Runge-Kutta method for first three values and subsequently, Adams-Moulton predictor-corrector method was applied for one correction per step and a fixed increment. The corrections to the initial conditions Δx and Δy , which involves integrals of perturbation equations were determined. The process was repeated until the relative changes in the correction terms Δx and Δy are less than small pre-assigned values. Least square error was found out and tested with a small pre-assigned value. Previous guesses were corrected and the whole process was repeated until the desired accuracy was achieved, i.e. the least square error was found less than a small preassigned value.

The set of equations (4.2.1) and its' associated perturbation differentials equations (4.2.10) and (4.2.11), which are all third order in η , can be expressed as an equivalent system of fifteen first order differential equations with five equations coming from each set. Thirteen initial conditions in total are known, and two more conditions are to be guessed as initial estimates. These equations subject to the given numerical method, lends to the solution within desired accuracy.

The two other sets of coupled equations of the boundary layer respectively (4.3.9) and (4.3.10), with their corresponding perturbation differential equations (4.3.11), (4.3.12), (4.3.13) and (4.3.14) can be expressed as an equivalent system of twentyfour first order differential equation for each set. This is because each of the set of equations constitutes four dependent variables. Because of the involvement of the dependent variables X_1 and Y_1 in these equations, the number of initial conditions required to start with, are twenty eight and two conditions are guessed as before for each set. These initial conditions comprise all the given conditions required for the solution of equations (4.2.1), besides their own initial conditions. The solutions of equations (4.2.1) achieved by the method just outlined in the foregoing paragraphs, one had in particular good approximations for $X_1''(0)$ and $Y_1'(0)$. These values are then used as a complete information of the initial conditions required for the subsequent solutions of equations (4.2.10) and (4.2.11). The computational technique is exactly the same for these equations.

The method described above was programmed in FORTRAN IV on the DEC-10 Computer system. A general flow chart (Fig. 5.1) is presented for the main program adapted for all the system of equations. The flow chart of integration subroutine is presented in the Fig. 5.2. The FORTRAN listings of the method are enclosed in the appendix D. The integration formulas, used in the integration subroutine are also given in Appendix B.

4.5 RESULTS

With trial initial guesses 0.60 and -0.50 for $\frac{d^2X_1(o)}{d\eta^2}$ and $\frac{dY_1(o)}{d\eta}$ respectively, the set of equations (4.2.1) were integrated to a value of η_{edge} equal to 5.0 with initial step size of 0.05 for first four steps and subsequently raised to 0.1 for further steps. The preassigned values to compare least square error and increments in the initial estimates in the iteration process was kept 0.005 and 0.005 respectively. The final results are quoted in Table II. From this solution, we have in particular better approximations for $\frac{d^2X_1(o)}{d\eta^2} = 0.796700$ and $\frac{dY_1(o)}{d\eta} = -0.438100$. The least square error was found out to be 0.000972.

These values are utilized further to integrate the other two sets of equations (4.3.9) and (4.3.10) with the initial step size of 0.05 for first four steps and subsequently raised to 0.1 for further steps, for the same range of the value of η_{edge} i.e. 5.0. The initial values $\frac{d^2X_2(o)}{d\eta^2}$ and $\frac{dY_2(o)}{d\eta}$, corresponding to the solution of set of equations (4.3.9) are 0.004316 and -0.054234 respectively. The initial values of $\frac{d^2X_3(o)}{d\eta^2}$ and $\frac{dY_3(o)}{d\eta}$, corresponding to the solution of set of equations (4.3.10) are 0.008510 and 0.001510 respectively.

Solutions of equations (4.2.1) give approximately the velocity and temperature profile and their corresponding gradients in the adjacent boundary layer. These are plotted in figures 4.1 through (4.4) respectively. The perturbations to

the velocity and temperatures comes from the solutions of sets of equations (4.3.9) and (4.3.10) are plotted in figures (4.5) through (4.8).

The set of equation (3.2.27) are rewritten with the value of Grashoff number substituted from the data given in Appendix III as follows:

$$Nu_D = -(0.4262 \times 10^8)^{1/4} \left[\frac{dY_1(o)}{d\eta} + \bar{x}^2 \left(a \frac{dY_2(o)}{d\eta} + \frac{dY_3(o)}{d\eta} \right) \right] \quad (4.5.1)$$

for non-linear variation of the temperature,

$$Nu_D = -(0.4262 \times 10^8)^{1/4} \left[\frac{dY_1(o)}{d\eta} + \bar{x} \left(a \frac{dY_2(o)}{d\eta} + \frac{dY_3(o)}{d\eta} \right) \right] \quad (4.5.2)$$

for linear variation of temperature,

$$Nu_D = -(0.4262 \times 10^8)^{1/4} \left[\frac{dY_1(o)}{d\eta} + \bar{x} \frac{dY_3(o)}{d\eta} \right] \quad (4.5.3)$$

for isothermal case, when $a = 0$.

Now, the dimensionless heat transfer, i.e. Nusselt number can be computed from the above equations utilizing the solution of boundary layer equations with respect to the dimensionless distance. Three cases of non-isothermal conditions are considered with three different values of a taken as 0.1, 0.5 and 2.5 respectively. The results are tabulated in table III and (IV) and corresponding plots are displayed in figures (4.9) through (4.12).

η in steps	X_1	X_1'	X_1''	Y_1	Y_1'
0.0000	0.00000000	0.00000000	0.79670000	1.00000000	-0.43810000
0.0500	0.00081756	0.04043711	0.74118671	0.97218671	-0.43804183
0.1000	0.00381879	0.07474550	0.69898994	0.95619158	-0.43803864
0.1500	0.00134321	0.10237435	0.65795813	0.93721567	-0.43784128
0.2000	0.01463159	0.13996232	0.60620739	0.91240416	-0.43762473
0.3000	0.03151091	0.19616526	0.51877114	0.86868884	-0.43654889
0.4000	0.05358281	0.24390416	0.43697600	0.82512514	-0.43454978
0.5000	0.08002921	0.28375378	0.36100693	0.78181656	-0.43141548
0.6000	0.11009054	0.31630196	0.29095379	0.73888508	-0.42698513
0.7000	0.14306626	0.34214126	0.22682333	0.69646619	-0.42114964
0.8000	0.17831503	0.36186126	0.16855065	0.65470369	-0.41385131
0.9000	0.21525402	0.37604189	0.11600961	0.61374470	-0.40508199
1.0000	0.25335769	0.38524783	0.06902254	0.57373477	-0.39487986
1.1000	0.29215598	0.39002376	0.02736919	0.53481352	-0.38332460
1.2000	0.33123216	0.39089059	-0.00920497	0.49711079	-0.37053164
1.3000	0.37022025	0.38834237	-0.04098105	0.46074333	-0.35664531
1.4000	0.40880224	0.38284402	-0.06825965	0.42581234	-0.34183161
1.5000	0.44670511	0.37482967	-0.09135439	0.39240164	-0.32627084

Contd...

η in steps	X_L	X_L'	X_L''	Y_L	Y_L'
1. 6000	0.48369763	0.36470171	-0.11058603	0.36057659	-0.31015044
1. 7000	0.51958722	0.35283032	-0.12627725	0.33038375	-0.29365838
1. 8000	0.55421671	0.33955349	-0.13874800	0.30185107	-0.27697737
1. 9000	0.61922462	0.30997792	-0.15527107	0.24979029	-0.24372476
2. 0000	0.64943731	0.29420041	-0.15991703	0.22623429	-0.22745360
2. 1000	0.67805253	0.27806245	-0.16252492	0.20428601	-0.21158983
2. 2000	0.70504399	0.26175475	-0.16335370	0.18389934	-0.19623740
2. 3000	0.73040319	0.24544301	-0.16264469	0.16501875	-0.18148089
2. 4000	0.75413705	0.22926970	-0.16062095	0.14758120	-0.16738602
2. 5000	0.77626564	0.21335590	-0.15748702	0.13151799	-0.15400085
2. 6000	0.79682014	0.19780318	-0.15342903	0.11675643	-0.14135718
2. 7000	0.81584099	0.18269538	-0.14861511	0.10322137	-0.12947235
2. 8000	0.83337620	0.16810042	-0.14319597	0.09083661	-0.11835100
2. 9000	0.84947985	0.15407198	-0.13730573	0.07952602	-0.10798703
3. 0000	0.86421075	0.14065112	-0.13106288	0.06921455	-0.09836541
3. 1000	0.87763123	0.12786778	-0.12457126	0.05982902	-0.08946388
3. 2000	0.88980615	0.11574224	-0.11792115	0.05129877	-0.08125462
3. 3000	0.90080193	0.10428633	-0.11119043	0.04355615	-0.07370564
3. 4000	0.91068583	0.09350470	-0.10444562	0.03653684	-0.06678207
3. 5000	0.91952524	0.08339587	-0.09774298	0.03018015	-0.06044725
3. 6000	0.92738716	0.07395320	-0.09112958	0.02442905	-0.05466363

η in steps	x_1	x_1'	x_1''	y_1	y_1'
3.7000	0.93433768	0.06516575	-0.08464424	0.01923032	-0.04939357
3.8000	0.94044163	0.05701909	-0.07831853	0.01453447	-0.04459990
3.9000	0.94576225	0.04949594	-0.07217756	0.01029568	-0.04024643
4.0000	0.95036092	0.04257681	-0.05524084	0.00647168	-0.03629832
4.1000	0.95429701	0.03624052	-0.06052298	0.00302362	-0.03272231
4.2000	0.95762768	0.03046461	-0.05503439	0.00208414	-0.02948695
4.3000	0.96040782	0.02522580	-0.04978181	0.00188415	-0.02656265
4.4000	0.96268994	0.02050029	-0.04476893	0.00140612	-0.02392178
4.5000	0.96362121	0.01806210	-0.04036812	0.00081752	-0.02272165
4.6000	0.96452418	0.01626402	-0.03999682	0.00067710	-0.02153864
4.7000	0.96595825	0.01249296	-0.03546437	0.00052166	-0.01938947
4.8000	0.96703748	0.00916327	-0.031116865	0.00045620	-0.01745237
4.9000	0.96780483	0.00251501	-0.00410525	0.00021854	-0.01570722
5.0000	0.96830094	0.00105468	-0.00126859	0.00010931	-0.01413561

LEAST SQUARE ERROR IS GIVEN AS = 0.000972

INITIAL ESTIMATES : $x_1''(0) = 0.796700$

$y_1'(0) = -0.438100$

Table III

Nusselt Number for isothermal and non-isothermal
surface conditions on the fuel rod
($a = 0.0$, $a = 0.1$)

Dimensionless distance from the origin \bar{x}	Isothermal surface condition $a = 0.0$	Nusselt number for non-isothermal surface conditions $a = 0.1$	
		Temperature vation of the form $\phi = 1+a\bar{x}$ (linear)	Temperature vation of the form $\phi = 1+a\bar{x}^2$ (non-linear)
0.0	35.399	35.399	35.399
0.1	35.393	35.609	35.415
0.2	35.387	35.822	35.479
0.3	35.380	36.043	35.587
0.4	35.371	36.256	35.739
0.5	35.365	36.472	35.933
0.6	35.357	36.688	36.171
0.7	35.349	36.905	36.451
0.8	35.341	37.119	36.774
0.9	35.328	37.336	37.142
1.0	35.315	37.551	37.551
1.1	35.301	37.788	38.004
1.2	35.286	37.982	38.512
1.3	35.269	38.198	39.151
1.4	35.249	38.414	39.881
1.5	35.223	38.629	40.491

Table IV

Nusselt number for non-isothermal
surface conditions on the fuel rod
($a = 0.5$, $a = 2.5$)

Dimensionless distance from origin $X \bar{x}$	Nusselt Number			
	$a = 0.5$		$a = 2.5$	
	Temperature variation of the form $\phi = (1+a\bar{x})$ (linear)	Temperature variation of the form $\phi = (1+a\bar{x}^2)$ (Non-linear)	Temperature variation of the form $\phi = (1+a\bar{x})$ (linear)	Temperature variation of the form $\phi = (1+a\bar{x}^2)$ (Non-linear)
0.0	35.399	35.399	35.399	35.399
0.1	35.837	35.437	36.517	35.505
0.2	36.281	35.571	37.649	36.845
0.3	36.724	35.793	38.777	36.409
0.4	37.168	36.103	39.905	37.198
0.5	37.611	36.502	41.033	38.213
0.6	38.055	36.990	42.161	39.452
0.7	38.498	37.567	43.288	40.120
0.8	39.942	38.232	44.416	42.612
0.9	39.385	38.986	45.544	44.529
1.0	39.829	39.829	46.672	46.672
1.1	40.273	40.760	47.800	49.040
1.2	40.716	41.781	48.928	51.634
1.3	41.160	42.889	50.055	54.454
1.4	41.603	44.081	51.183	57.499
1.5	42.047	45.328	52.311	60.770

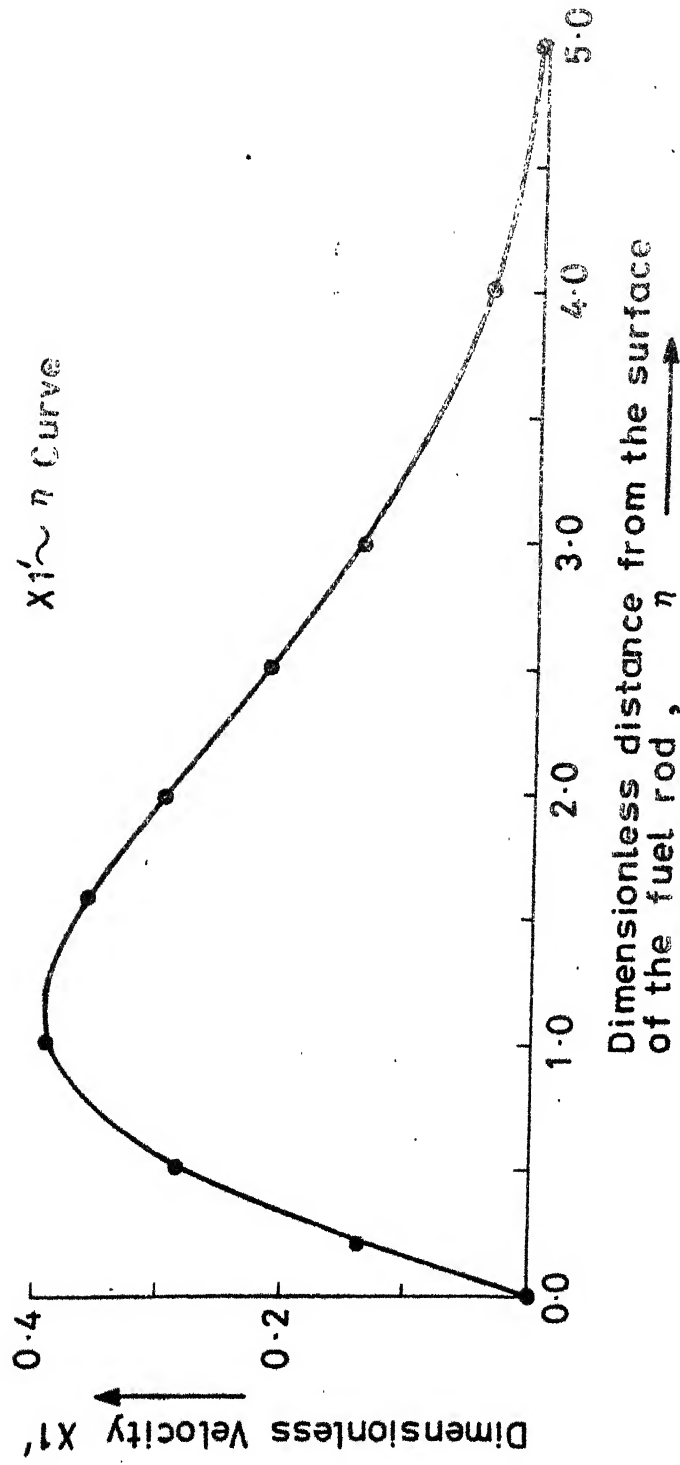


Fig. 4-1 Velocity Distribution in the boundary layer

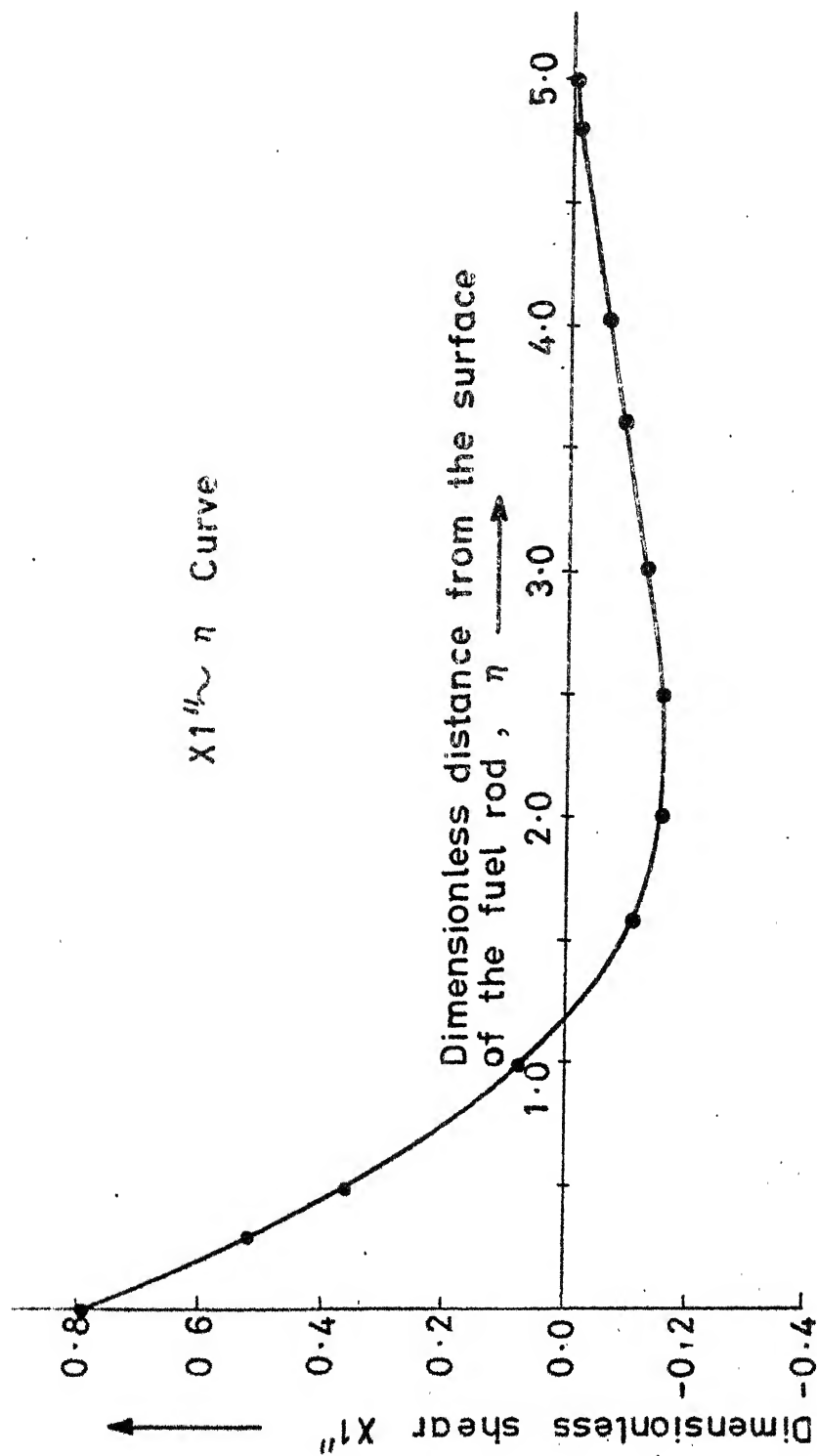


Fig. 4.2 Distribution of shear in the boundary layer

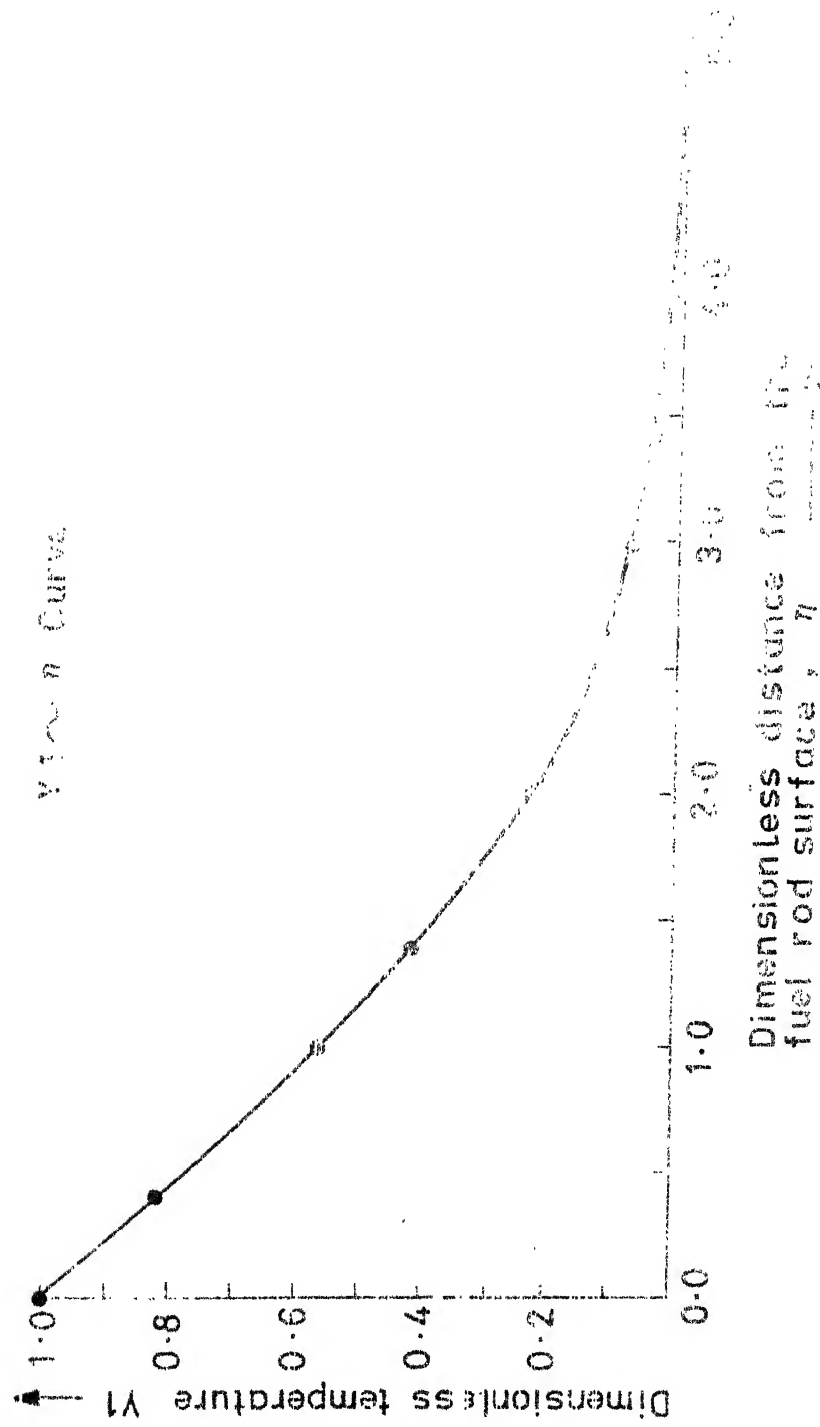


Fig. 4-3 Temperature distribution in the boundary layer

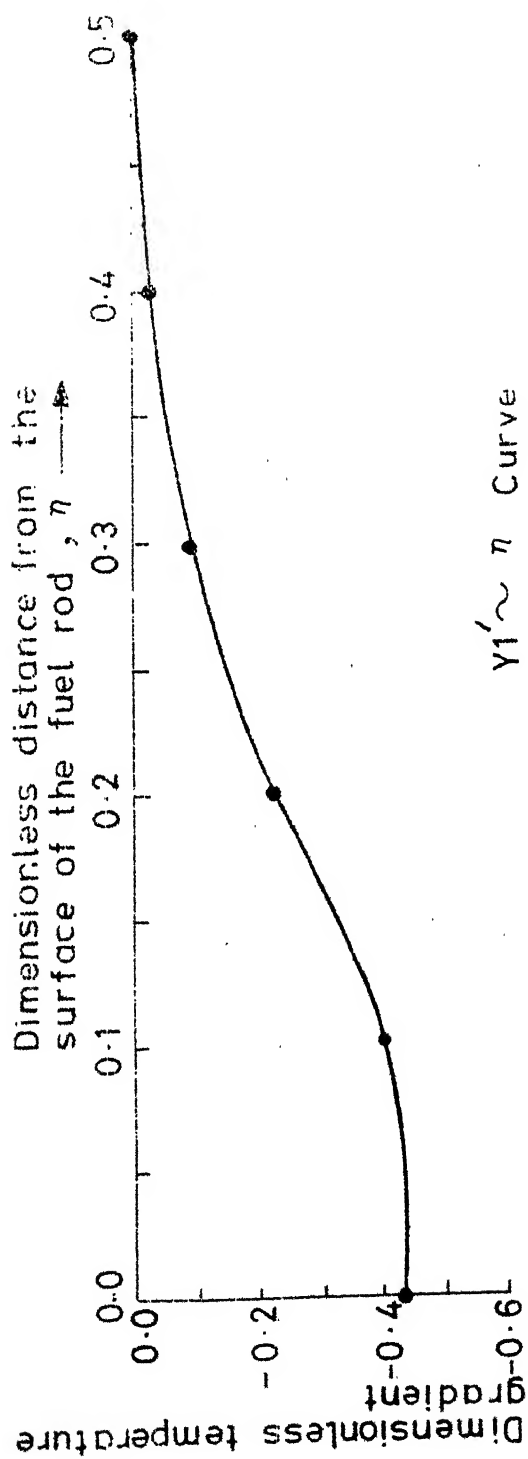


Fig. 4.4 Variation of temperature gradient

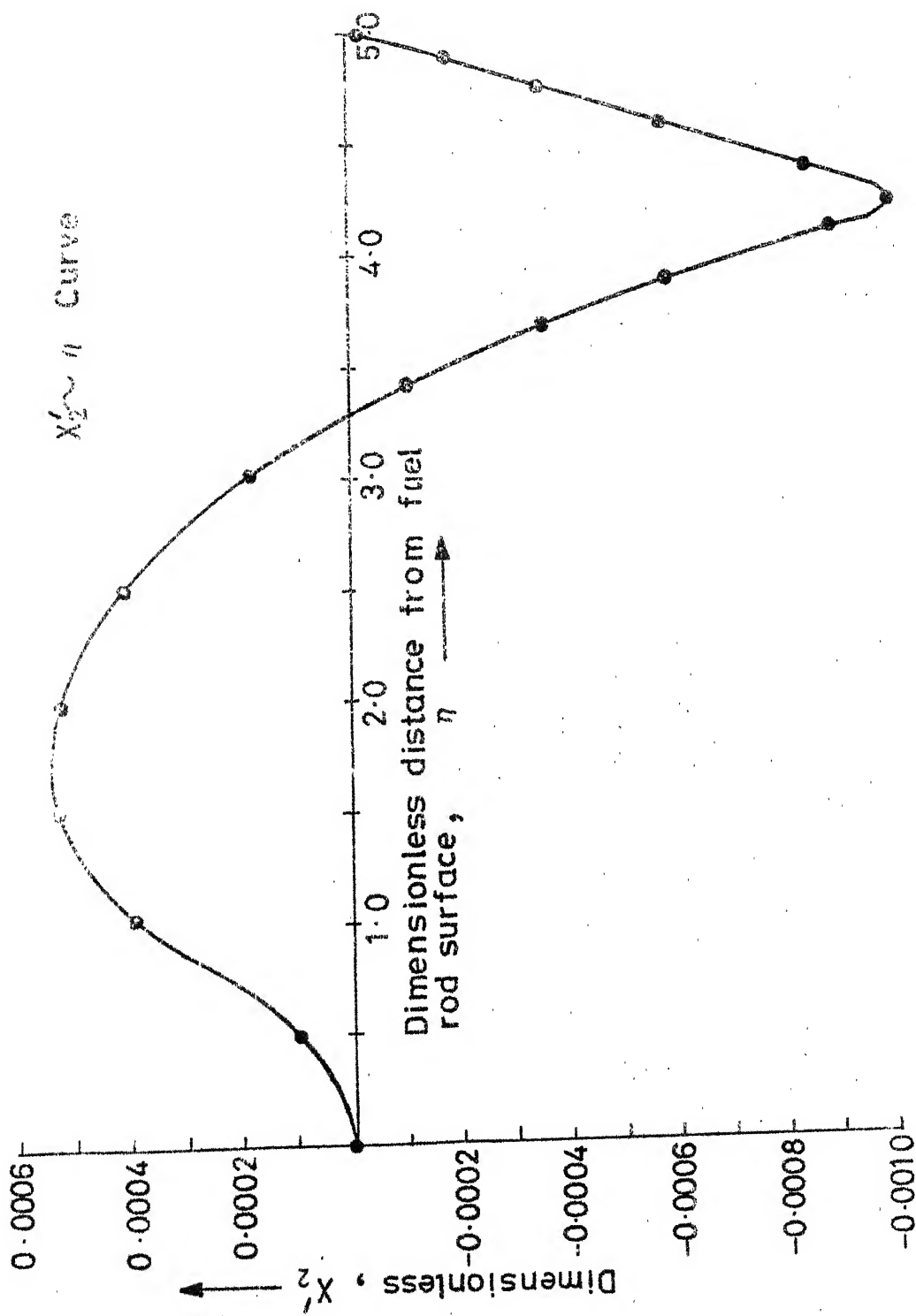


Fig. 4.5 Perturbations to the dimensionless velocity

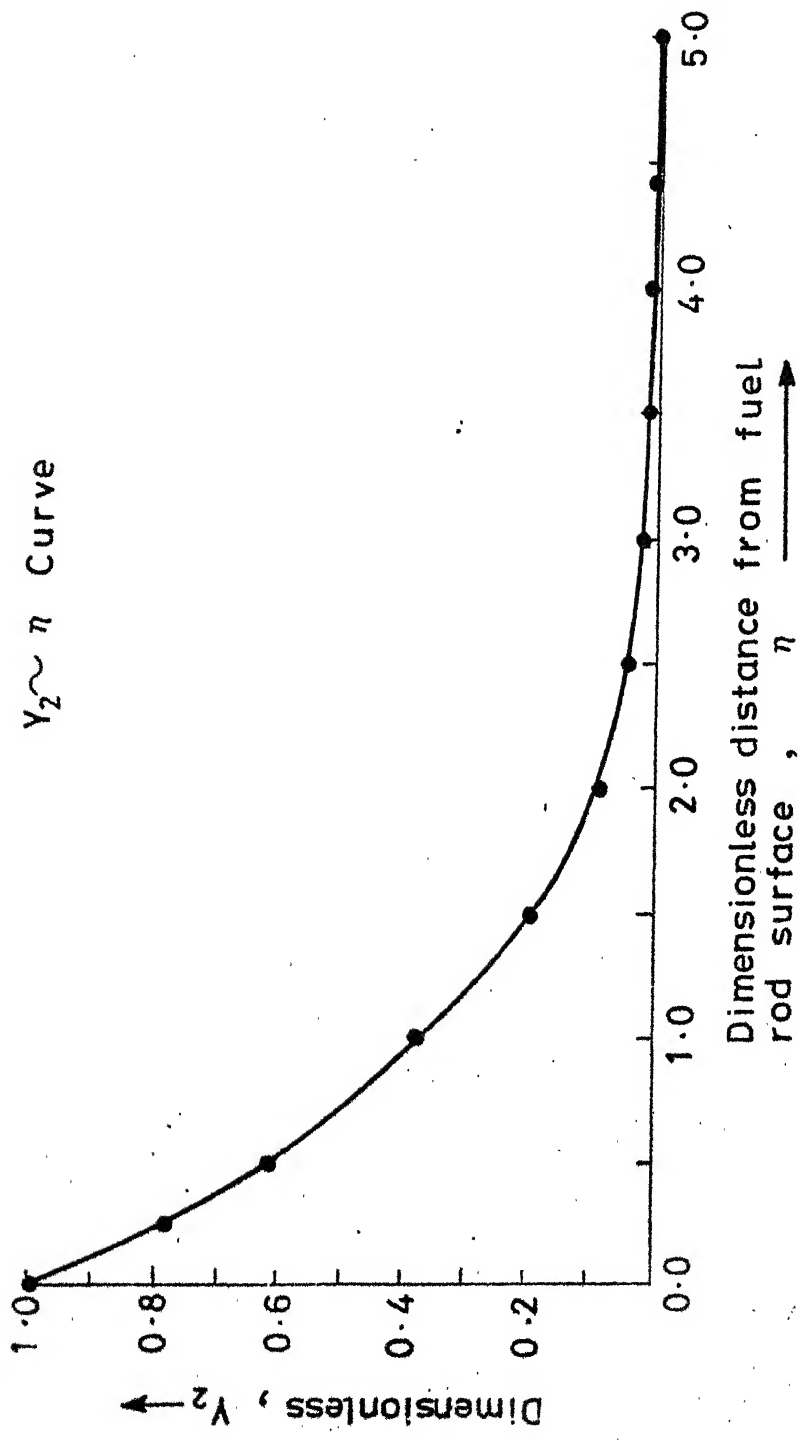


Fig. 4.6 Perturbations to the dimensionless temperature ∞

Fig. 4-7

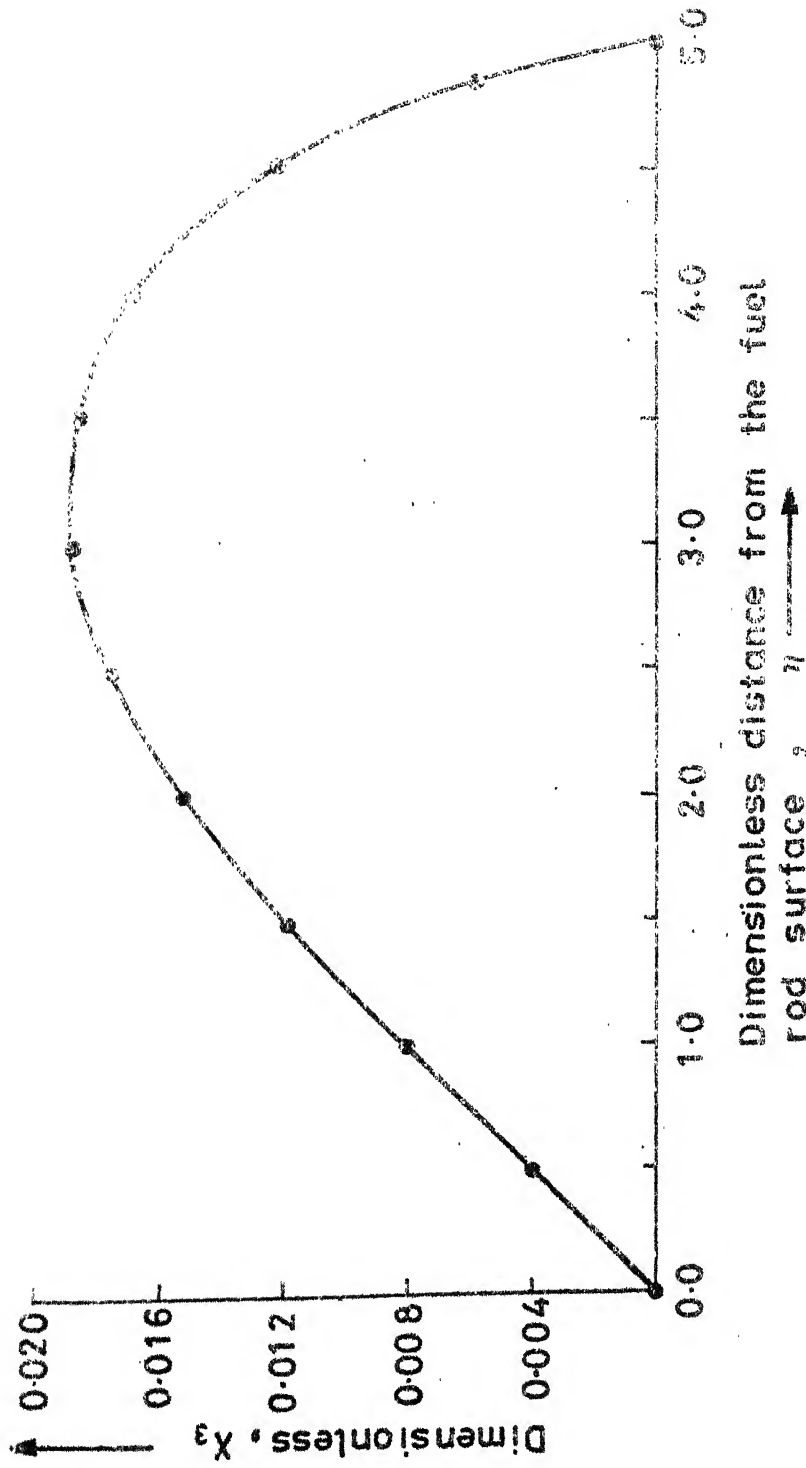


Fig. 4-7 Perturbations to the dimensionless velocity ∞

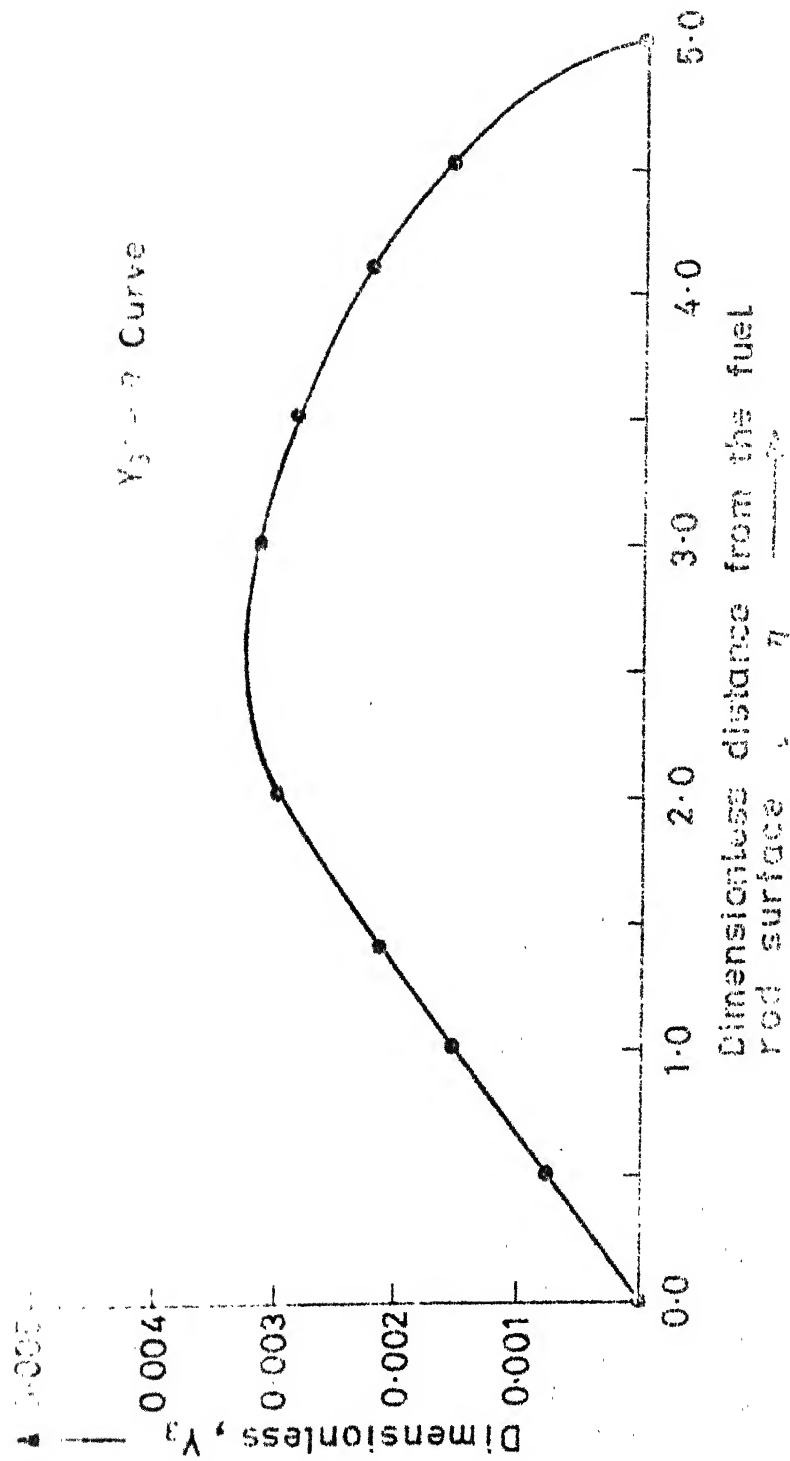
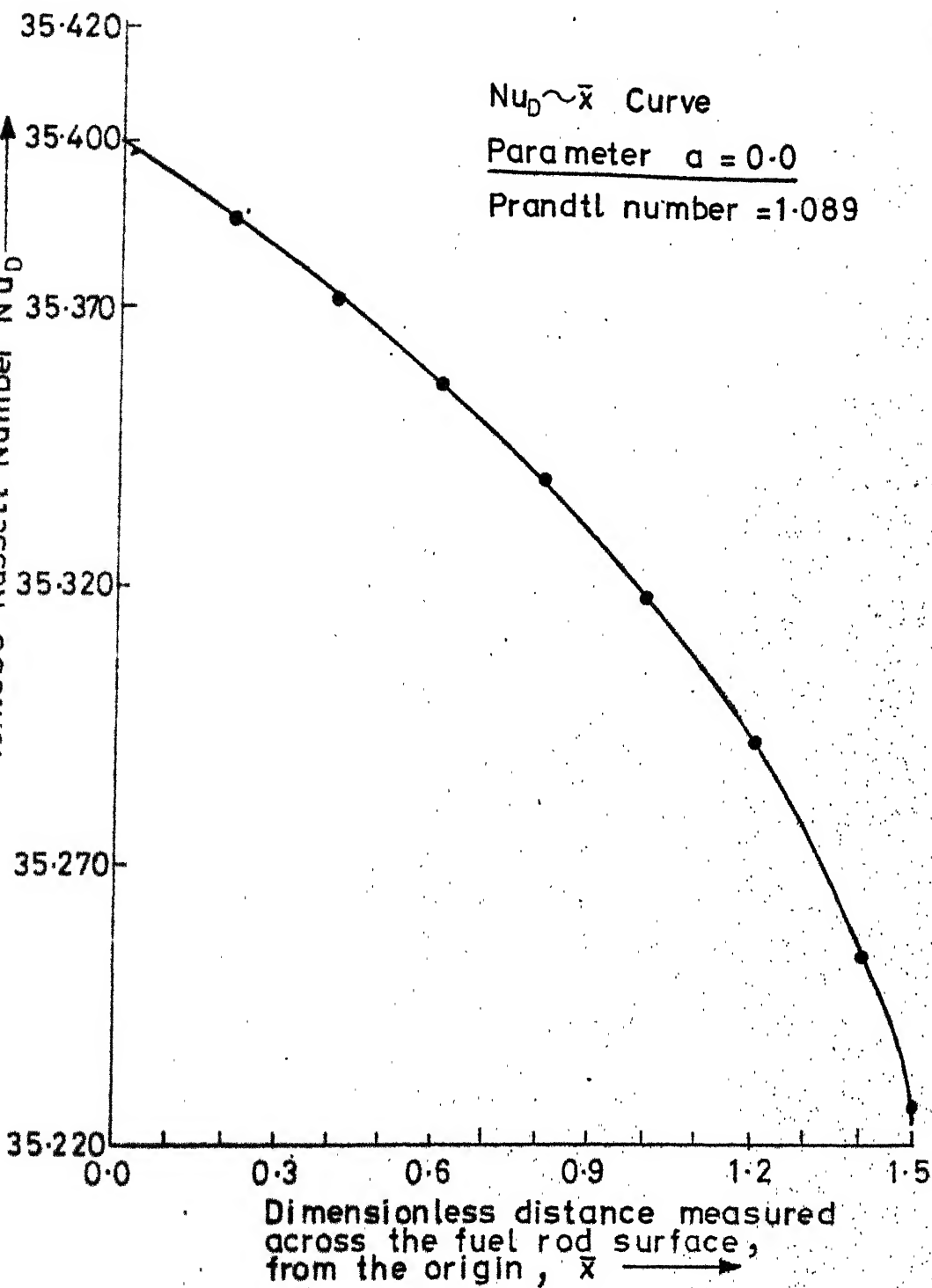


Fig. 4.8 Perturbations to the dimensionless temperature



g. 4.9 Isothermal surface condition on the fuel rod

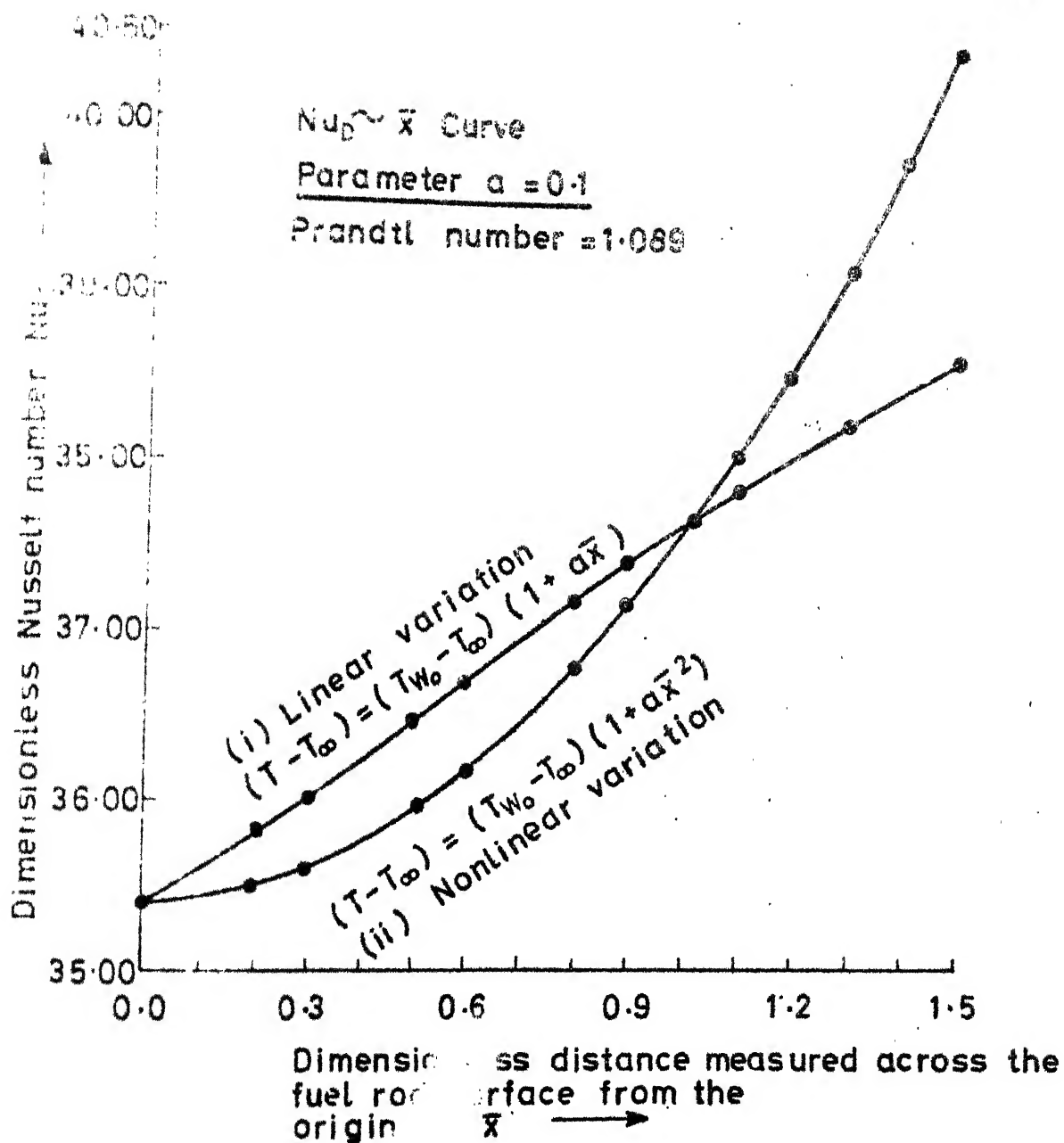


Fig. 4-10 Non isothermal surface condition on the fuel rod for $a = 0.1$

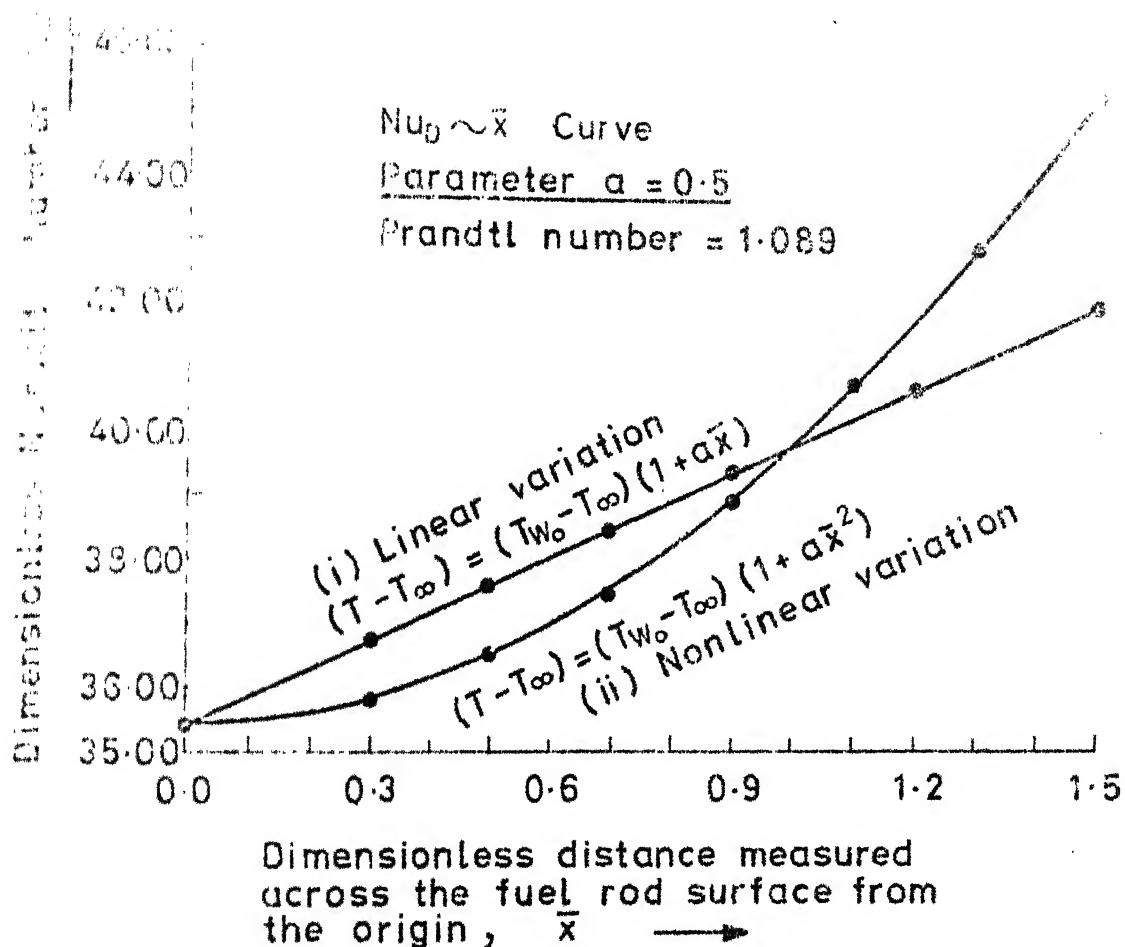


Fig. 4.11 Non-isothermal surface condition on the fuel rod for $a = 0.5$

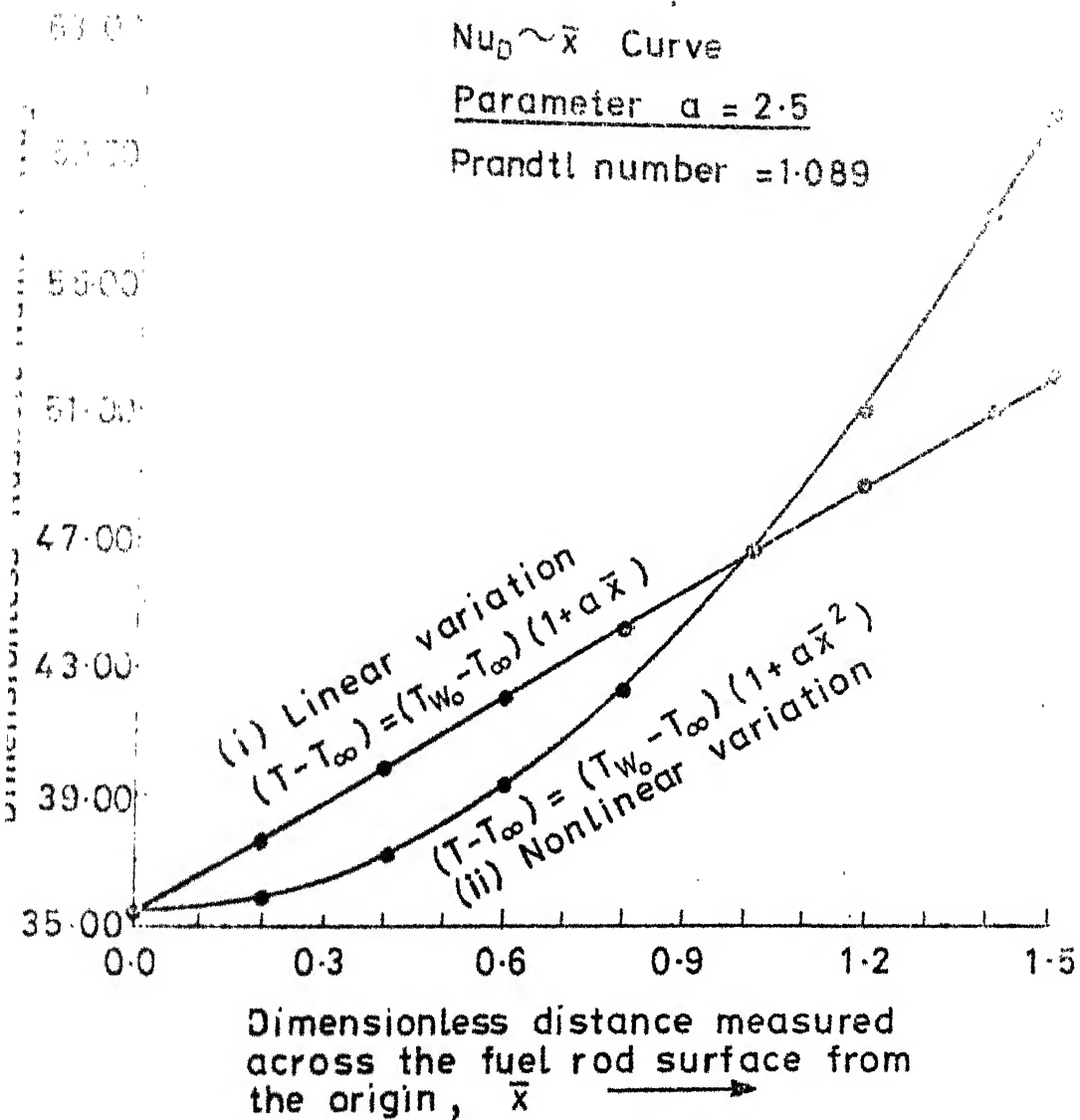


Fig. 4.12 Nonisothermal surface condition on the fuel rod for $a = 2.5$

CHAPTER V

DISCUSSION OF RESULTS AND CONCLUSION

5.1 DISCUSSION OF RESULTS

The preponderance of the preceeding chapters are devoted to study the problem of transient flow and temperature behaviour associated with loss-of-flow accident in a CANDU Reactor core and principally following the transient, the thermosyphon (Natural convection) cooling effects are assessed in situations, when there is a variation of temperature on the fuel rod surface.

The results leading to a flow coastdown curve, Fig. 2.2, represents situations when pump flywheel inertia is large. Consequently, the pump will continue to circulate the fluid for a substantial length of time and the flow coastdown will be relatively slow. Following the total loss of pumping power, the driving pressure is found incapable of establishing natural circulation in the primary circuit.

The temperature distribution in the core under the transient condition, induced by loss-of-flow accident, assuming an initial sinusoidal heat flux distribution can be known from the solution of the transient heat conduction equation as cited in the equation (3.1.25). The steady state temperature distribution of the core follows from the same equation, when time is considered very large.

The natural convection thermosyphon results leading to velocity and temperature profiles show an asymptotic decrease as the edge of the boundary layer is approached. The thermosyphoning effects are attributed to the velocity distribution in the boundary layer. Nusselt number is calculated for natural convection around horizontal cylindrical objects by Hyman correlation as given in equation (1.3.10). It gives, $Nu_D = 37.38$.

The present heat transfer results as given in Table (IV) 3 III for isothermal and non-isothermal surface conditions are in close agreement with this value. Furthermore, the present results are approximately one fifteenth of forced convection Nusselt number (for coolant velocity 27.2 ft/sec) as shown in the text by K. Sri Ram [32]. The variation of surface temperature of the fuel rod in the manner $(1 + a\bar{x}^2)$ gives a sharp rise in the Nusselt number compared to the variation in the form $(1 + a\bar{x})$ for the values of $\bar{x} > 1$, as shown in Fig. 4.11.

5.2 CONCLUSION

On the basis of the analysis given in the foregoing chapters, the following principal conclusions can be drawn:

(1) The hydraulic modelling to determine the transient flow behaviour associated with the loss-of-flow accidents for coolant pumps designed with sufficiently large flywheels shows that, the flow coastdown will be slow. However, if the reactor trip is immediate, the after heat from the decay of fission products can be transported out of the core for a substantial length of time.

(2) The steady state temperature distribution in the core is attained approximately after 2 minutes.

(3) Since, the natural circulation can not be established in the primary flow circuit, thermosyphoning in the vicinity of each fuel rod provides immediate cooling. To investigate this phenomena, following Lighthills' [7] approach, the boundary layer differential equations for free convection flows around horizontal cylindrical fuel elements are formulated and solved by numerical methods. For non-isothermal conditions, the surface temperature of the fuel rod is assumed to be varied in two different manners, i.e. of the forms $(1 + a\bar{x})$ and $(1 + a\bar{x}^2)$. Suitable transformations are used so that the solutions will be independent of parameter a and hence, the method will be applicable for all reasonable values of a . Furthermore, it is found that the surface temperature variation has a significant effect on heat transfer.

5.3 SUGGESTIONS FOR FURTHER WORK

The present work can be extended in many ways as quoted below :

- (a) The hydraulic transient analysis can be extended for very fast transients, where acoustical phenomena becomes important or to situations where transient boiling and rapid depressurization of the systems cause rapid time changes in the fluid density to occur. These can be accomplished by formulating appropriate mass, momentum and energy balance equations to such situations.

conceive of the pure convection process being relevant for the random nature of the flow in the boundary layer regime and possibly, neighbouring boundary layer interactions becomes prevalent. This may also be investigated.

REFERENCES

1. T.H. Davies and W.D. Morris : Industrial Engg. Digest, 26 (1965).
2. R.T. Foyle : Proc. Institute of Mech. Engineers (London) 1951.
3. H. Cohen and F.J. Bayley : Heat Transfer Problems of liquid cooled Gas turbine blades, Proc. Institute of Mech. Engineers, Vol. 169, 1955.
4. E. Schmidt : General Discussion on Heat transfer, Institution of Mechanical Engineers, London, 1951.
5. H. Cohen and B.W. Martin : British Journal of Applied Physics, Vol. 5, March 1954.
6. J.P. Hartnett and W.E. Weish : Experimental Studies of free convection Heat transfer in a vertical tube with uniform heat flux, TRANS. ASME, Vol. 79, 1957.
7. M.J. Lighthill : Theoretical considerations on free convection in tubes, Quarterly Journal of Mech. and Appl. Math, Vol. 6, 1953.
8. B.W. Martin : Free convection in an open thermosyphon, Proceedings of Royal Society of London Series A, Vol. 230, 1955.
9. F.J. Bayley and G.S.H. Lock : Heat transfer characteristics of a closed thermosyphon, Journal of heat transfer, TRANS, ASME, Feb. 1965.
10. D. Japikse and E.R.F. Winter : Proceedings of International Heat transfer conference, 4th paper (1970).

11. S.C. Hyman, C.F. Bonilla : Natural convection transfer processes I. Heat transfer to liquid metals and non-metals at horizontal cylinders, Chemical Engineering Progress Symposium Series 49 (1953).
12. R. Herman : Laminar free convection from inclined cylinders, NACA, TM, 1366 (1954).
13. S. Levy : Integral methods in Natural convection Flow, J. Appl. Mech. 22 (1955).
14. E.R.G. Eckert and E. Soehngen : Studies on heat transfer in Laminar Free Convection with the Zehnder-Mach Interferometer, USAF. Tech. Report (1948).
15. R.B. Bird, W.E. Stewart and E.N. Lightfoot : Transport phenomena, 1960.
16. E.E. Lewis : Power Reactor Safety, 1979.
17. D. Burgreen : Flow Coastdown in a Loop after pumping power cut-off, Nucl. Sci. and Engg. 306-312 (1959)
18. M.M. Elwakil : Nuclear Power Engg., McGraw-Hill (1962).
19. Louis Brand : Differential and Difference equations, John-Wiley and Sons, 1966.
20. J.E. Mayer : Hydrodynamic Models for the treatment of reactor thermal transients, Nucl. Sc. and Engg. 10 (1961).
21. J. Crank and P. Nicholson : A practical method for numerical evaluation of solution of partial differential equation of heat conduction type, Proc. Cambridge Philosophical Society (1947).

22. J.C.Y. Koh and J.F. Price : Laminar free convection from horizontal axisymmetric bodies, Journal of heat transfer, TRANS, ASME, April 1965.
23. E. Schmidt : Heat transfer by natural convection, paper 1961 International Heat Transfer Conference.
24. H.R. Vallentine : Applied Hydrodynamics.
25. T. Chaing and J. Kaye : On laminar free convection from cylinder, Proceedings of the US National Congress of a Applied Mechanics, Berkeley, June 1962.
26. R.A. Struble : Non-linear differential equations, McGraw-Hill, 1962.
27. Simon Ostrach : An analysis of laminar free convection flow and heat transfer about a flat plate parallel to the direction of the generating body force, NACA Report, 1111, 1953.
28. Leslie Fox : Numerical solution of ordinary and partial differential equations, Pergamon Press, 1962.
29. John R. Radbill : Application of quasilinearization to the boundary layer equations, AIAA, J. Vol. 2, Oct. 1964.
30. D.R. Hartree : Numerical analysis, Clarendon Press (Oxford), 1952.
31. P.R. Nachtsheim and P. Swigert : Numerical solution of systems of non-linear equations of boundary layer type NASA TN, 3112, 1965.
32. K. Sri Ram : Basic Nuclear Engineering, Wiley Eastern Limited, 1977.

APPENDIX A

Some aspects of solution of equation (2.2.10)

Equation (2.2.10) can be written as

$$t_{\ell} \frac{dy}{dt} + y^2 = \frac{1}{(1 + t/t_p)} \quad (A.1)$$

subject to initial condition,

$$y = 1 \text{ at } t = 0, \text{ i.e. } y(0) = 1, \text{ where, } y = \frac{W}{W_0}$$

Equation (A.1) may be reduced to the form

$$t_{\ell} \left(\frac{dz}{dt} + z^2 \right) - f(t) = 0 \quad (A.2)$$

by the substitution $y = Z t_{\ell}$, where $f(t) = \frac{1}{(1+t/t_p)^2}$

Equation (A.2) is a special case of Riccati equation

$$P_0(t) \left[\frac{dz}{dt} + z^2 \right] + P_1(t)z + P_2(t) = 0 \quad (A.3)$$

where, $P_0 = t_{\ell}$, $P_1 = 0$ and $P_2 = -f(t)$

A theorem, Brand [19] states that the Riccati equation (A.3)

and the associated linear equation

$$P_0(t) \frac{d^2u}{dt^2} + P_1(t) \frac{du}{dt} + P_2(t)u = 0 \quad (A.4)$$

have corresponding solutions, which satisfy the equations

$$u(t) = \exp \int Z(t)dt, \quad Z(t) = \frac{1}{u} \frac{du}{dt}$$

By the above theorem, associated linear equation of (A.2) is found out to be

$$\frac{d^2u}{dt^2} - f(t)u = 0 \quad (A.5)$$

with transformed initial condition

$$\frac{1}{u(t)} \frac{du(t)}{dt} \Big|_{t=0} = \frac{1}{t_{\ell}}$$

Equation (A.5) is of the form of Schrodinger equation. There ~~is~~ is no standard method of solution of this, equation and usually approximation theory is used for analytical solution.

APPENDIX BINTEGRATION FORMULAS

Runge-Kutta 4th Order Formulas :

A pth order differential equations can be expressed as a system of p 1st order differential equations, i.e.

$$\frac{d^p y}{dx^p} = f(x, y, \frac{dy}{dx}, \frac{d^2 y}{dx^2}, \dots, \frac{d^{p-1} y}{dx^{p-1}}) \quad (B.1)$$

It we take, $y_1 = y$, $y_2 = \frac{dy}{dx}$ and $y_p = \frac{d^{p-1} y}{dx^{p-1}}$,
the system of equations, i.e.,

$$\frac{dy_1}{dx} = f_1(x, y, \dots, y_p)$$

$$\frac{dy_2}{dx} = f_2(x, y, \dots, y_p)$$

$$\frac{dy_p}{dx} = f_p(x, y, \dots, y_p)$$

Vectorially, $\frac{d\vec{Y}}{dx} = \vec{f}(x, \vec{Y})$ where, \vec{Y} , \vec{f} are column vectors.

For a coupled equation of the form,

$$\frac{dy}{dx} = f(x, y, z) \text{ and } \frac{dz}{dx} = g(x, y, z)$$

the 4th order Runge-Kutta method is given as :

$$y_{n+1} = y_n + \frac{1}{6} (K_1 + 2K_2 + 2K_3 + K_4) \quad (B.2)$$

$$z_{n+1} = z_n + \frac{1}{6} (\ell_1 + 2\ell_2 + 2\ell_3 + \ell_4)$$

where,

$$K_1 = hf(x_n, y_n, z_n)$$

$$\ell_1 = hg(x_n, y_n, z_n)$$

$$K_2 = hf\left(x_n + \frac{h}{2}, y_n + \frac{K_1}{2}, z_n + \frac{\ell_1}{2}\right)$$

$$K_3 = hf\left(x_n + \frac{h}{2}, y_n + \frac{K_2}{2}, z_n + \frac{\ell_2}{2}\right)$$

$$\ell_2 = hg\left(x_n + \frac{h}{2}, y_n + \frac{K_1}{2}, z_n + \frac{\ell_1}{2}\right)$$

$$\ell_3 = hg\left(x_n + \frac{h}{2}, y_n + \frac{K_2}{2}, z_n + \frac{\ell_2}{2}\right)$$

$$K_4 = hf(x_n + h, y_n + K_3, z_n + \ell_3)$$

$$\ell_4 = hg(x_n + h, y_n + K_3, z_n + \ell_3)$$

where, h is the step size. Three values are first determined from the above method to use them in Adam-Moulton predictor corrector for better accuracy, as corrector an implicit iteration technique is used for next predictor value.

Adams-Moulton Predictor Corrector Scheme:

$$\text{Predictor : } y_{n+1}^{(0)} = y_n + \frac{h}{24}[55f(x_n, y_n, z_n) - 59f(x_{n-1}, y_{n-1}, z_{n-1}) + 37f(x_{n-2}, y_{n-2}, z_{n-2}) - 9f(x_{n-3}, y_{n-3}, z_{n-3})]$$

$$z_{n+1}^{(0)} = z_n + \frac{h}{24}[55g(x_n, y_n, z_n) - 59f(x_{n-1}, y_{n-1}, z_{n-1}) + 37g(x_{n-2}, y_{n-2}, z_{n-2}) - 9g(x_{n-3}, y_{n-3}, z_{n-3})]$$

Corrector :

$$y_{n+1}^{(1)} = y_n + \frac{h}{24}[9f(x_{n+1}, y_{n+1}^{(0)}, z_{n+1}^{(0)}) + 19f(x_n, y_n, z_n) - 5f(x_{n-1}, y_{n-1}, z_{n-1}) + f(x_{n-2}, y_{n-2}, z_{n-2})]$$

APPENDIX CCANDU (RAPP) REACTOR DATA

The following Rajasthan Atomic Power Plant data of a CANDU type reactor is used here for the required calculations.

Each fuel bundle consists of 19 fuel rods of Natural UO_2 .

- (1) Reactor inlet temperature $T_1 = 480^\circ\text{F}$
- (2) Reactor outlet temperature $T_2 = 560^\circ\text{F}$
- (3) Mean D_2O temperature $T = 515^\circ\text{F}$
- (4) Temperature at the centre of the core T_o (calculated)
 $= 580^\circ\text{F}$
- (5) D_2O temperature at low power $= 504^\circ\text{F}$
- (6) Specific heat at constant pressure of the D_2O coolant C_p
 $= 1.7744 \text{ Btu/lb-F}^\circ$
- (7) Dynamic viscosity of the D_2O coolant $\mu = 0.2838 \text{ lb/ft-hr}$
- (8) Thermal conductivity of D_2O coolant $K = 0.3066 \frac{\text{Btu}}{\text{hr-F}^\circ\text{-ft}}$
- (9) Reactor channel length $2\ell = 16.404 \text{ ft}$
- (10) Mean D_2O density $\bar{\rho} = 52.91 \text{ lb/ft}^3$
- (11) Mean D_2O density in the riser at outlet temperature
(calculated) $\bar{\rho}_r = 52.91 \frac{\text{lbm}}{\text{ft}^3}$
- (12) Mean D_2O density in the downcomer at the inlet
temperature $\bar{\rho}_d = 57.29 \text{ lbm/ft}^3$
- (13) Total system losses (calculated) $\sum \Delta P = 1.413 \text{ lbf/in}^2$
- (14) Driving pressure (calculated) $\sum \Delta P_d = 0.1827 \text{ lbf/in}^2$

- (15) Pump halftime for a typical recirculation pump,
 $t_p = I/c \omega_0 = 5 \text{ sec.}$
- (16) Height of the riser (hotleg) and downcomer (coldleg)
 of the U-tube heat exchanger = 6 ft
- (17) Prandtl number of pr = $\mu C_p / K = 1.089$
- (18) Reynolds number of Re = $\rho v D / \mu = 3.68 \times 10^5$
 (for the coolant velocity 27.2 ft/sec)
- (19) Nusselt number (for the coolant velocity 27.2 ft/sec)
 $= Nu = 654$
- (20) Heat transfer coefficient (calculated for the given
 Nusselt number) $h = Nu K / D = 9300 \text{ Btu/hr-ft}^2\text{-F}$
- (21) Hydraulic diameter $D = 0.0216 \text{ ft}$
- (22) Steady state Grashoff number basing on the diameter
 of the fuel rod (calculated) $Gr_D = \frac{g \beta (T_w - T_\infty) D^3}{\nu^2}$
 $= 0.4262 \times 10^8$
- (23) Kinematic viscosity $\nu = \frac{\mu}{\rho} = 5.3638 \times 10^{-3} \text{ ft}^2/\text{hr}$
- (24) Clad surface temperature $T_w = 573.8^\circ\text{F}$
- (25) Thermal expansion coefficient $\beta = 4.0 \times 10^{-4} \text{ F}^{-1}$
- (26) Volumetric thermal source strength at the centre
 of the core $q_0''' = 1.648 \text{ Btu/ft}^3\text{-sec}$
- (27) Diffusivity $\alpha = \frac{K}{\rho C_p} = 0.0032 \text{ ft}^2/\text{sec.}$

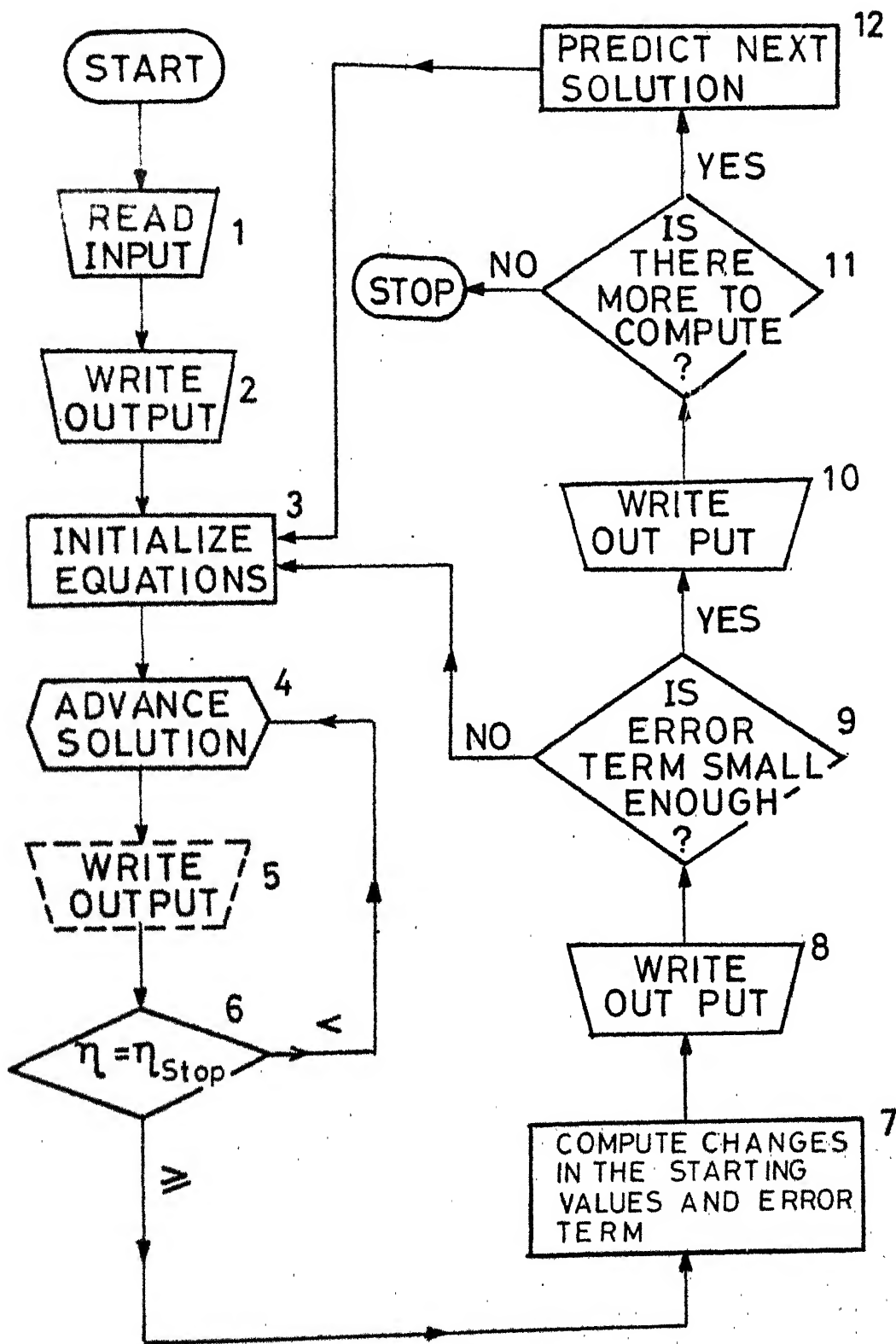


Fig. 5-1 General flow chart for the main program applied to all the equations

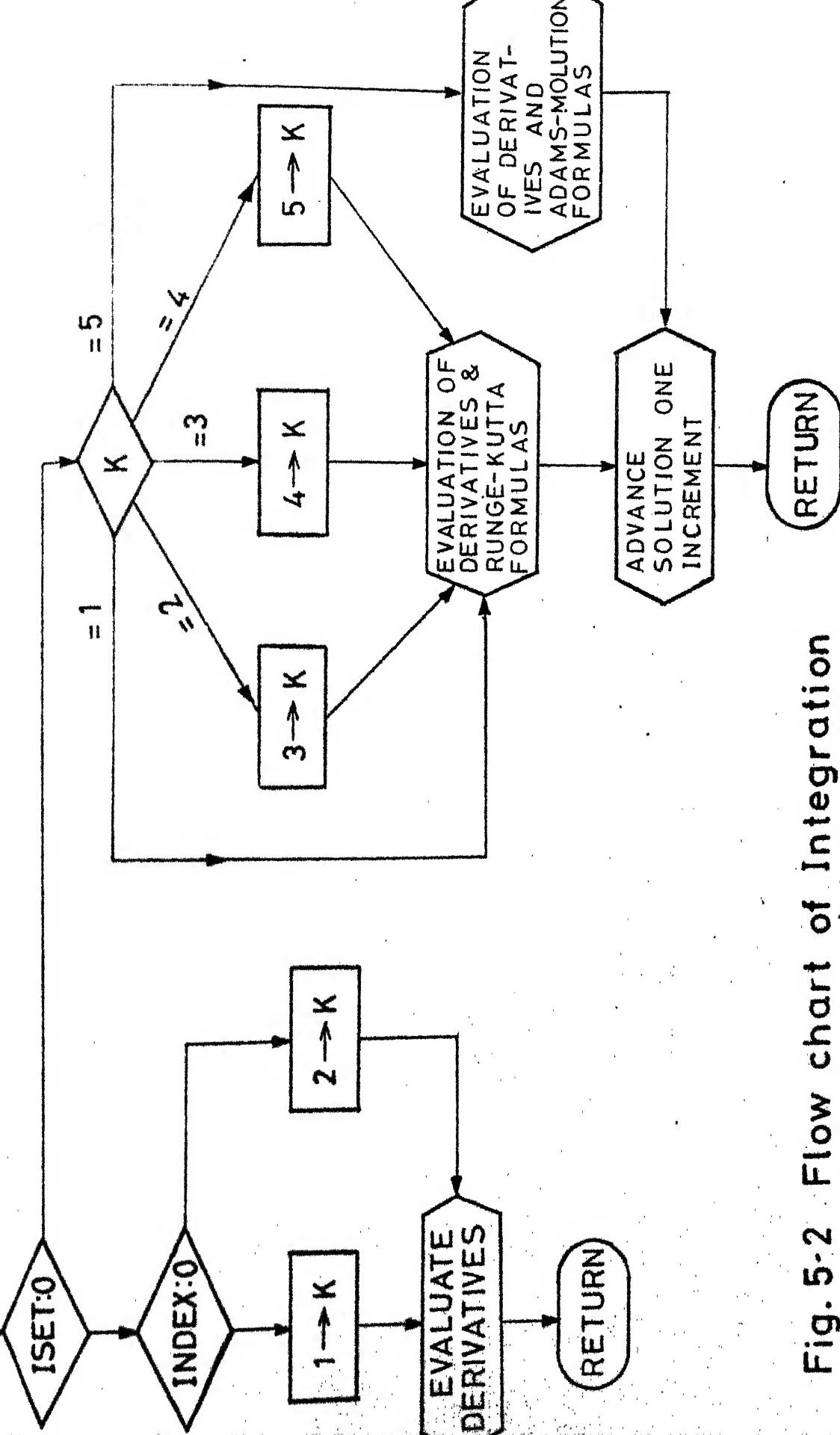


Fig. 5-2 Flow chart of Integration Subroutine Adams

APPENDIX DCOMPUTER PROGRAM

LAMINAR FLOW CONVECTION DIFFERENTIAL EQUATIONS ARE SOLVED
 SOLVING A SYSTEM OF NONLINEAR DIFFERENTIAL EQUATIONS
 THIS IS AN ASYMPTOTIC BOUNDARY VALUE PROBLEM FOR A NONLINEAR
 COUPLED THIRD ORDER DIFFERENTIAL EQUATION
 INITIAL VALUE METHOD IS APPLIED WITH RACHUNSHIN-SWIGERT
 ITERATION SCHEME USING LEAST SQUARE ERROR MINIMIZATION
 TO THE GIVEN PROBLEM

DECLARATION OF THE PROGRAM DEC

COMMON DATA

DIMENSION Y(30), D1(30), ETAEND(10), TEST(10)

READ*, N, Y, Z, PR, DELPR, LTEST

READ*, N, C, TAPAD(I), I=1, N

READ*, C, DELT(I), I=1, N

TEST(10), ACCURACY CRITERIA IMPOSED ON CORRECTION FOR
 INITIAL CONDITIONS DELX AND DELZ

TYPE 101, A, Z, TEST

TYPE 102, C, TAPAD(I), I=1, N

TYPE 103, C, DELT(I), I=1, N

TYPE 201, N, PR

I=1

SIYPE=DELPR

'DELPR' IS THE TYPE INTERVAL WHICH WE KEEP SAME AS STEP SIZE
 INITIAL SURFACE CONDITIONS ARE GIVEN BELOW

THESE ARE INITIAL CONDITIONS GIVEN AT THE CLAD SURFACE
 FACET, Y(3) AND Y(5) WHICH ARE TO BE GAUSSSED

ETA=0.0

Y(1)=0.0

Y(2)=0.0

Y(3)=A

Y(4)=1.0

Y(5)=Z

Y(6)=0.0

Y(7)=0.0

Y(8)=1.0

Y(9)=0.0

Y(10)=0.0

Y(11)=0.0

Y(12)=0.0

Y(13)=0.0

Y(14)=0.0

Y(15)=1.0

LET US FIRST CALCULATE THE DERIVATIVES FOR ONLY FIRST VALUE

OF ETA AS A TRAIL TO SEE THE RESULTS

CALL ADAMS(15, N, ETA, 0, Y, DY, 1)

TYPE 100, ETA, Y(1), Y(2), Y(3), Y(4), Y(5)

TYPE 90

TYPE 45

CALL ADAMS(15, N, ETA, 1, Y, DY, 1)

TYPE 202, ETA, Y(1), Y(2), Y(3), Y(4), Y(5)

IF (ETA, LT, SIYPE) GO TO 6

SIYPE=SIYPE+DELPR

IF (ETA, LT, ETAEND(1)) GO TO 4

RACHUNSHIN-SWIGERT LEAST SQUARE ITERATION SCHEME IS

NOW APPLIED

A11=Y(7)**2+Y(9)**2+Y(9)**2+Y(10)**2

A12=Y(7)*Y(12)+Y(9)*Y(14)+Y(18)*Y(13)+Y(10)*Y(15)

A21=A12

A22=Y(12)**2+Y(14)**2+Y(13)**2+Y(15)**2

R1=-(Y(2)*Y(7)+Y(4)*Y(9)+Y(3)*Y(8)+Y(5)*Y(10))

R2=-(Y(2)*Y(12)+Y(4)*Y(14)+Y(3)*Y(13)+Y(5)*Y(15))

DELX=A11*A22-A21*A12

CORRECTION IS FOR INITIAL CONDITIONS ARE GIVEN BELOW

CORRECTION IN X IS DELX AND Z IS DELZ


```

C      DY(8)=Y(7)
C      DY(7)=Y(8)
C      DY(8)=2.0*Y(2)*Y(7)-(Y(3)*Y(6)+Y(1)*Y(8))-Y(9)
C      DY(9)=Y(10)
C      DY(10)=-PR*(Y(5)*Y(6)+Y(1)*Y(10))
C      EQUATIONS CONTAINING Y DERIVATIVES ARE NOW WRITTEN
C      DY(11)=Y(12)
C      DY(12)=Y(13)
C      DY(13)=2.0*Y(2)*Y(12)-(Y(3)*Y(11)+Y(1)*Y(13))-Y(14)
C      DY(14)=Y(15)
C      DY(15)=-PR*(Y(5)*Y(11)+Y(1)*Y(15))
C      RETURN
C      END
C      INTEGRATION SUBROUTINE
C      SUBROUTINE I1 INTEGRATE DIFFERENTIAL EQUATION OF THE TYPE
C      DY=FX(X,Y) BY FOURTH ORDER RUNGE-KUTTA AND ADAMS MOULTON
C      FORMULAS
C      FIRST RUNGE-KUTTA METHOD APPLIED TO OBTAIN FIRST THREE VALUES
C      OF ADAMS-MOULTON PREDICTOR CORRECTOR WHICH IS SUBSEQUENTLY
C      APPLIED FOR BETTER ACCURACY
C      SUBROUTINE ADAMS(V,H,X,ISET,Y,DY,INDEX)
C      COMMON PR,K
C      DIMENSION Y(30),DY(30),P(30),YR(30),DYLL(30),DYLL(30),DYLL(30),
C      DYR(30),C2(30),C3(30),C4(30)
C      IF(ISET.C1.C)GO TO 6
C      IF(INDEX.NT.0)GO TO 4
C      K=2
C      GO TO 5
C      K=1
C      CALL DIFF(X,Y,DY)
C      RETURN
C      GO TO(10,7,8,9,11),K
C      K=3
C      GO TO 10
C      K=4
C      GO TO 10
C      K=5
C      FIRST RUNGE-KUTTA METHOD APPLIED
C      DO 1001 I=1,N
C      P(I)=Y(I)+(H/2.0)*DY(I)
C      CALL DIFF(X+H/2.0,P,C2)
C      DO 1002 I=1,N
C      P(I)=Y(I)+(H/2.0)*C2(I)
C      CALL DIFF(X+H/2.0,P,C3)
C      DO 1003 I=1,N
C      P(I)=Y(I)+H*C3(I)
C      CALL DIFF(X+H,P,C4)
C      DO 1004 I=1,N
C      YR(I)=Y(I)+(H/6.0)*(DY(I)+2.0*C2(I)+2.0*C3(I)+C4(I))
C      CALL DIFF(X+H,YR,DYR)
C      GO TO 12
C      ADAMS-MOULTON PREDICTOR CORRECTOR IS NOW APPLIED
C      DO 1101 I=1,N
C      P(I)=Y(I)+(H/24.0)*(55.0*DY(I)-59.0*DYLL(I)+37.0*DYLL(I)-
C      19.0*DYLL(I))
C      CALL DIFF(X+H,P,DYR)
C      DO 1102 I=1,N
C      YR(I)=Y(I)+(H/24.0)*(9.0*DYR(I)+19.0*DY(I)-5.0*DYLL(I)+DYLL(I))
C      CALL DIFF(X+H,YR,DYR)
C      X=X+H
C      DO 1201 I=1,N
C      Y(I)=YR(I)
C      DYLL(I)=DYLL(I)
C      DYLL(I)=DYLL(I)
C      DYLL(I)=DY(I)
C      DY(I)=DYR(I)
C      RETURN
C      END

```

LAMINAR FREE CONVECTION DIFFERENTIAL EQUATION 2
 THE ITERATION PROCEDURE IS SAME AS GIVEN IN EQUATION 1
 INITIAL CONDITIONS AND DIFFERENTIAL EQUATION SUBROUTINE
 ARE ONLY CHANGED
 INITIAL CONDITIONS ARE GIVEN BELOW

```
ETA=0.0
Y(1)=0.0
Y(2)=0.0
Y(3)=1
Y(4)=1.0
Y(5)=2
Y(6)=0.0
Y(7)=0.0
Y(8)=1.0
Y(9)=0.0
Y(10)=0.0
Y(11)=0.0
Y(12)=0.0
Y(13)=0.0
Y(14)=0.0
Y(15)=1.0
Y1(1)=0.0
Y1(2)=0.0
Y1(3)=0.67
Y1(4)=1.0
Y1(5)=-0.81
Y1(6)=0.0
Y1(7)=0.0
Y1(8)=1.0
Y1(9)=0.0
Y1(10)=0.0
Y1(11)=0.0
Y1(12)=0.0
Y1(13)=0.0
Y1(14)=0.0
Y1(15)=1.0
SUBROUTINE 17 COMPUTE THE ORIGINAL AND CORRESPONDING
PERTURBATION DIFFERENTIAL EQUATIONS FOR SYSTEM OF EQUATIONS 2
PERTURBATION EQUATIONS ARE USED TO DETERMINE THE PARTIAL
DERIVATIVES IN THE CORRECTION TERMS
THESE PARTIAL DERIVATIVES KNOWN AS CONVERGENCE DERIVATIVES
SUBROUTINE DIFF(ETA,Y,DY) FOR DIFFERENTIAL EQUATION 2
COMMON PP,K
DIMENSION Y(30),DY(30),Y1(30),DY1(30)
FIRST ORIGINAL EQUATION IS WRITTEN AS FIVE EQUIVALENT
ORDINARY FIRST ORDER DIFFERENTIAL EQUATIONS
D1(1)=Y1(2)
D1(2)=Y1(3)
DY(1)=Y(2)
DY(2)=Y(3)
DY(3)=- (Y1(1)*Y(3)-4.0*Y1(2)*Y(2)+3.0*Y1(3)*Y(1)-Y(4))
DY1(4)=Y1(5)
DY(4)=Y(5)
DY(5)=-PP*(Y1(1)*Y(5)-2.0*Y1(2)*Y(4)+3.0*Y(1)*Y1(5))
DY1(6)=Y1(7)
DY1(7)=Y1(8)
DY(6)=Y(7)
DY(7)=Y(8)
DY(8)=- (Y1(6)*Y(3)+Y1(1)*Y(8)-4.0*Y1(2)*Y(7)-4.0*Y1(7)*Y(2)
1+3.0*Y1(8)*Y(1)+3.0*Y1(3)*Y(6)-Y(9))
DY1(9)=Y1(10)
DY(9)=Y(10)
DY(10)=-PP*(Y1(1)*Y(10)+Y(7)*Y1(6)-2.0*Y1(7)*Y(4)
1-2.0*Y1(2)*Y(9)+3.0*Y(1)*Y1(10)+3.0*Y(6)*Y1(5))
D1(11)=Y1(12)
D1(12)=Y1(13)
DY(11)=Y(12)
DY(12)=Y(13)
DY(13)=- (Y1(11)*Y(3)+Y1(1)*Y(13)-4.0*Y1(2)*Y(12)-4.0*Y1(12)
1+Y(7)+3.0*Y1(13)*Y(1)+3.0*Y1(3)*Y(11)-Y(14))
DY1(14)=Y1(15)
DY(14)=Y(15)
DY(15)=-PP*(Y1(1)*Y(15)+Y(5)*Y1(11)-2.0*Y1(12)*Y(4)
1-2.0*Y1(2)*Y(14)+3.0*Y(1)*Y1(15)+3.0*Y(11)*Y1(5))
RETURN
END
```


V (1) 1000
 V (2) 1000
 V (3) 1000
 V (4) 1000
 V (5) 1000
 V (6) 1000
 V (7) 1000
 V (8) 1000
 V (9) 1000
 V (10) 1000
 V (11) 1000
 V (12) 1000
 V (13) 1000
 V (14) 1000
 V (15) 1000
 V (16) 1000
 V (17) 1000
 V (18) 1000
 V (19) 1000
 V (20) 1000
 V (21) 1000
 V (22) 1000
 V (23) 1000
 V (24) 1000
 V (25) 1000
 V (26) 1000
 V (27) 1000
 V (28) 1000
 V (29) 1000
 V (30) 1000
 V (31) 1000
 V (32) 1000
 V (33) 1000
 V (34) 1000
 V (35) 1000
 V (36) 1000
 V (37) 1000
 V (38) 1000
 V (39) 1000
 V (40) 1000
 V (41) 1000
 V (42) 1000
 V (43) 1000
 V (44) 1000
 V (45) 1000
 V (46) 1000
 V (47) 1000
 V (48) 1000
 V (49) 1000
 V (50) 1000
 V (51) 1000
 V (52) 1000
 V (53) 1000
 V (54) 1000
 V (55) 1000
 V (56) 1000
 V (57) 1000
 V (58) 1000
 V (59) 1000
 V (60) 1000
 V (61) 1000
 V (62) 1000
 V (63) 1000
 V (64) 1000
 V (65) 1000
 V (66) 1000
 V (67) 1000
 V (68) 1000
 V (69) 1000
 V (70) 1000
 V (71) 1000
 V (72) 1000
 V (73) 1000
 V (74) 1000
 V (75) 1000
 V (76) 1000
 V (77) 1000
 V (78) 1000
 V (79) 1000
 V (80) 1000
 V (81) 1000
 V (82) 1000
 V (83) 1000
 V (84) 1000
 V (85) 1000
 V (86) 1000
 V (87) 1000
 V (88) 1000
 V (89) 1000
 V (90) 1000
 V (91) 1000
 V (92) 1000
 V (93) 1000
 V (94) 1000
 V (95) 1000
 V (96) 1000
 V (97) 1000
 V (98) 1000
 V (99) 1000
 V (100) 1000

CONSIDER $Y(10), Y(20), Y(30), Y(40)$
 DIMENSION $Y(40)$ BY $Y(40), Y(40), Y(40)$
 FIRST ORIGINAL EQUATION IS WRITTEN AS FIVE EQUIVALENT
 ORDINARY FIRST ORDER DIFFERENTIAL EQUATIONS

FUNCTION V(40), DY(40), Y1(30), DY1(30)
 FIRST ORDER DIFFERENTIAL EQUATION IS WRITTEN AS FIVE EQUIVALENT
 FIRST ORDER DIFFERENTIAL EQUATIONS

$$Y(1) = Y(1)$$

$$Y(2) = Y(2)$$

$$Y(3) = Y(3)$$

$$Y(4) = Y(4)$$

$$Y(5) = Y(5)$$

$$Y(1) + Y(2) - 4.0 * Y(2) * Y(3) + 3.0 * Y(3) * Y(1) + Y(4)$$

$$Y(1) * Y(5) - 2.0 * Y(2) * Y(4) + 3.0 * Y(1) * Y(5)$$

$$Y(1) + Y(3) + Y(5) * Y(6) = 4.0 * Y(2) * Y(7) - 4.0 * Y(7) * Y(2)$$

$$Y(1) + 3.0 * Y(1) * Y(6) + Y(6) + Y(6) = 0.166 * Y(9)$$

$$Y(1) + Y(10) + Y(7) * Y(6) = 4.0 * Y(7) * Y(4)$$

$$Y(1) + Y(1) + 3.0 * Y(1) * Y(13) + Y(11) + Y(14) = 0.166 * Y(16)$$

$$Y(1) + Y(15) + Y(15) * Y(15) + 3.0 * Y(15) * Y(15)$$

Date Slip **A66872**

This book is to be returned on the
date last stamped.

6

CD 6.72.9

L

NETP-1981-M-DAS-THE